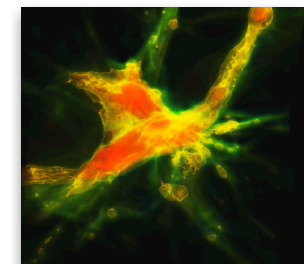
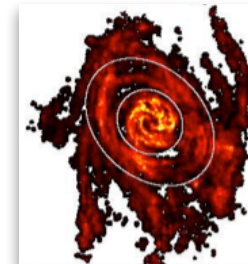
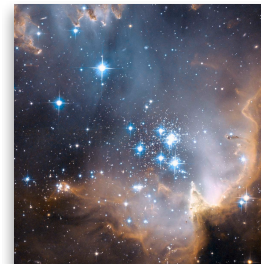
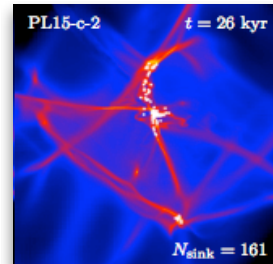
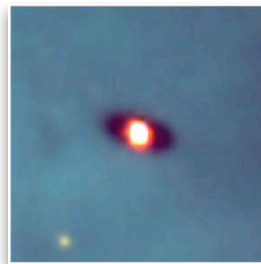
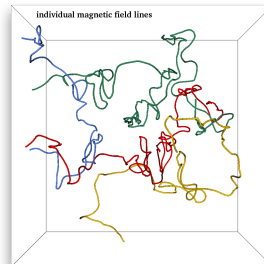


Modeling ISM Dynamics and Star Formation



Ralf Klessen



Universität Heidelberg, Zentrum für Astronomie
Institut für Theoretische Astrophysik



disclaimer

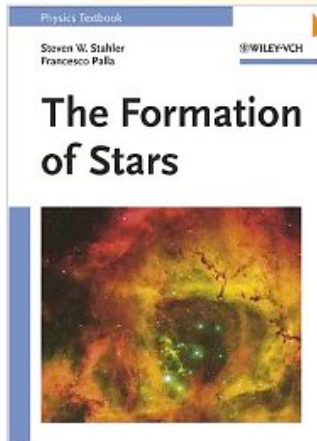
Disclaimer

- I try to cover the field as broadly as possible, however, there will clearly be a bias towards my personal interests and many examples will be from my own work.

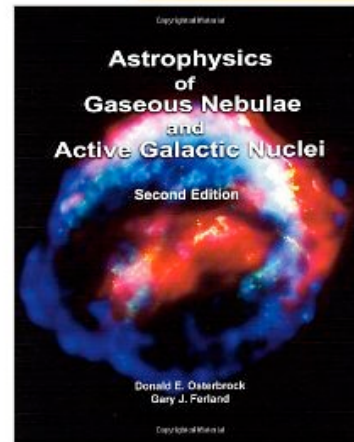
literature

Literature

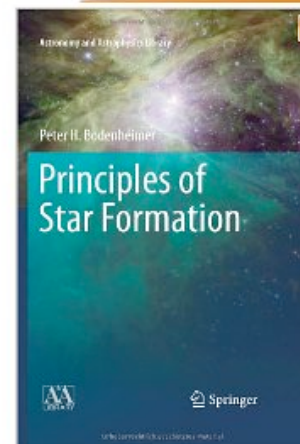
Click to **LOOK INSIDE!**



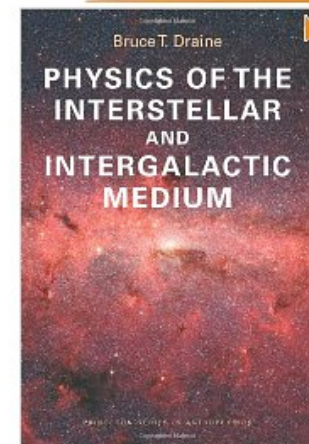
Click to **LOOK INSIDE!**



Click to **LOOK INSIDE!**



Click to **LOOK INSIDE!**

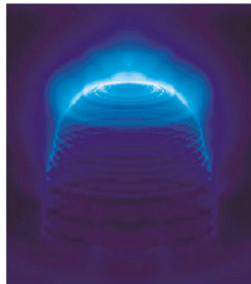


PHYSICS TEXTBOOK

George B. Rybicki
Alan P. Lightman

WILEY-VCH

**Radiative Processes
in Astrophysics**

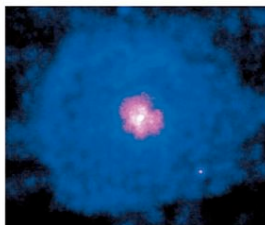


PHYSICS TEXTBOOK

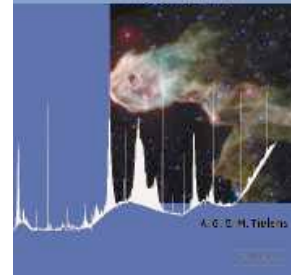
Lyman Spitzer, Jr.

WILEY-VCH

**Physical Processes in the
Interstellar Medium**



The Physics and Chemistry of the
**Interstellar
Medium**



Stars in Atmospheres and Atmospheres



**NUMERICAL METHODS
IN ASTROPHYSICS**

An Introduction

Peter Bodenheimer
Gerson P. Luger
Mohit Riey
Ramon N. Toral

Taylor & Francis

🌟 Books

- 🌟 Spitzer, L., 1978/2004, Physical Processes in the Interstellar Medium (Wiley-VCH)
- 🌟 Rybicki, G.B., & Lightman, A.P., 1979/2004, Radiative Processes in Astrophysics (Wiley-VCH)
- 🌟 Stahler, S., & Palla, F., 2004, "The Formation of Stars" (Weinheim: Wiley-VCH)
- 🌟 Tielens, A.G.G.M., 2005, The Physics and Chemistry of the Interstellar Medium (Cambridge University Press)
- 🌟 Osterbrock, D., & Ferland, G., 2006, "Astrophysics of Gaseous Nebulae & Active Galactic Nuclei, 2nd ed. (Sausalito: Univ. Science Books)
- 🌟 Bodenheimer, P., et al., 2007, Numerical Methods in Astrophysics (Taylor & Francis)
- 🌟 Draine, B. 2011, "Physics of the Interstellar and Intergalactic Medium" (Princeton Series in Astrophysics)
- 🌟 Bodenheimer, P. 2012, "Principles of Star Formation" (Springer Verlag)





Literature

● Review Articles

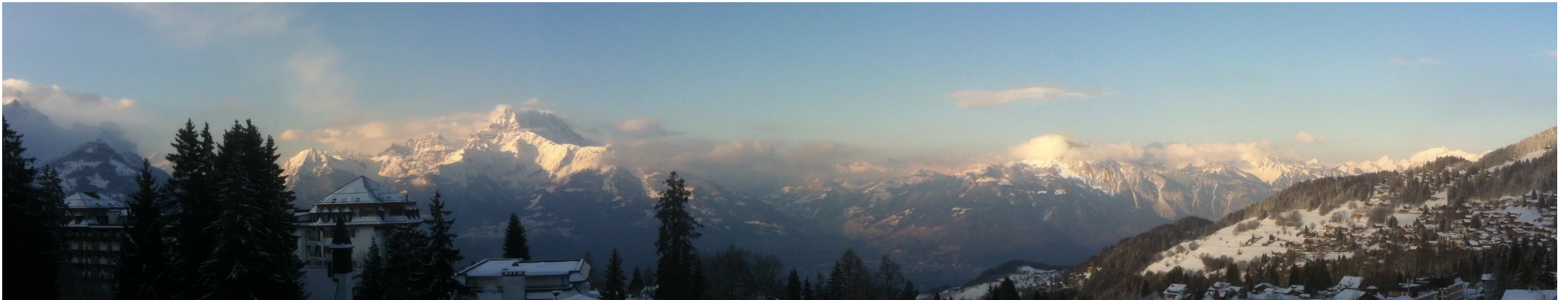
- Mac Low, M.-M., Klessen, R.S., 2004, "The control of star formation by supersonic turbulence", Rev. Mod. Phys., 76, 125
- Elmegreen, B.G., Scalo, J., 2004, "Interstellar Turbulence 1", ARA&A, 42, 211
- Scalo, J., Elmegreen, B.G., 2004, "Interstellar Turbulence 2", ARA&A, 42, 275
- Bromm, V., Larson, R.B., 2004, "The first stars", ARA&A, 42, 79
- Zinnecker, H., Yorke, McKee, C.F., Ostriker, E.C., 2008, "Toward Understanding Massive Star Formation", ARA&A, 45, 481 - 563
- McKee, C.F., Ostriker, E.C., 2008, "Theory of Star Formation", ARA&A, 45, 565
- Kennicutt, R.C., Evans, N.J., 2012, "Star Formation in the Milky Way and Nearby Galaxies", ARA&A, 50, 531

Further resources

Internet resources

-  Cornelis Dullemond: *Radiative Transfer in Astrophysics*
http://www.ita.uni-heidelberg.de/~dullemond/lectures/radtrans_2012/index.shtml
-  Cornelis Dullemond: *RADMC-3D: A new multi-purpose radiative transfer tool*
<http://www.ita.uni-heidelberg.de/~dullemond/software/radmc-3d/index.shtml>
-  List of molecules in the ISM (wikipedia):
http://en.wikipedia.org/wiki/List_of_molecules_in_interstellar_space
-  Leiden database of molecular lines (LAMBDA)
<http://home.strw.leidenuniv.nl/~moldata/>

Part 3: Star Formation



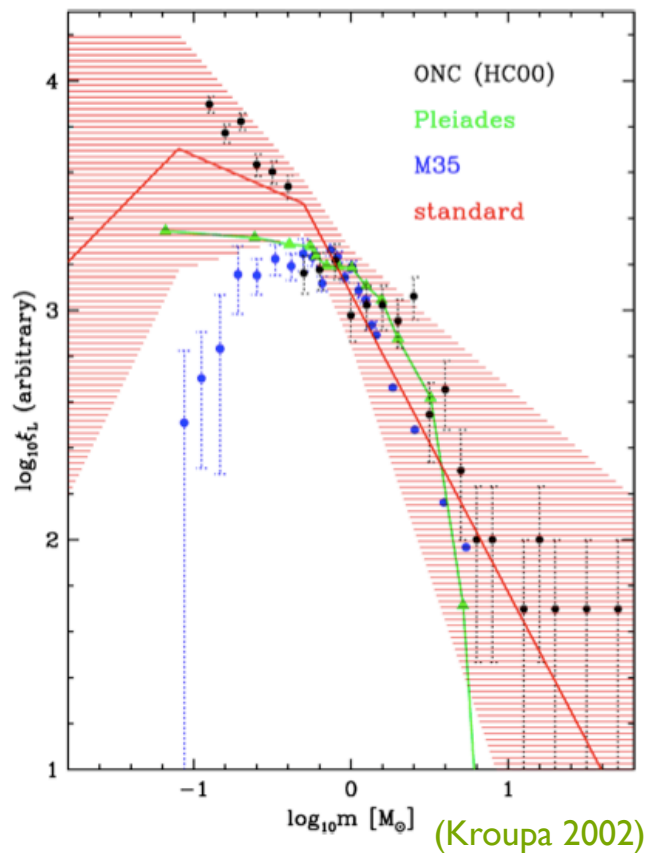
Ralf Klessen

Universität Heidelberg, Zentrum für Astronomie
Institut für Theoretische Astrophysik



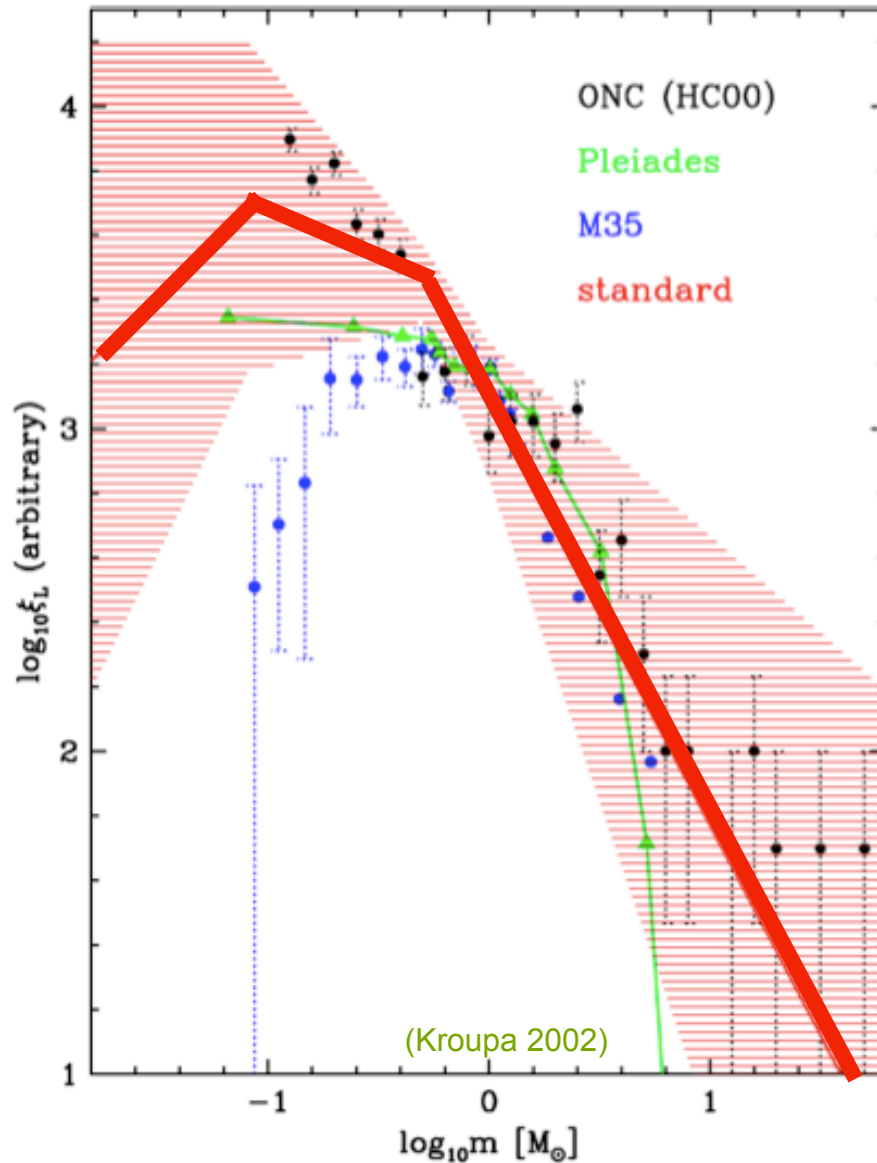
stellar mass function

stars seem to follow a universal mass function at birth --> IMF



Orion, NGC 3603, 30 Doradus
(Zinnecker & Yorke 2007)

IMF: observations 1



power-law approximation to the IMF (Kroupa, Tout, Gilmore 1993, Kroupa 2002)

$$\xi(m)dm \propto m^{-\alpha}dm,$$

$$\xi(m) = \begin{cases} 0.26 m^{-0.3} & \text{for } 0.01 \leq m < 0.08 \\ 0.035 m^{-1.3} & \text{for } 0.08 \leq m < 0.5 \\ 0.019 m^{-2.3} & \text{for } 0.5 \leq m < \infty. \end{cases}$$

IMF: observations 2

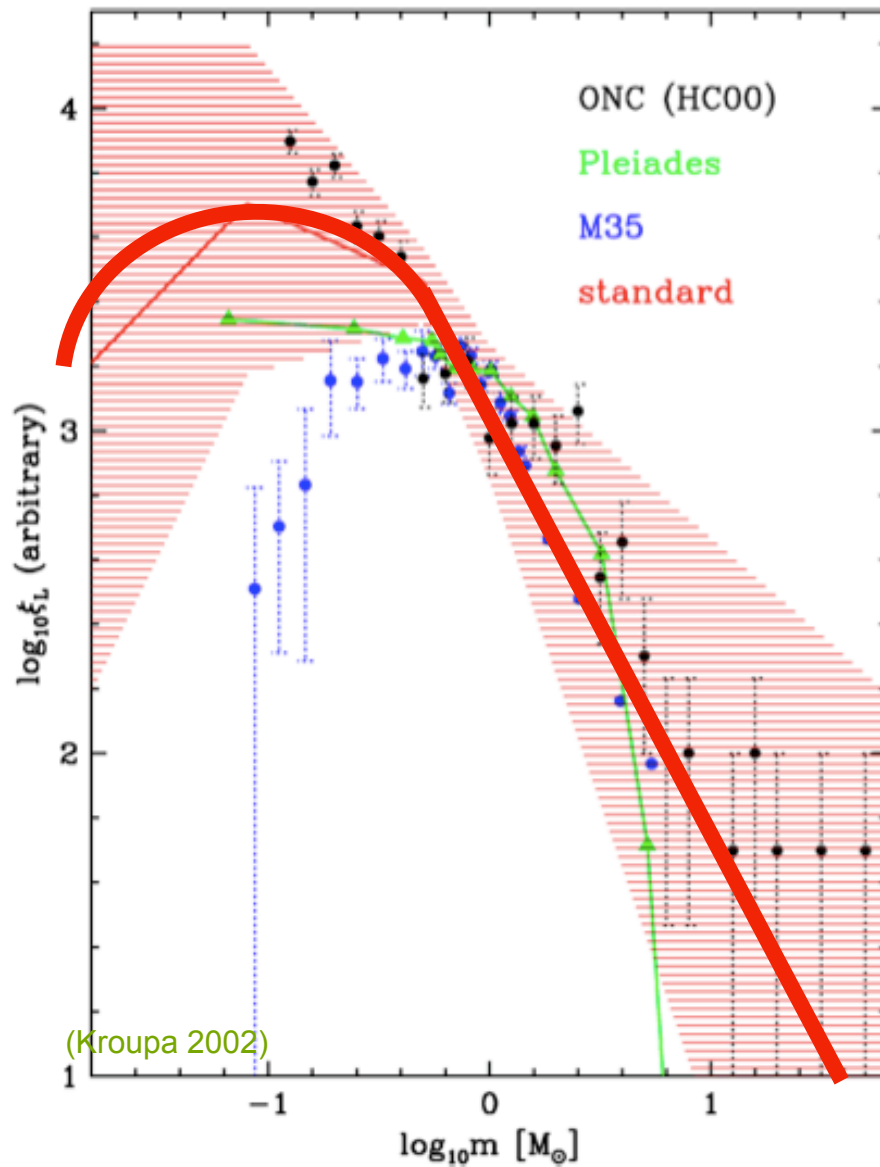
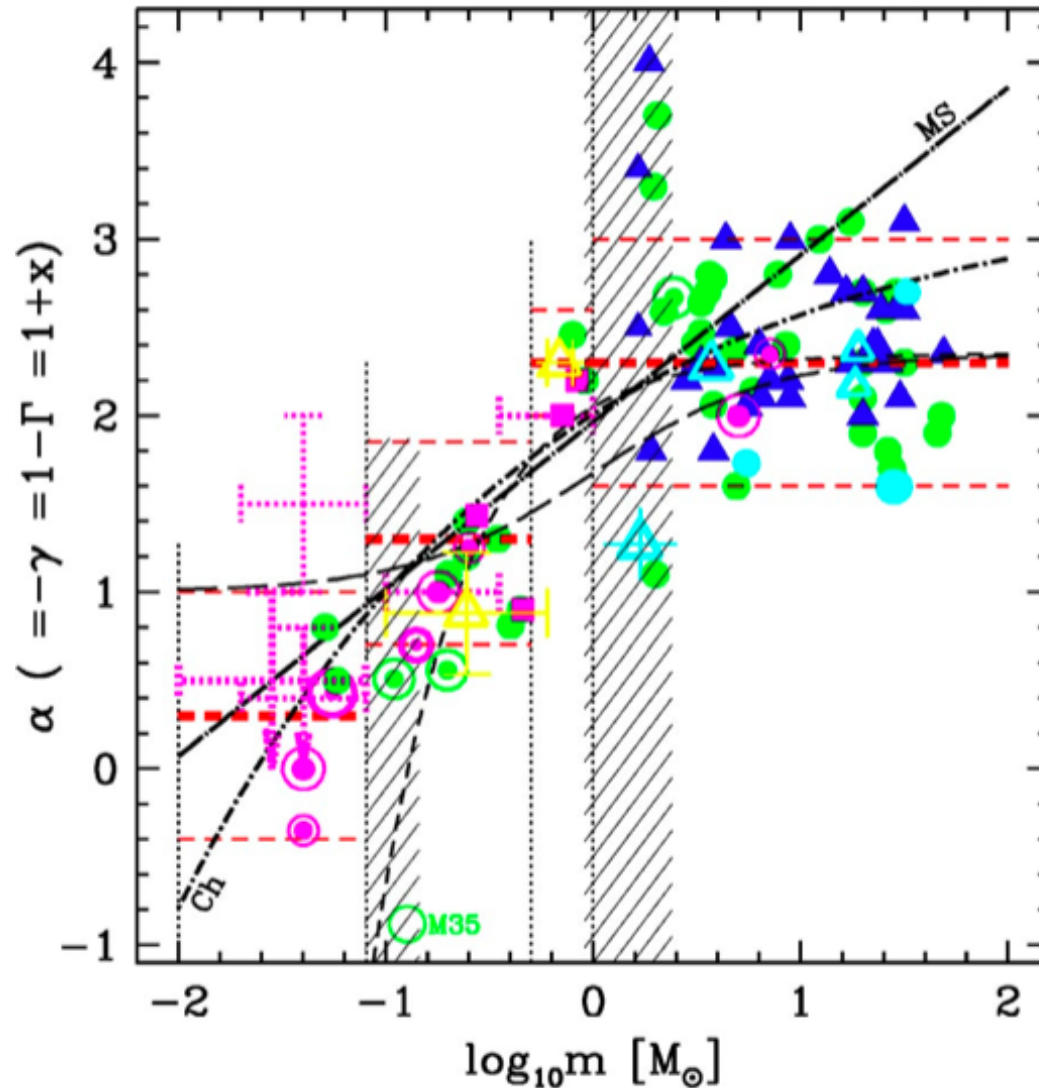


TABLE 1
 DISK IMF AND PDMF FOR SINGLE OBJECTS

Parameter	IMF	PDMF
$m \leq 1.0 M_{\odot}, \xi(\log m) = A \exp [-(\log m - \log m_c)^2/2\sigma^2]$		
A	$0.158^{+0.051}_{-0.046}$	0.1
m_c	$0.079^{+0.021}_{-0.016}$	0.0
σ	$0.69^{+0.05}_{-0.01}$	0.6
$m > 1.0 M_{\odot}, \xi(\log m) = Am^{-x}$		
A	4.43×10^{-2}	
x	1.3 ± 0.3	

(Chabrier 2003)

IMF: observations 3



but notice possible influence of dynamical evolution in star cluster on transformation from present-day mass function (PDMF) to IMF.

IMF: observations 4

notice alternative functional forms for the IMF

- log-normal form (Miller & Scalo 1979):

$$\log_{10} \xi(\log_{10} m) = A - \frac{1}{2(\log_{10} \sigma)^2} \left[\log_{10} \left(\frac{m}{m_0} \right) \right]^2.$$

with $m_0 = 0.23$, $\sigma = 0.42$, $A = 0.1$.

- combined log-normal & power-law (Chabrier 2003):

$$m \leq 1.0 M_{\odot}, \xi(\log m) = A \exp [-(\log m - \log m_c)^2/2\sigma^2]$$

$$m > 1.0 M_{\odot}, \xi(\log m) = Am^{-x}$$

A	$0.158^{+0.051}_{-0.046}$	A	4.43×10^{-2}
m_c	$0.079^{-0.016}_{+0.021}$	x	1.3 ± 0.3
σ	$0.69^{-0.01}_{+0.05}$		

IMF: observations 5

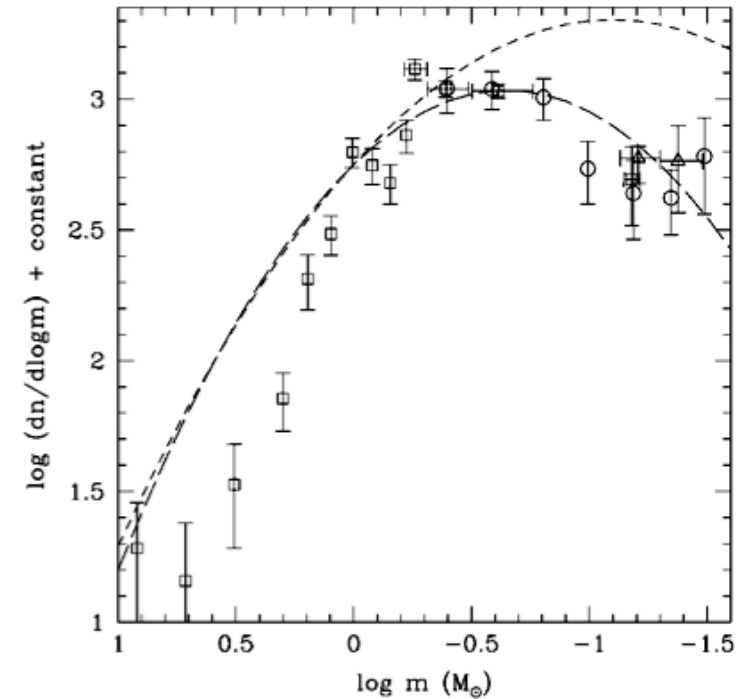
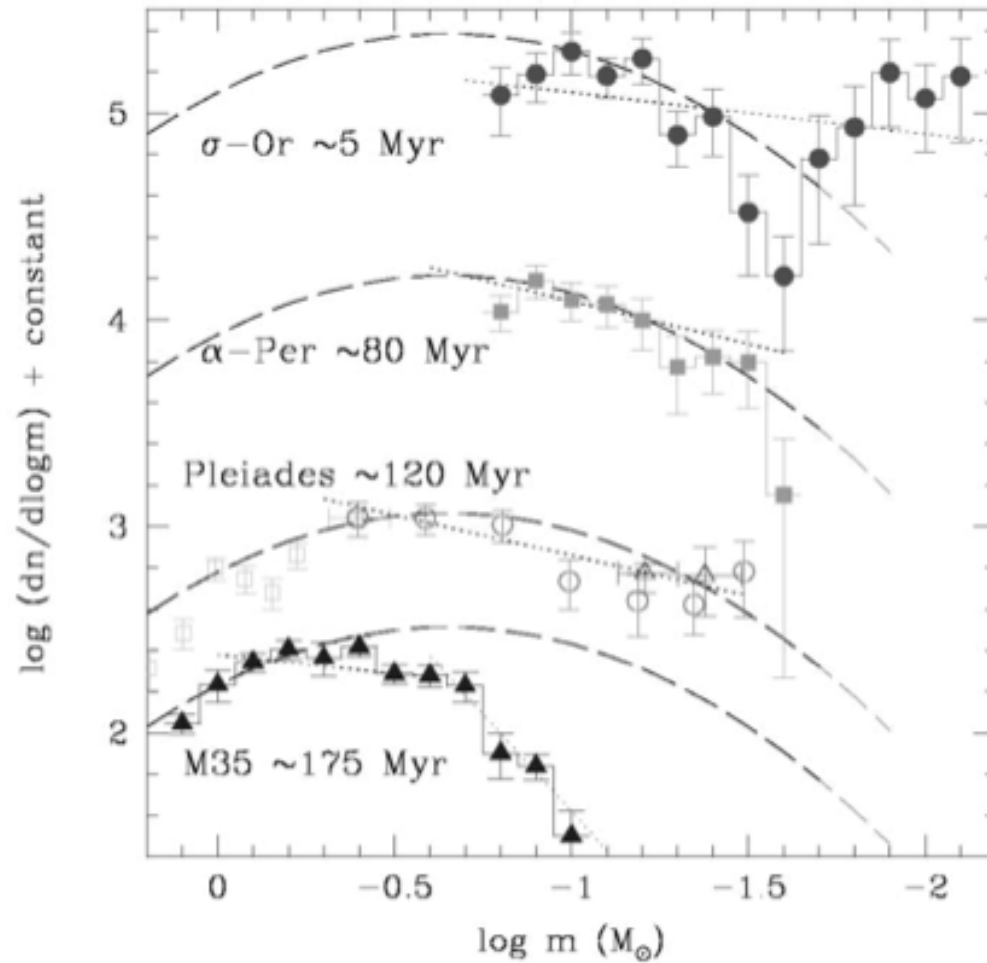


FIG. 4.—Pleiades mass function calculated with the BCAH98 and Chabrier et al. (2000a) MMRs from various observations. *Squares*: Hambly et al. (1999); *triangles*: Dobbie et al. (2002b); *circles*: Moraux et al. (2003). The short-dashed and long-dashed lines display the single (eq. [17]) and system (eq. [18]) field MFs, respectively, arbitrarily normalized to the present data.

system vs. single-star IMF

comparison at low-mass end

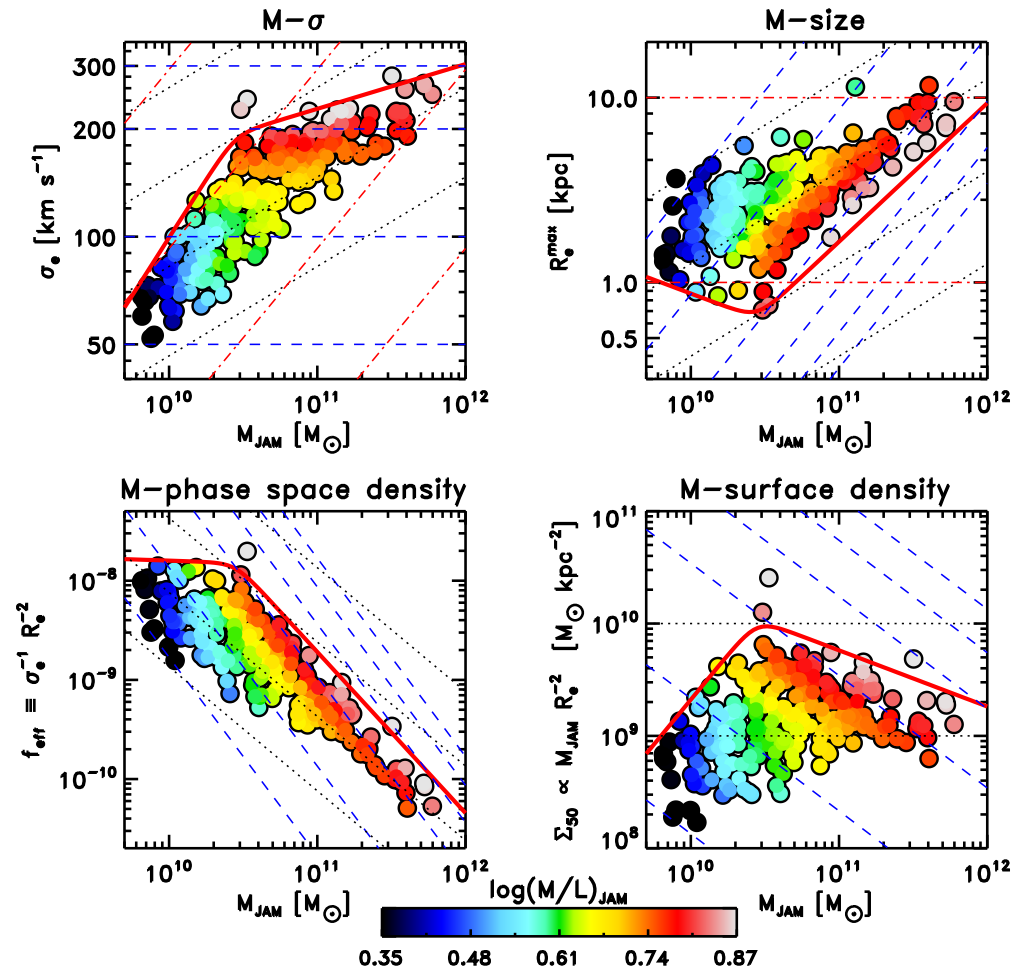
(Chabrier 2003)

IMF: observations 6

BUT: maybe variations with galaxy type (bottom heavy in the centers of large ellipticals)

from JAM (Jeans anisotropic multi Gaussian expansion) modeling

inferred excess of low-mass stars compared to Kroupa IMF



(Cappellari et al. 2012, Nature, 484, 485, Cappellari et al. 2012ab, MNRAS, submitted, also van Dokkum & Conroy 2010, Nature, 468, 940, Wegner et al. 2012, AJ, 144, 78, and others)

IMF: theoretical approach

- distribution of stellar masses depends on
 - turbulent initial conditions
 - > mass spectrum of prestellar cloud cores
 - collapse and interaction of prestellar cores
 - > competitive accretion and N -body effects
 - thermodynamic properties of gas
 - > balance between heating and cooling
 - > EOS (determines which cores go into collapse)
 - (proto) stellar feedback terminates star formation
 - ionizing radiation, bipolar outflows, winds, SN

IMF: theoretical approach

- distribution of stellar masses depends on

- *turbulent initial conditions*

- > *mass spectrum of prestellar cloud cores ???*

- collapse and interaction of prestellar cores

- > competitive accretion and N -body effects

- thermodynamic properties of gas

- > balance between heating and cooling

- > EOS (determines which cores go into collapse)

- (proto) stellar feedback terminates star formation

- ionizing radiation, bipolar outflows, winds, SN

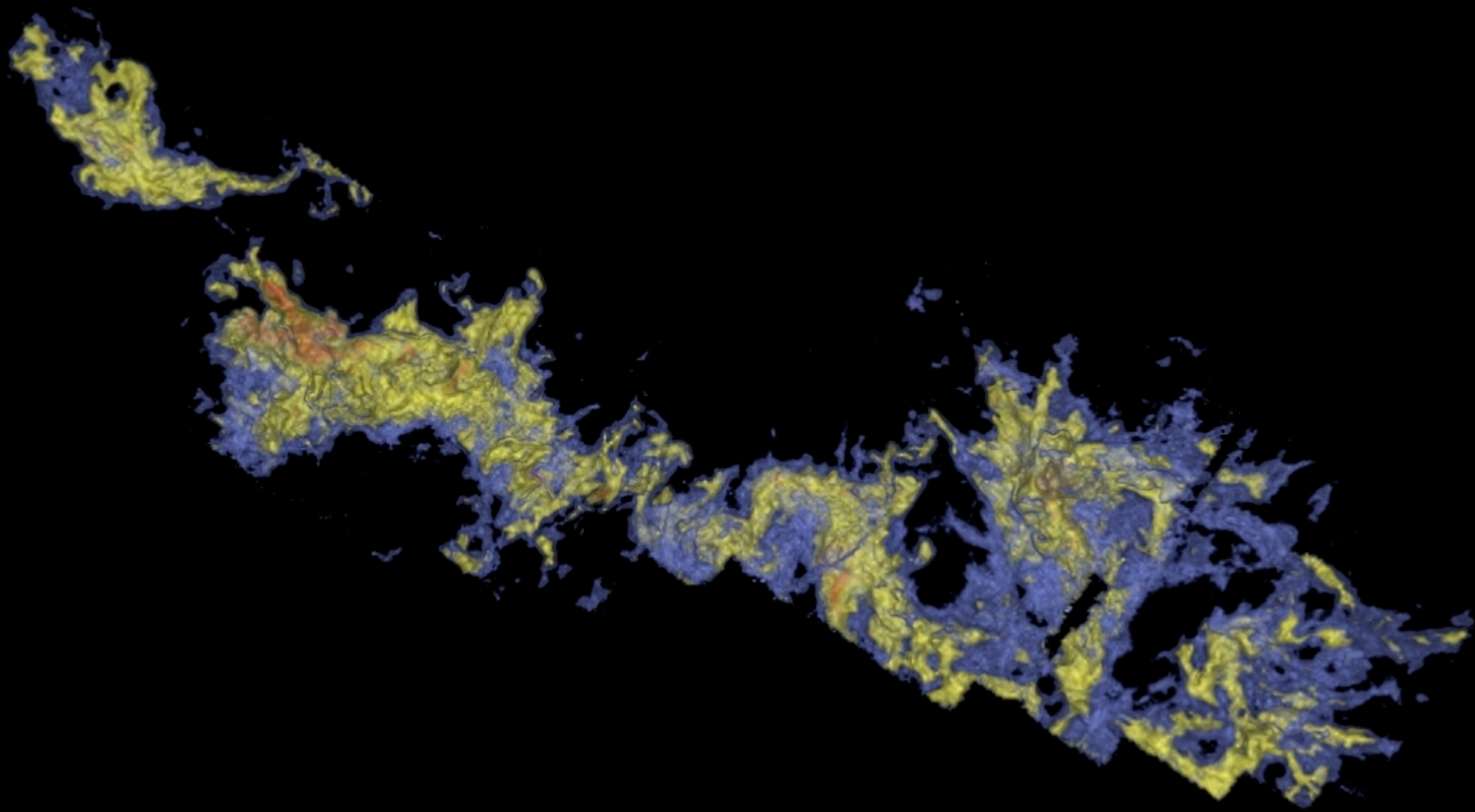
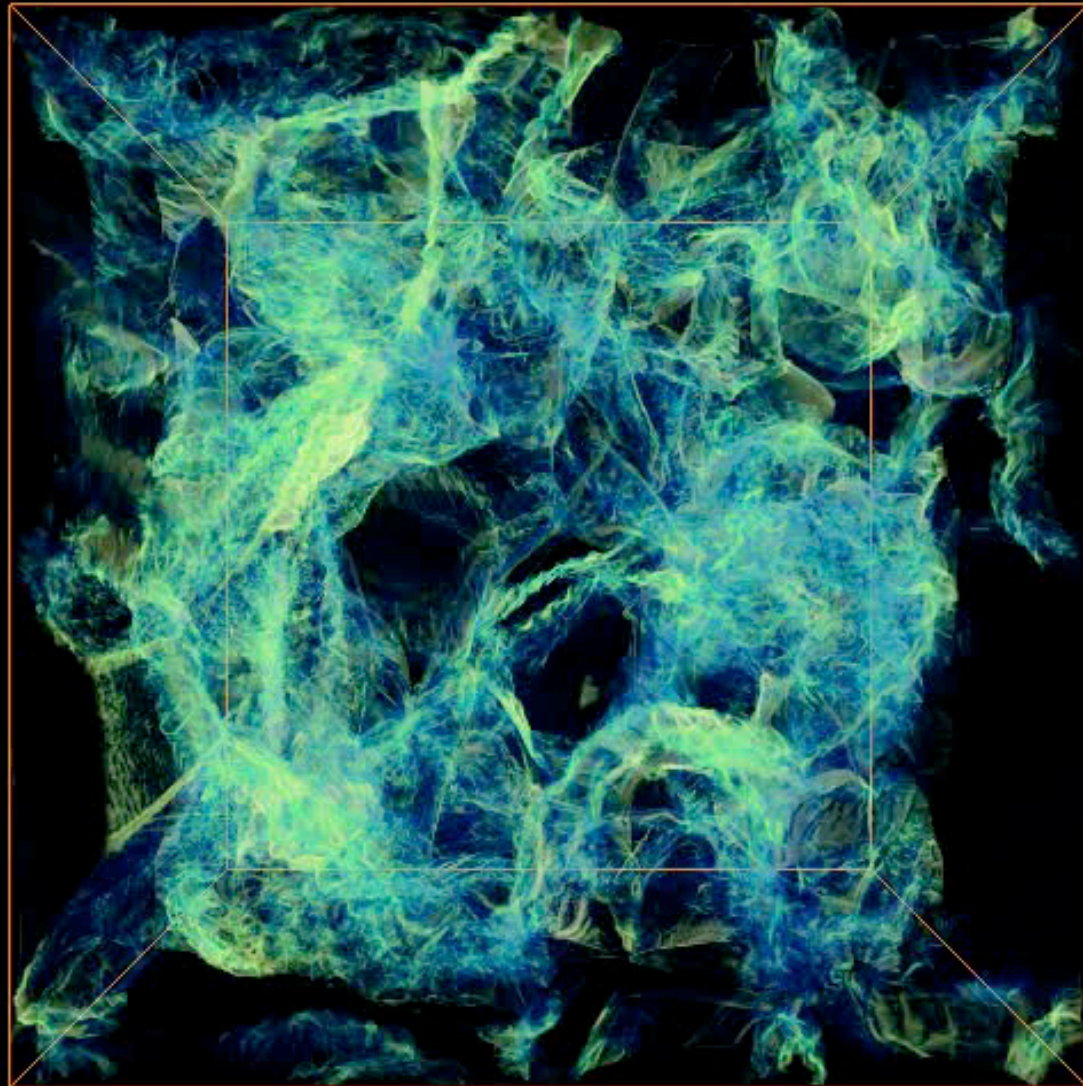
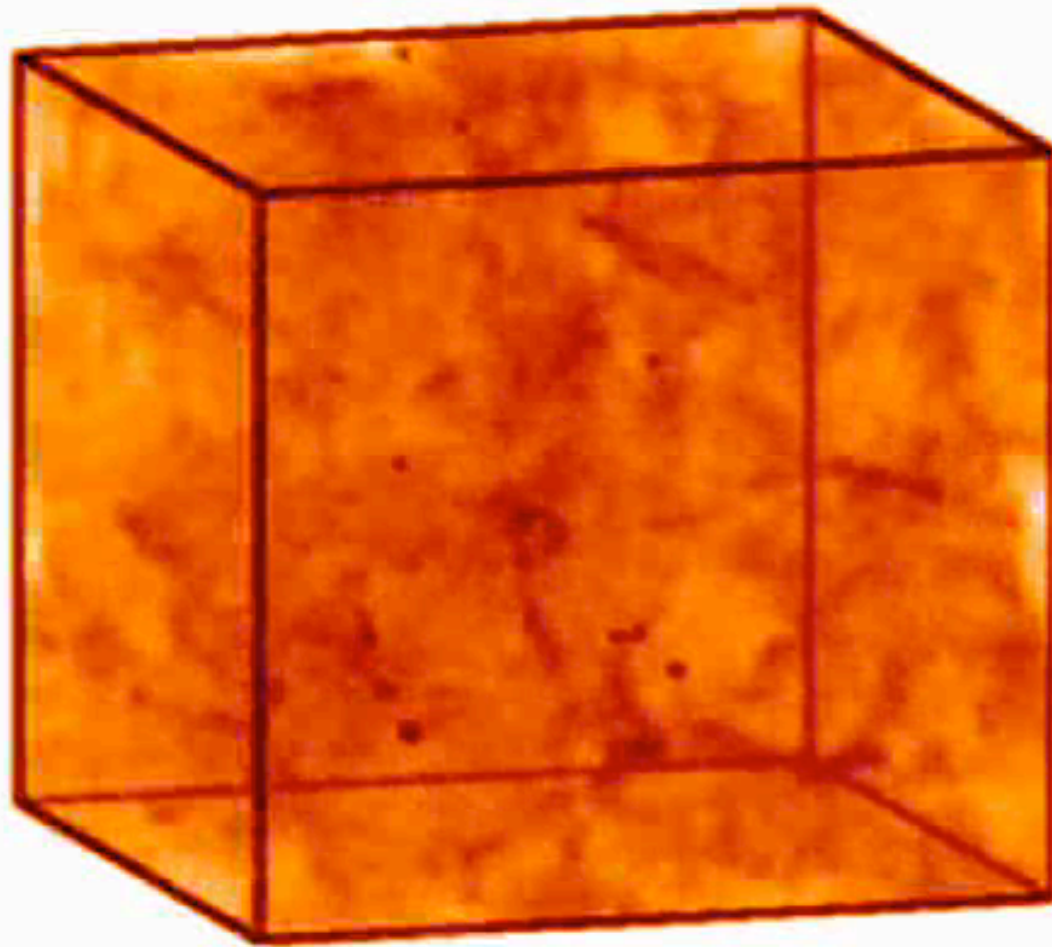


image from Alyssa Goodman: COMPLETE survey

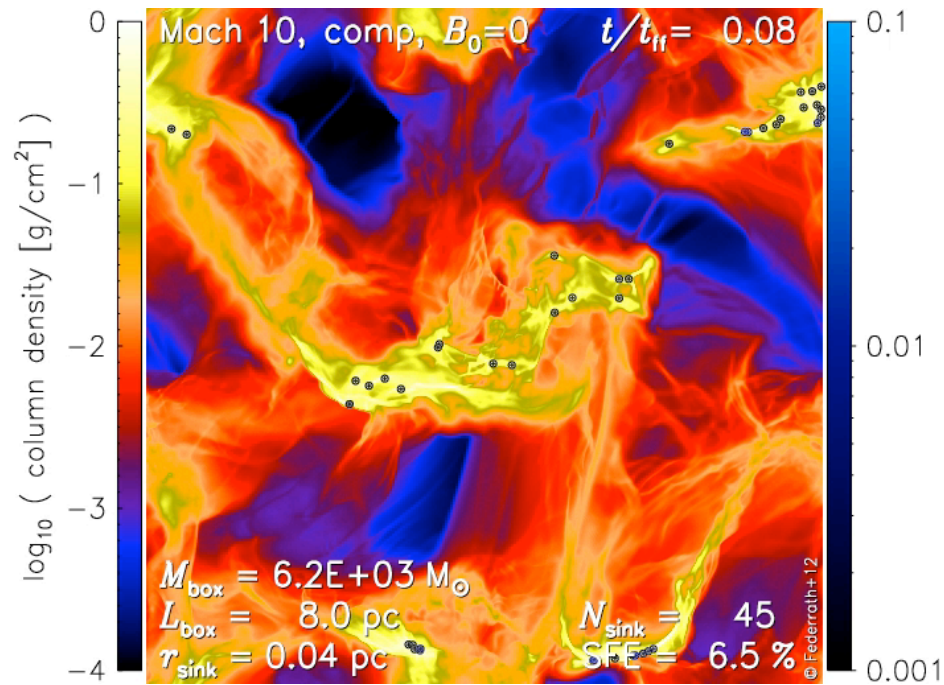


Schmidt et al. (2009, A&A, 494, 127)



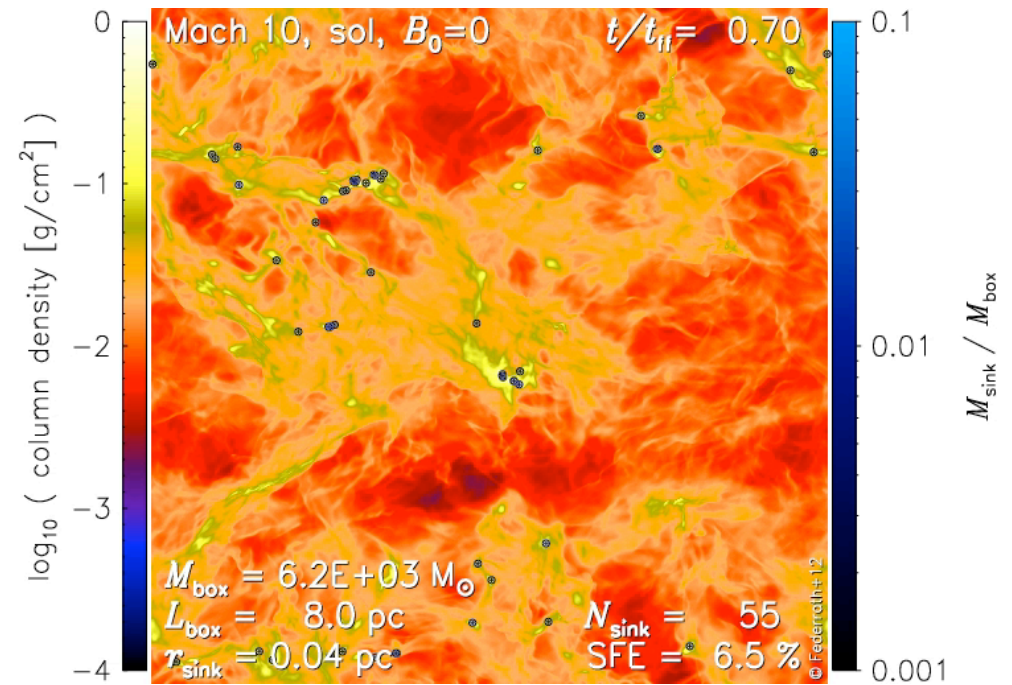
$$t = 4.53$$

compressive driving



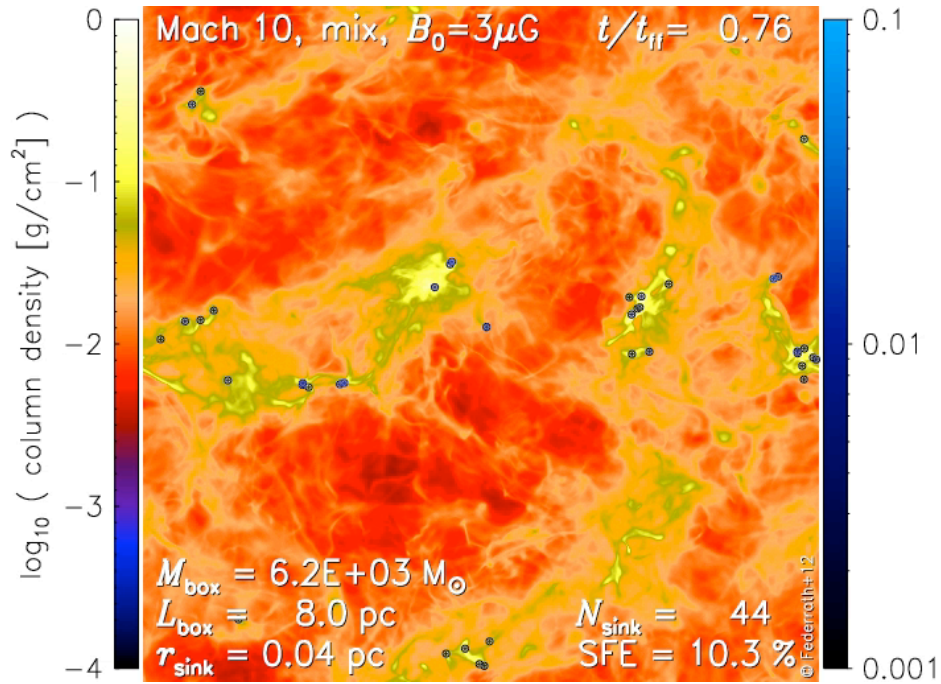
- evolves faster
(collapse sets in quickly)
- forms more 'sink' particles
- 'clustered' star formation

solenoidal driving

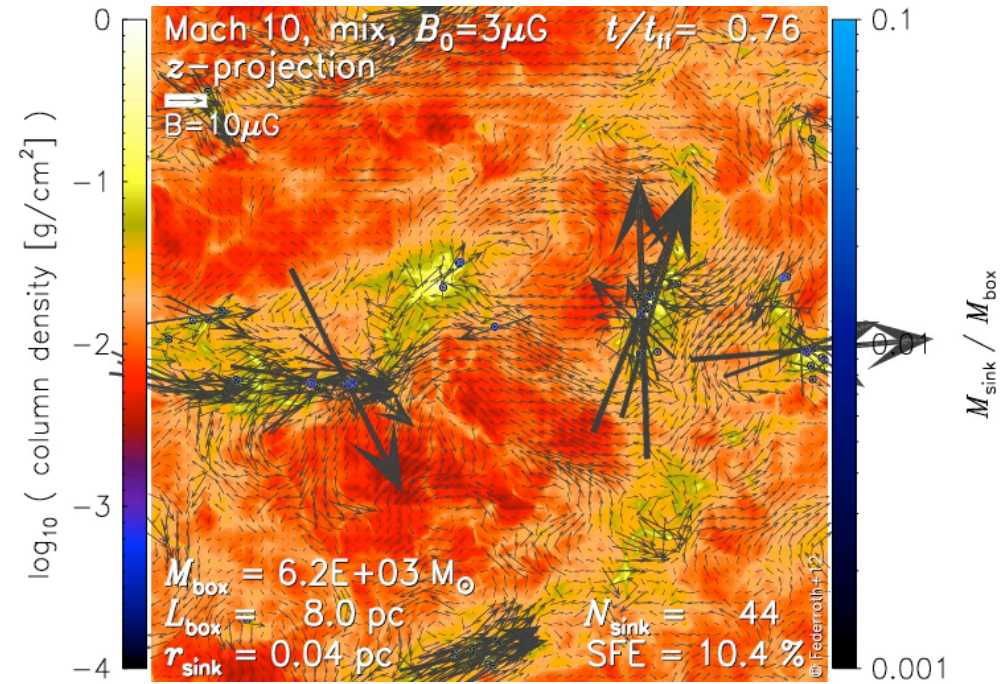


- evolves more slowly
(collapse needs time)
- forms fewer 'sink' particles
- 'distributed' star formation

with B field (no lines shown)



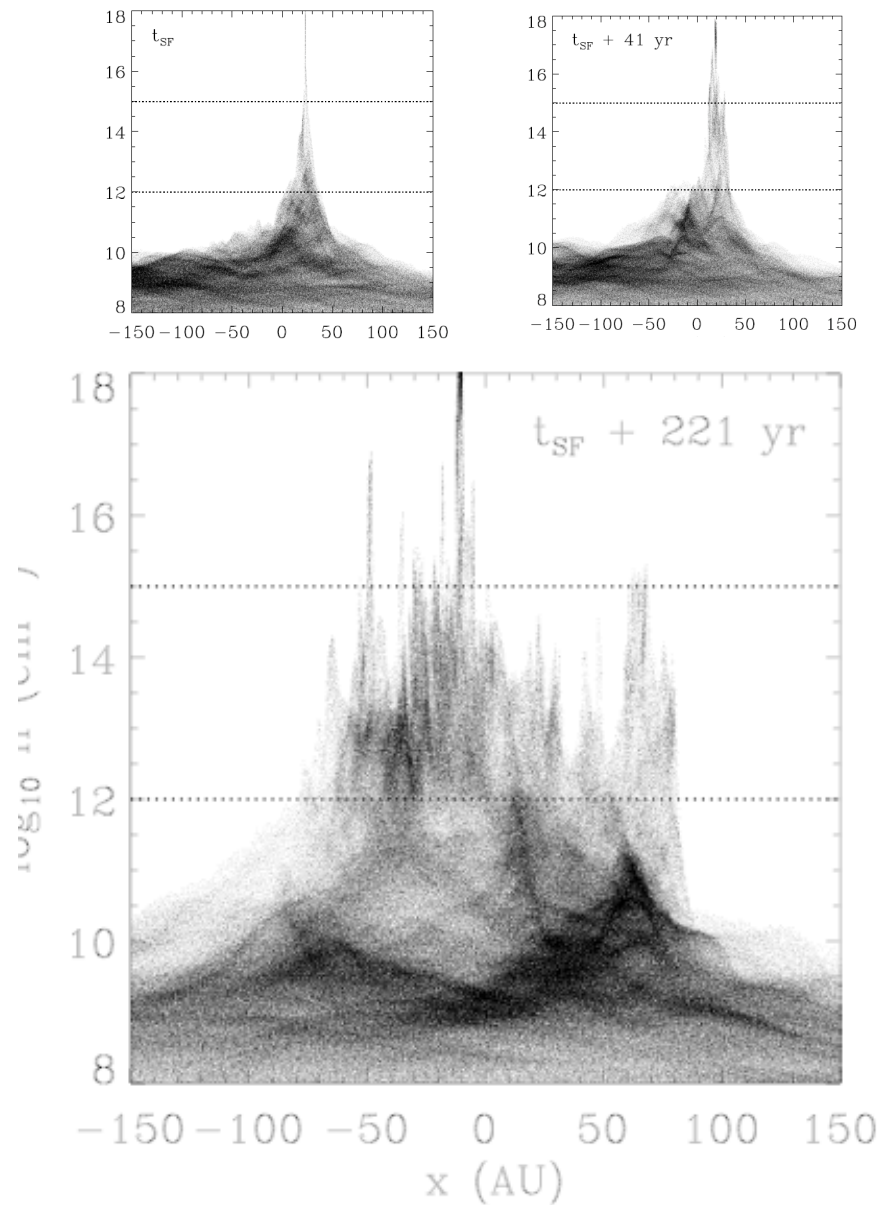
with B field (with field lines)



numerical intermezzo I

Sink Particles

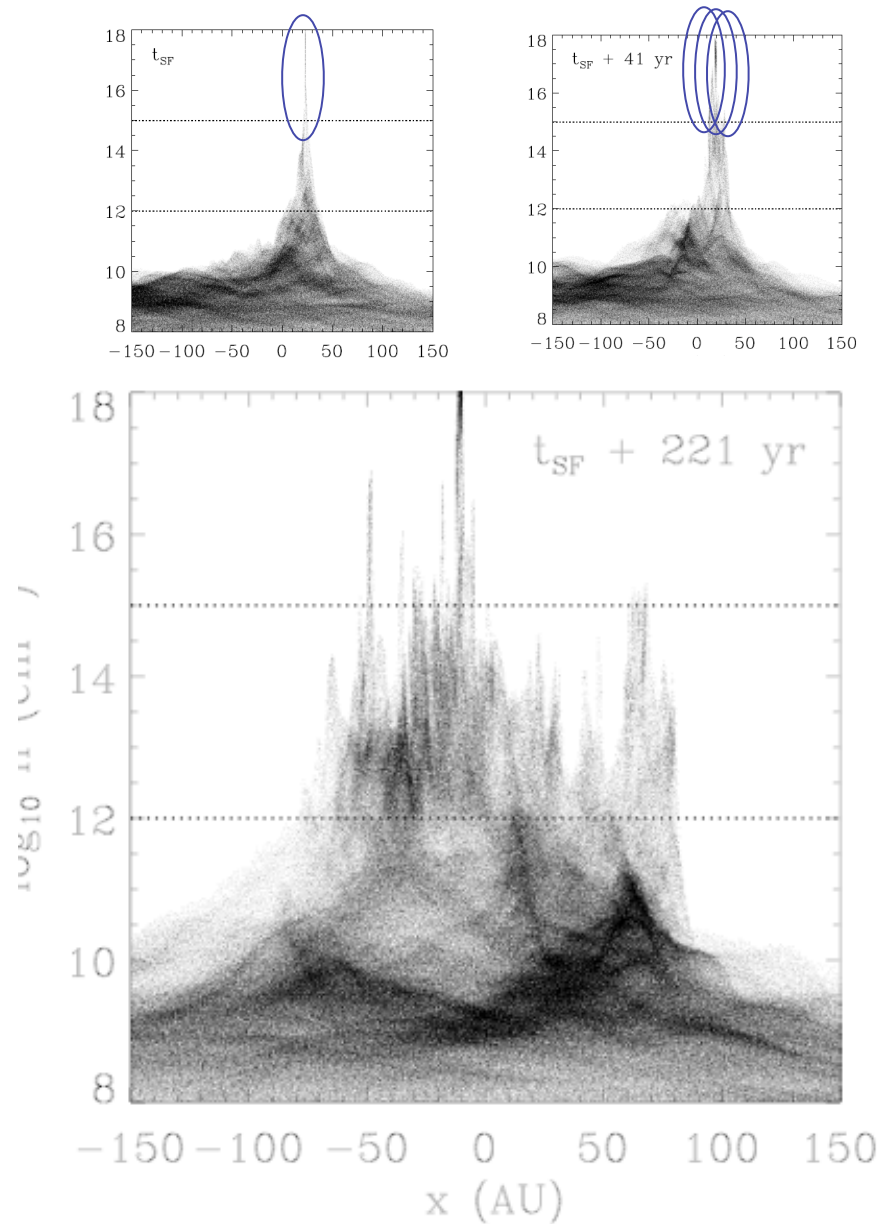
numerical intermezzo I



- as collapse sets in the densities grow exponentially on smaller and smaller scales
- Courant Friedrichs Lewy criterion \rightarrow timesteps get smaller \rightarrow code grains to a halt

(image from Clark et al. 2007)

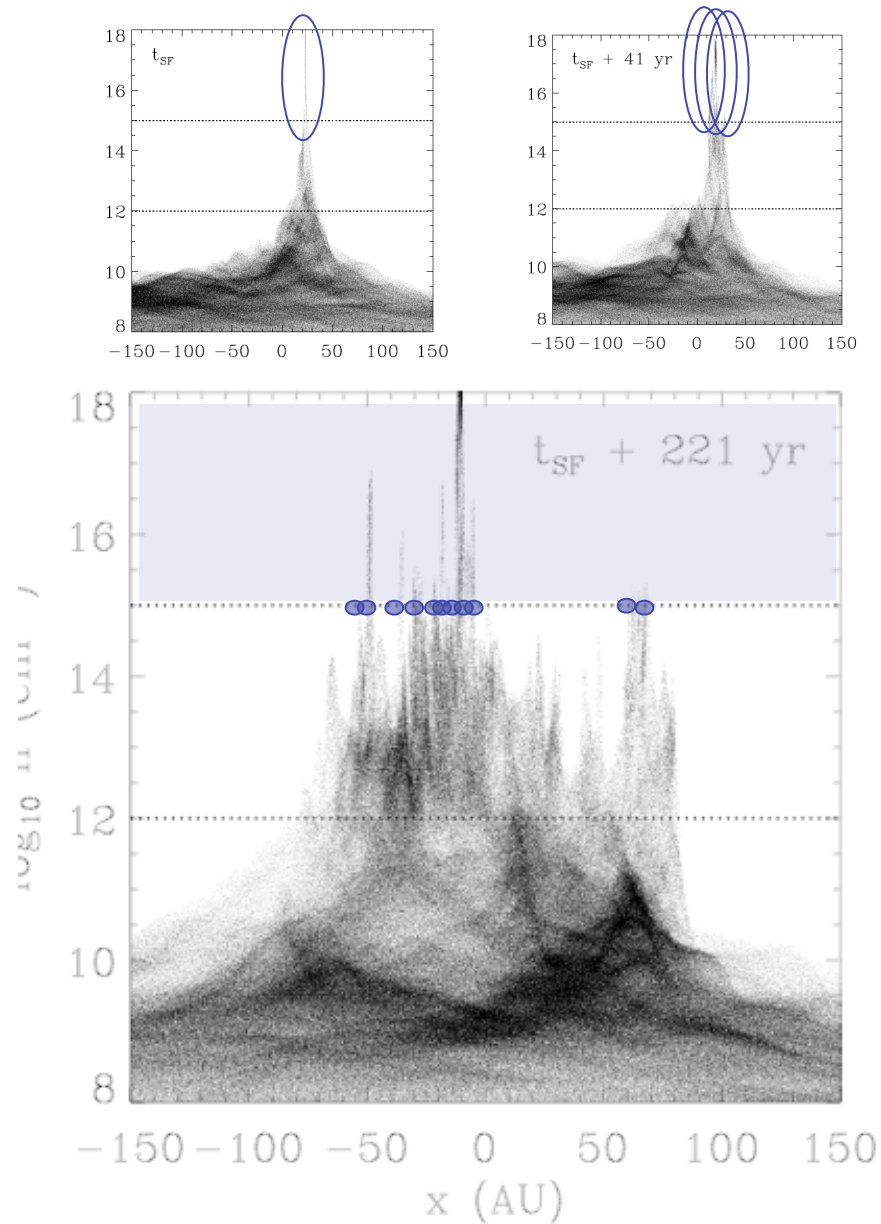
numerical intermezzo 2



- as collapse sets in the densities grow exponentially on smaller and smaller scales
- Courant Friedrichs Lewy criterion \rightarrow timesteps get smaller \rightarrow code grinds to a halt
- solution: *introduce sink particles that replace collapsing protostellar cores*

(image from Clark et al. 2007)

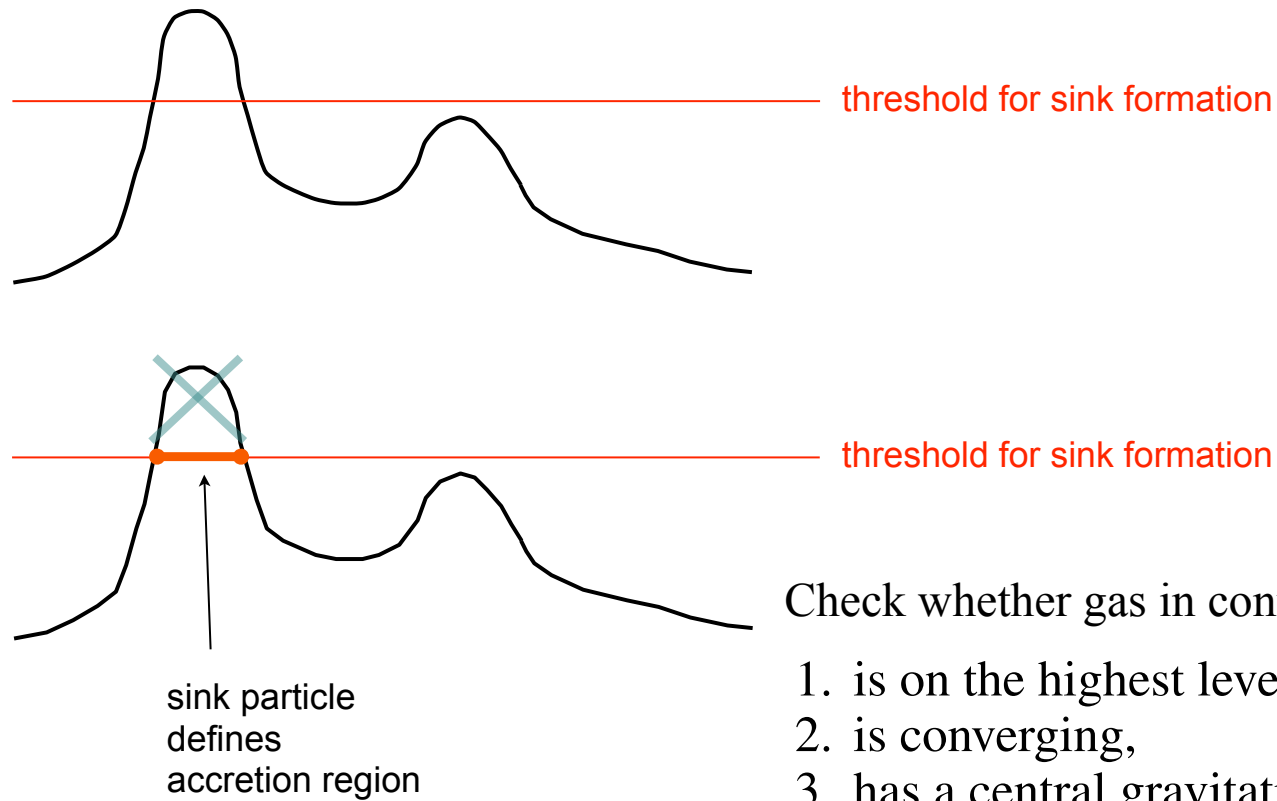
numerical intermezzo I



- as collapse sets in the densities grow exponentially on smaller and smaller scales
- Courant Friedrichs Lewy criterion \rightarrow timesteps get smaller \rightarrow code grinds to a halt
- solution: *introduce sink particles that replace collapsing protostellar cores*
- but: *how to place them*

(image from Clark et al. 2007)

numerical intermezzo I

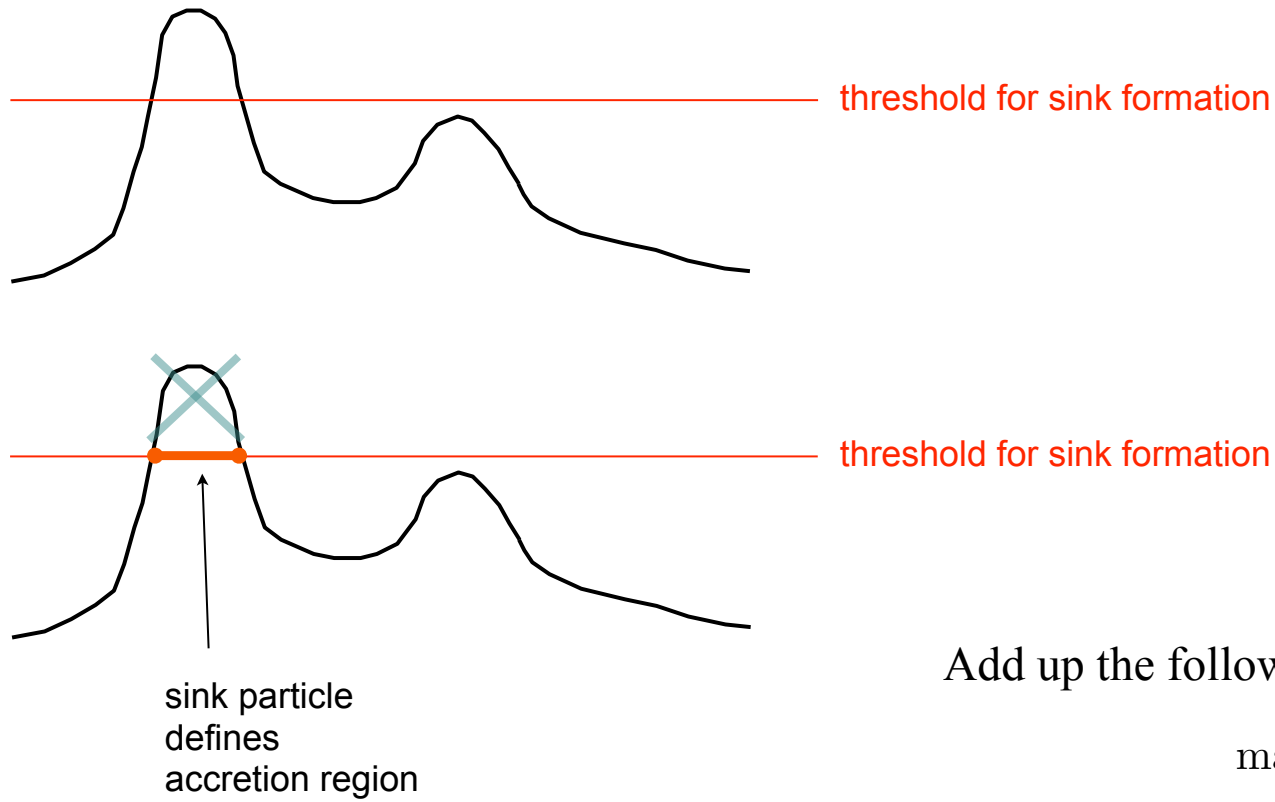


Check whether gas in control volume is

1. is on the highest level of refinement,
2. is converging,
3. has a central gravitational potential minimum,
4. is Jeans-unstable,
5. is bound, and
6. is not within r_{acc} of an existing sink particle.

If yes, then form new sink.

numerical intermezzo I



Add up the following quantities:

$$\text{mass } M_A = \sum_i m_i$$

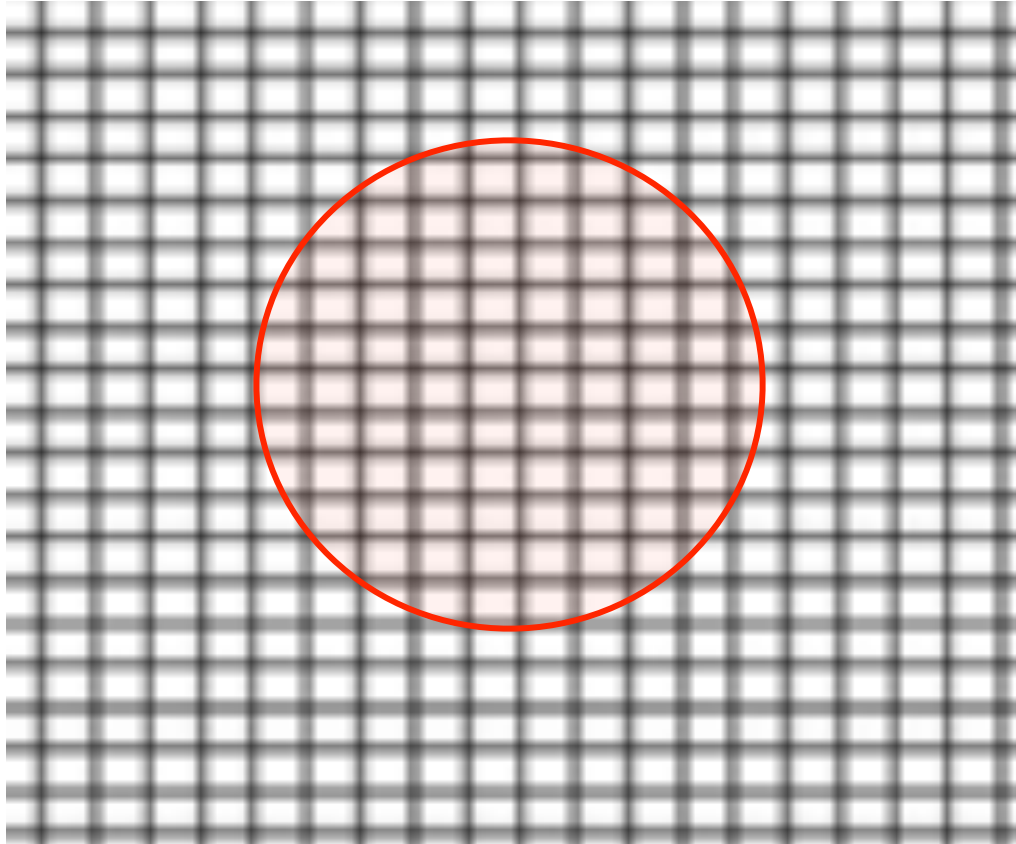
$$\text{center of mass } M_A \mathbf{R}_A = \sum_i m_i \mathbf{r}_i$$

$$\text{momentum } \mathbf{P}_A = \sum_i m_i \mathbf{v}_i$$

$$\text{angular momentum } \mathbf{L}_A = \sum_i \mathbf{r}_i \times m_i \mathbf{v}_i$$

Mass growth of sink particles with accretion:

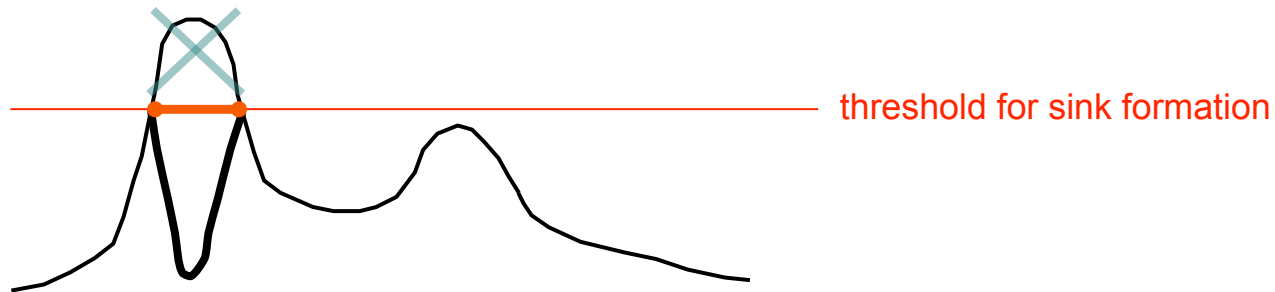
- particle based schemes (SPH, Arepo): remove particles or cells within the accretion volume
- Eulerian grid codes: remove *access* gas above the threshold within the accretion volume (but keep the cells)



Resolution requirements

- 4 cells across (Truelove 1997): pure hydro
- 8 cells across (Heitsch et al. 2001): MHD
- 32 cells across (Federrath et al. 2012): turbulence

numerical intermezzo I



Resolution requirements

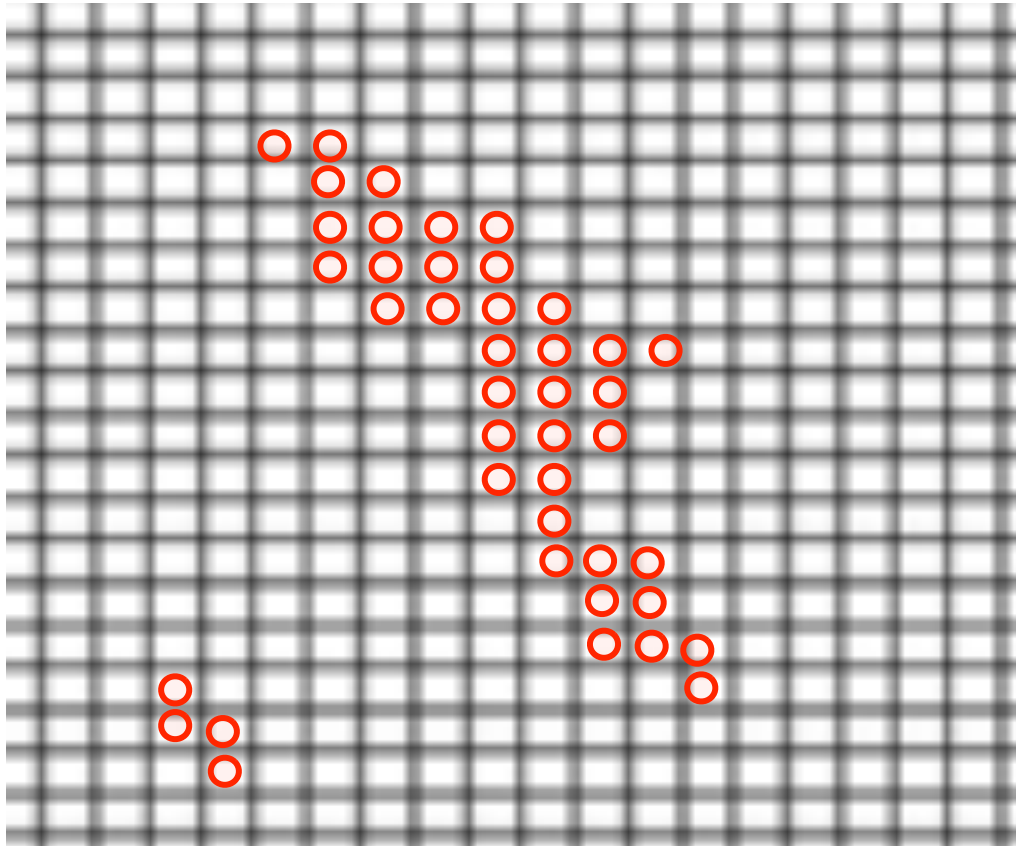
- 4 cells across (Truelove 1997): pure hydro
- 8 cells across (Heitsch et al. 2001): MHD
- 32 cells across (Federrath et al. 2012): turbulence

Mass growth of sink particles with accretion:

- particle based schemes (SPH, Arepo): remove particles or cells within the accretion volume
- Eulerian grid codes: remove *access* gas above the threshold within the accretion volume (but keep the cells)

Mass growth by sink particle merging:

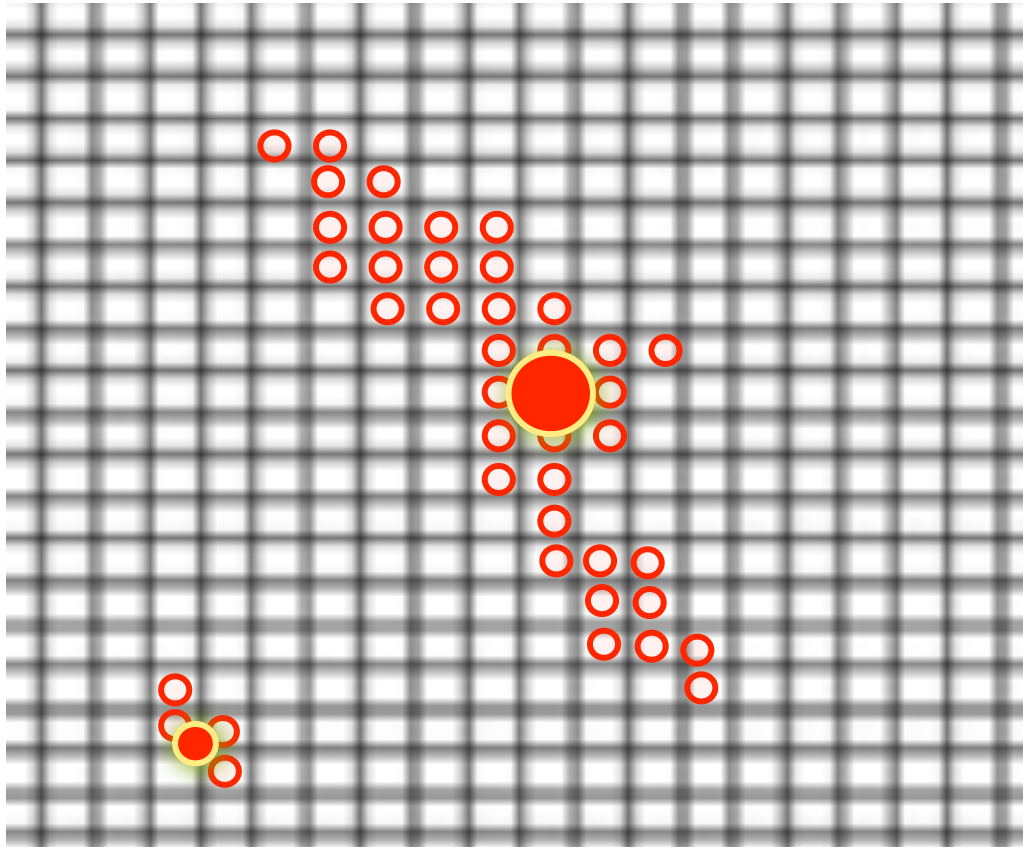
- span many new sink particles at each timestep if density is above threshold
- then merge all sinks in connected regions together



Resolution requirements

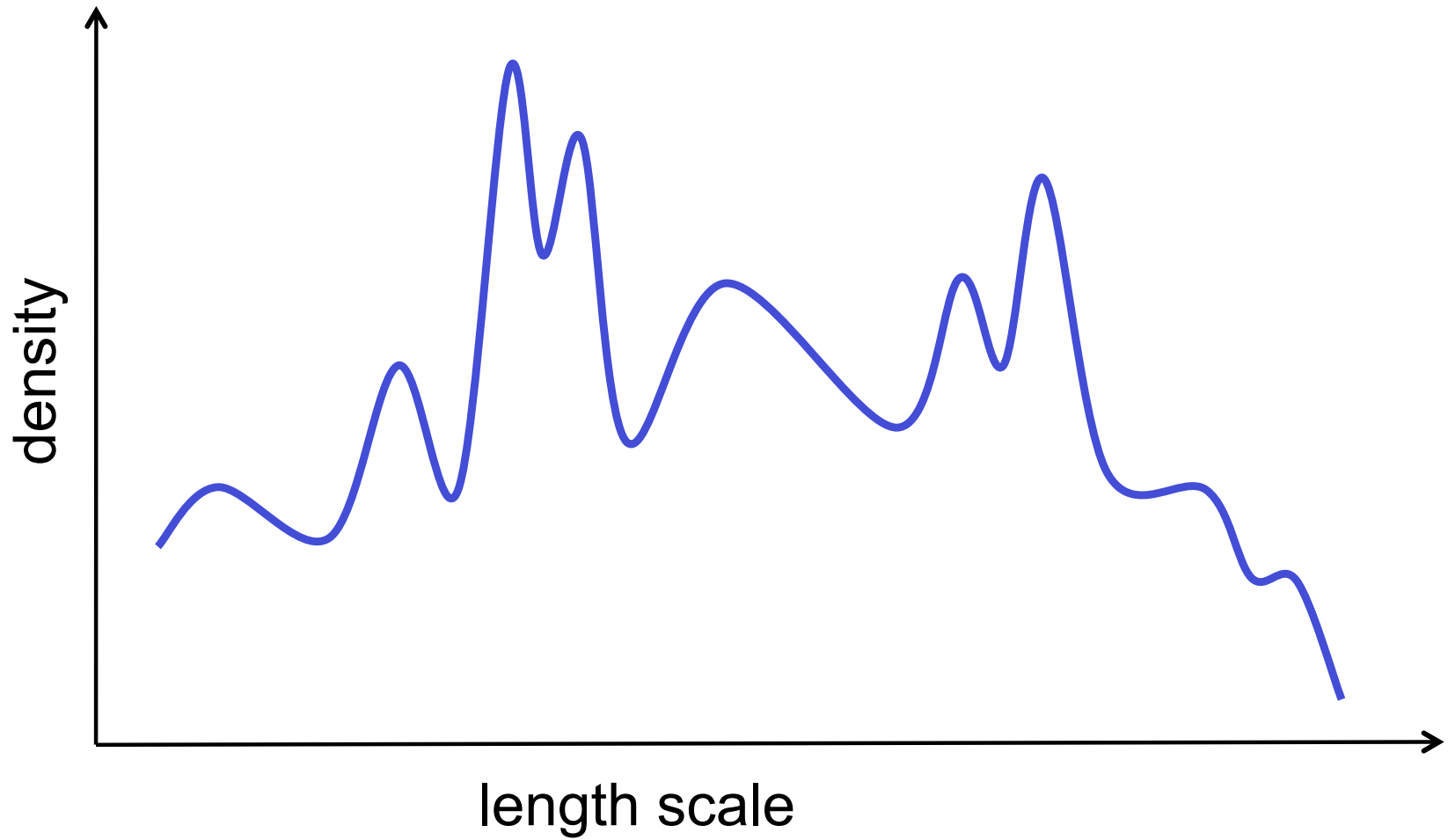
- 4 cells across (Truelove 1997): pure hydro
- 8 cells across (Heitsch et al. 2001): MHD
- 32 cells across (Federrath et al. 2012): turbulence

numerical intermezzo I



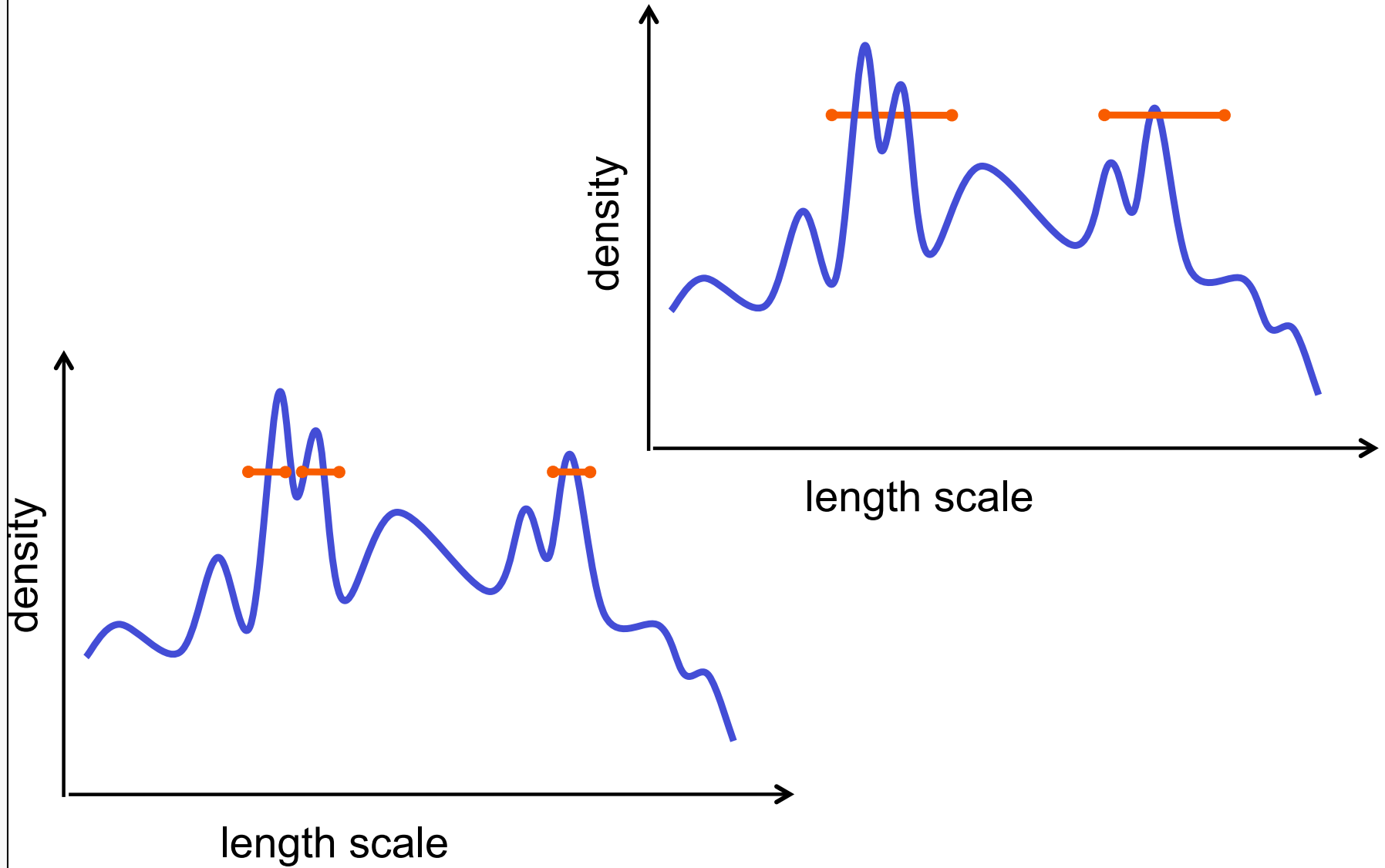
numerical intermezzo I

- sink particle diameter
- sink separation at formation
- sink density threshold



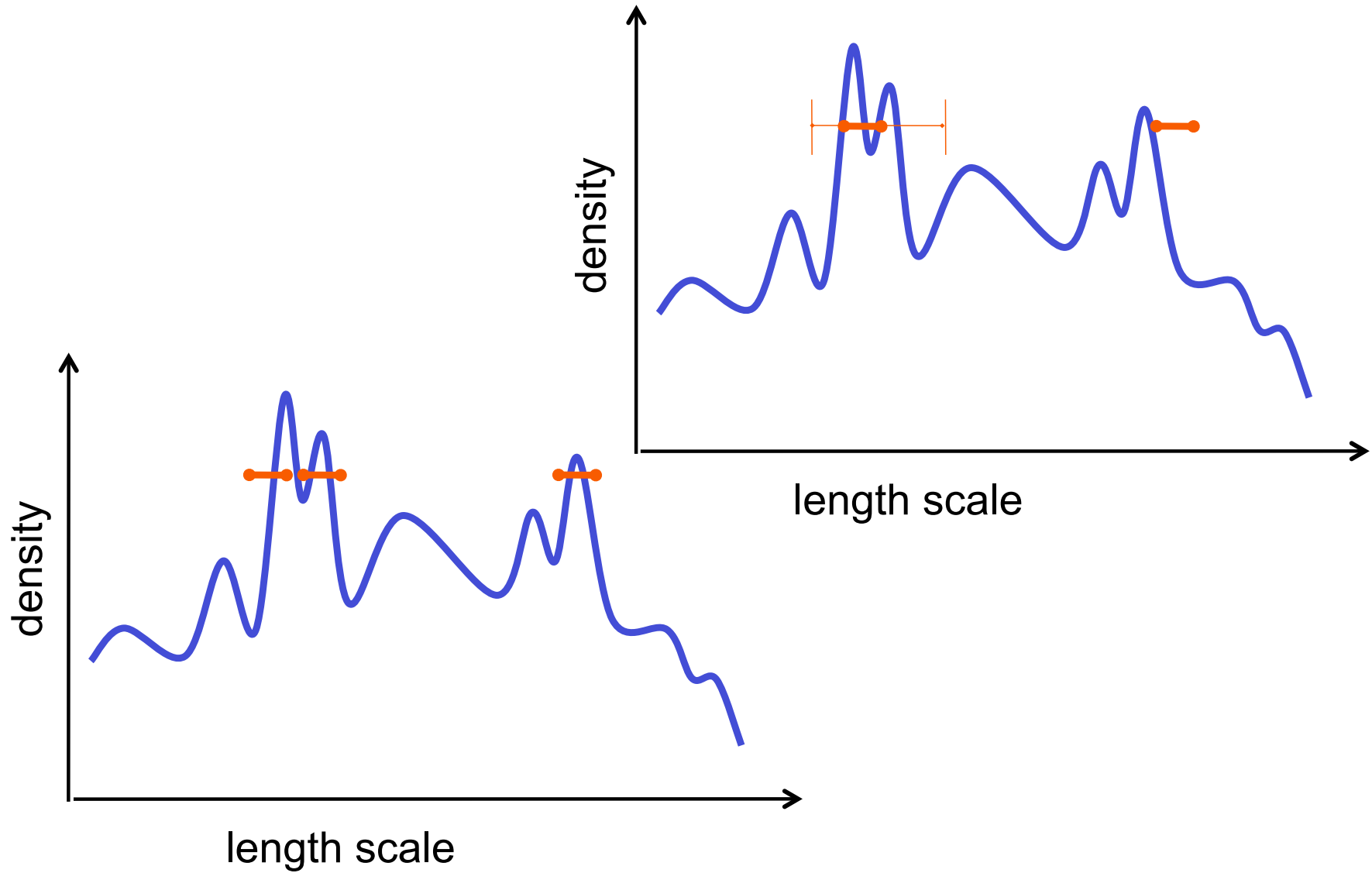
numerical intermezzo I

- sink particle diameter
- sink separation at formation
- sink density threshold



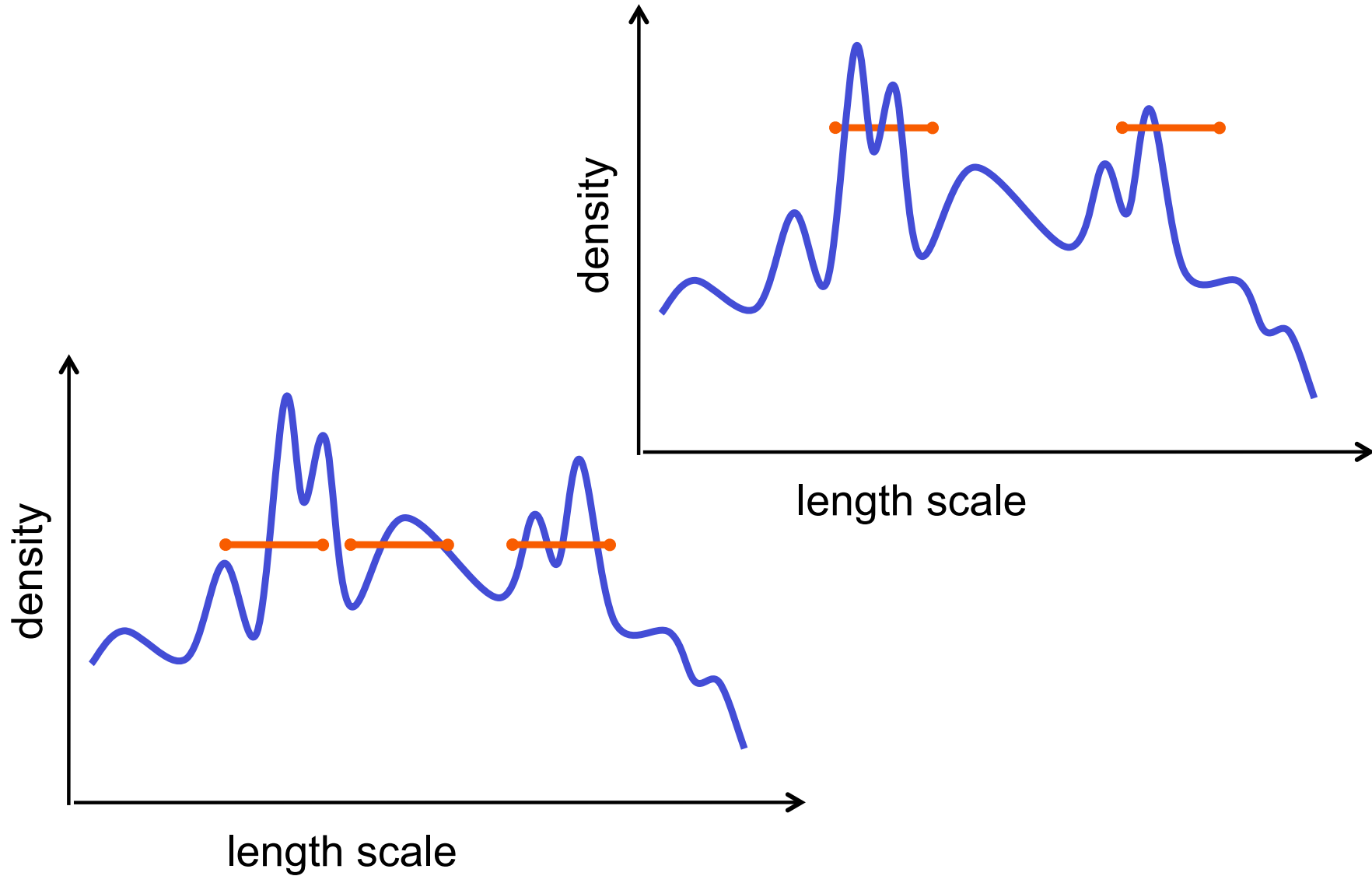
numerical intermezzo I

- sink particle diameter
- sink separation at formation
- sink density threshold



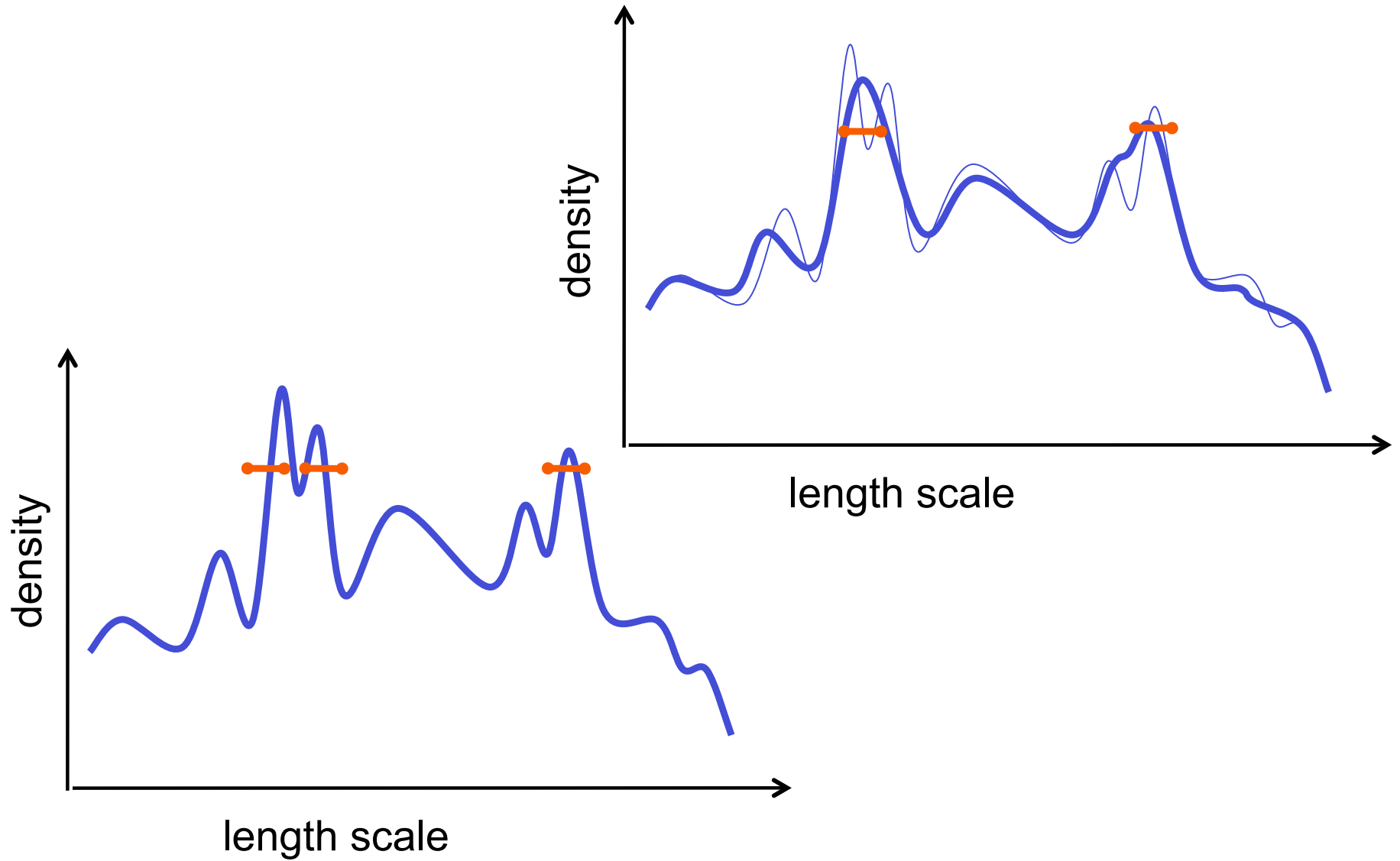
numerical intermezzo I

- sink particle diameter
- sink separation at formation
- sink density threshold



numerical intermezzo I

high-resolution runs vs. low-resolution calculations



Questions to address:

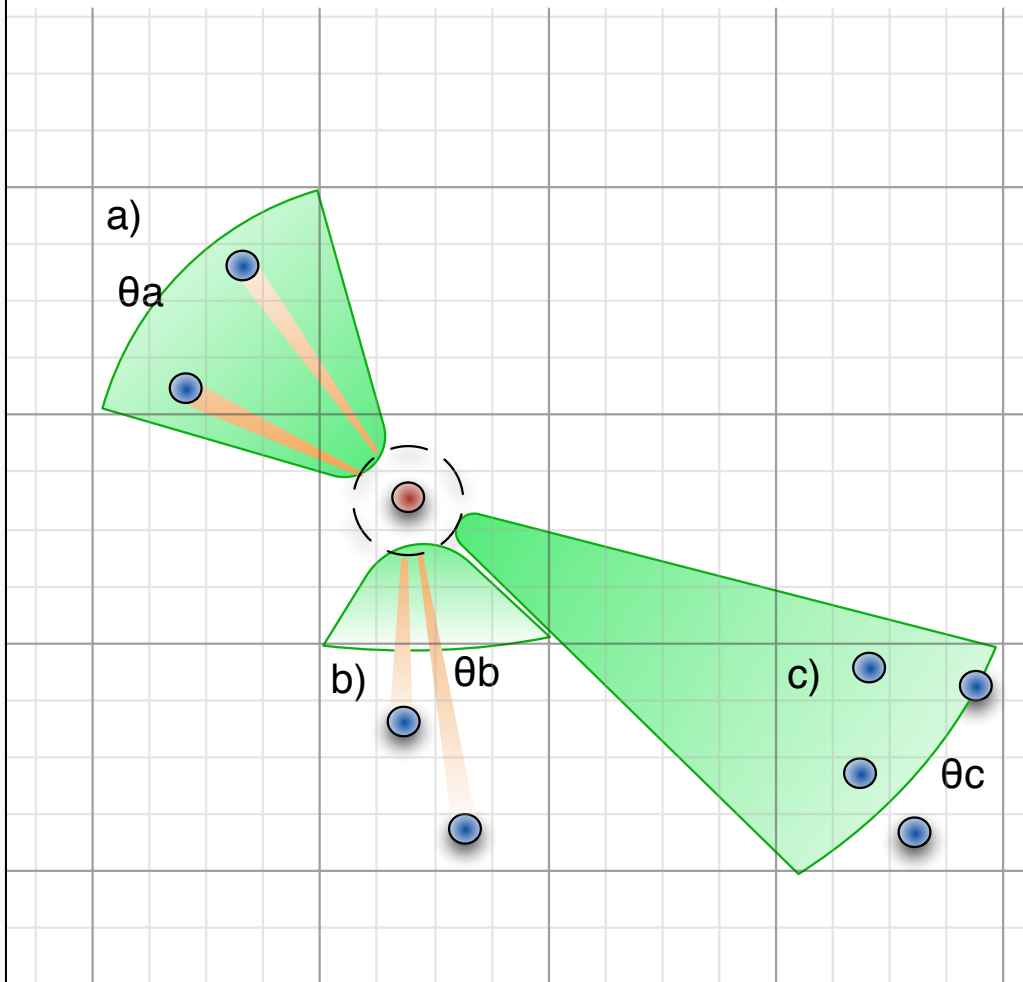
- how to decide on size?
- which criteria for sink formation?
- which criteria for accretion?
- how to do the sub-cycling?

- SUB-GRID scale model!!!
 - internal degrees of freedom (tides)
 - stellar evolution (stellar radii, luminosity)
 - binarity
 - radiation
 - outflows
 - stellar populations (star cluster sinks)
 - magnetic fields
 - disk evolution
 - and *MANY* more

TreeCol

TreeCol

numerical intermezzo 2



IDEA

- (gravitational) tree-walk
- calculated column densities
- accumulate on HEALPIX sphere

TreeCol

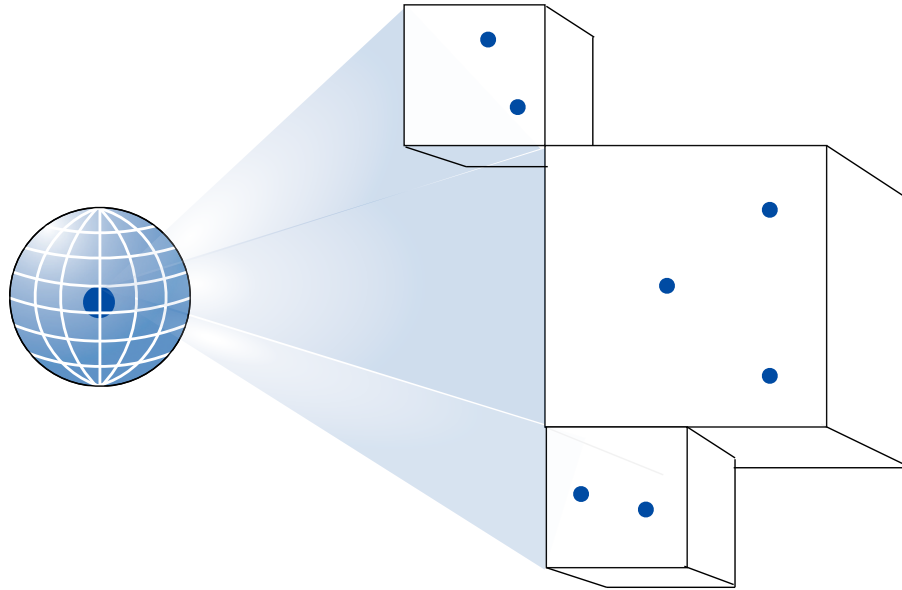


Figure 2. Schematic diagram illustrating the *TreeCol* concept. During the tree walk to obtain the gravitational forces, the projected column densities of the tree nodes (the boxes shown on the right) are mapped onto a spherical grid surrounding the particle for which the forces are being computed (the “target” particle, shown on the left). The tree already stores all of the information necessary to compute the column density of each node, the position of the node in the plane of the sky of the target particle, and the angular extent of the node. This information is used to compute the column density map at the same time that the tree is being walked to calculate the gravitational forces. Provided that the tree is already employed for the gravity calculation, the information required to create the 4π steradian map of the column densities can be obtained for minimal computational cost.

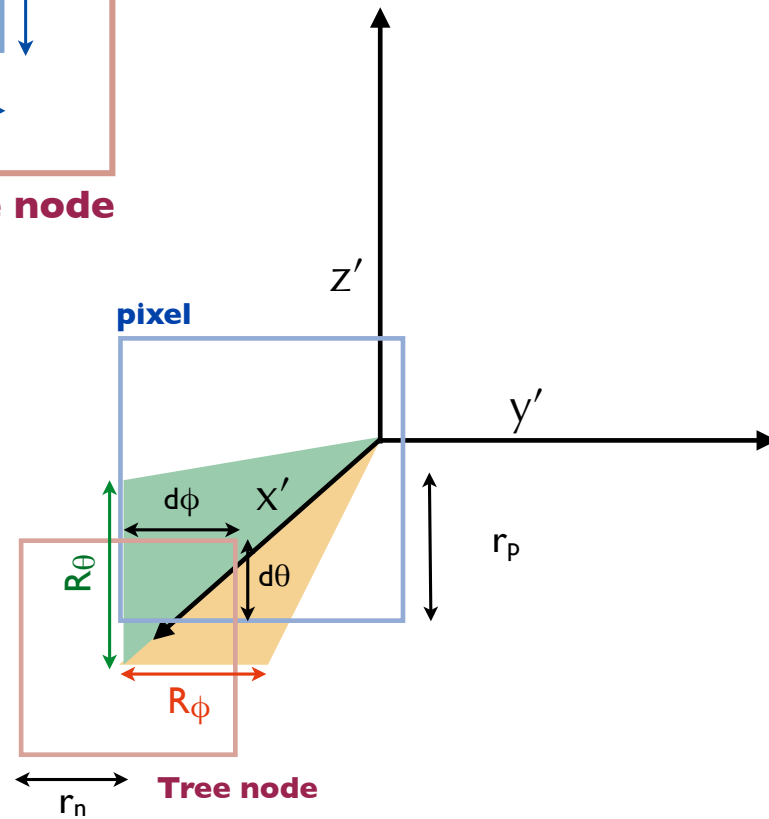
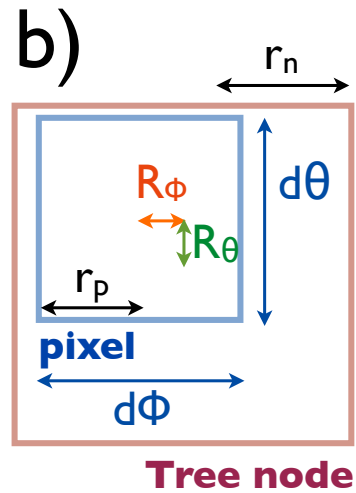
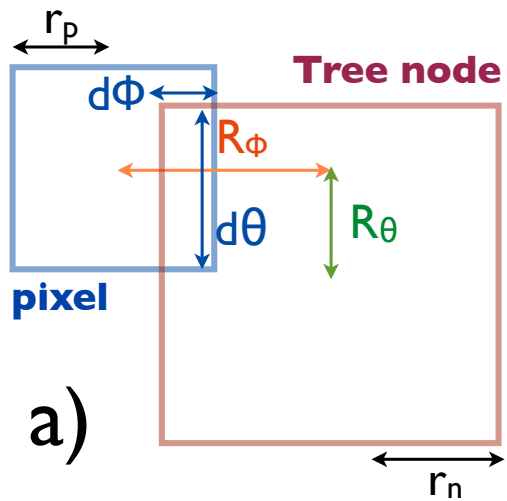
IDEA

- (gravitational) tree-walk
- calculated column densities
- accumulate on HEALPIX sphere

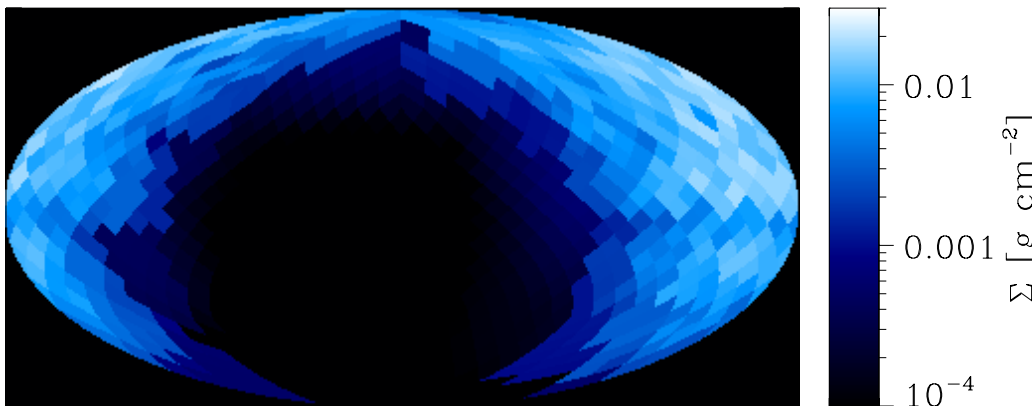
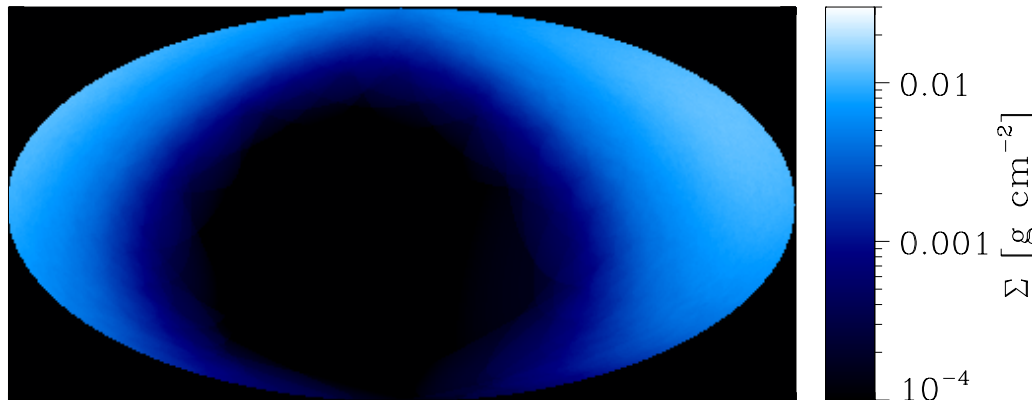
PERFORMANCE

- adds little computational overhead to gravitational tree-walk
- *but:* can add considerable memory overhead

TreeCol



TreeCol



IDEA

- (gravitational) tree-walk
- calculated column densities
- accumulate on HEALPIX sphere

PERFORMANCE

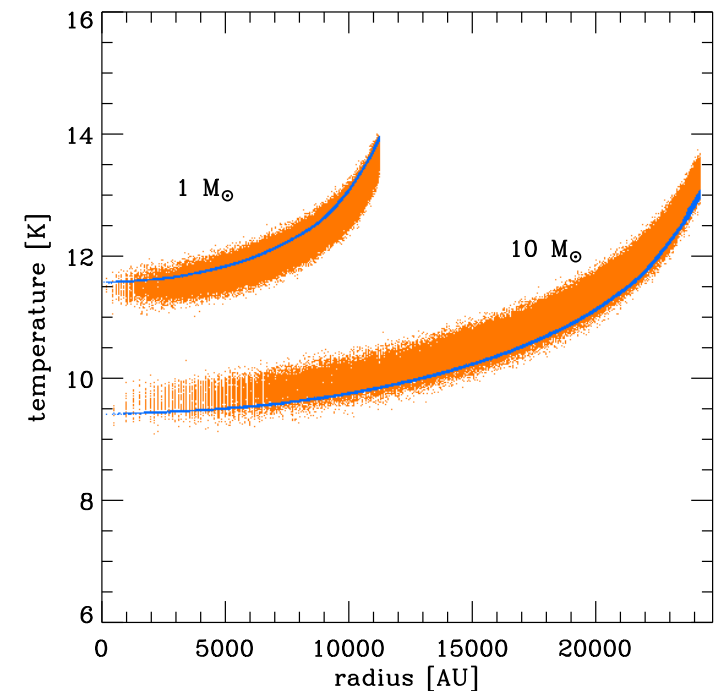
- adds little computational overhead to gravitational tree-walk
- but: can add considerable memory overhead
- approximation usually good to a few percent!

TreeCol

Model	N_{pix}	θ_{tot}	$\bar{\Sigma}$ [g cm^{-2}]	Error [%]
Spherical cloud			3.060×10^{-3}	
	48	0.3	3.234×10^{-3}	5.7
	48	0.5	3.274×10^{-3}	7.0
	192	0.3	3.205×10^{-3}	4.7
	192	0.5	3.239×10^{-3}	5.8
	768	0.3	3.192×10^{-3}	4.3
	768	0.5	3.226×10^{-3}	5.4
Turbulent cloud			1.151×10^{-2}	
	48	0.3	1.126×10^{-2}	2.2
	192	0.3	1.125×10^{-2}	2.3
	768	0.3	1.133×10^{-2}	1.6

PERFORMANCE

- approximation usually good to a few percent!
- example: protostellar core, comparison with RADMC



IMF: theoretical approach

- distribution of stellar masses depends on
 - *turbulent initial conditions*
 - > *mass spectrum of prestellar cloud cores ???*
 - collapse and interaction of prestellar cores
 - > competitive accretion and N -body effects
 - thermodynamic properties of gas
 - > balance between heating and cooling
 - > EOS (determines which cores go into collapse)
 - (proto) stellar feedback terminates star formation
 - ionizing radiation, bipolar outflows, winds, SN



different statistical approaches

- there are different quantitative IMF based on turbulence
 - Padoan & Nordlund (2002, 2007)
 - Hennebelle & Chabrier (2008, 2009)
 - Hopkins (2012)
 - all relate the mass spectrum to statistical characteristics of the turbulent velocity fields

THE ASTROPHYSICAL JOURNAL, 684:395–410, 2008 September 1
© 2008. The American Astronomical Society. All rights reserved. Printed in U.S.A.

ANALYTICAL THEORY FOR THE INITIAL MASS FUNCTION: CO CLUMPS AND PRESTELLAR CORES

PATRICK HENNEBELLE

Laboratoire de Radioastronomie, UMR CNRS 8112, École Normale Supérieure et Observatoire de Paris,
24 rue Lhomond, 75231 Paris Cedex 05, France

AND

GILLES CHABRIER¹

École Normale Supérieure de Lyon, CRAL, UMR CNRS 5574, Université de Lyon, 69364 Lyon Cedex 07, France

Received 2008 February 12; accepted 2008 May 4



different statistical approaches

- there are different quantitative IMF based on turbulence
 - Padoan & Nordlund (2002, 2007)
 - Hennebelle & Chabrier (2008, 2009)
 - Hopkins (2012)
 - all relate the mass spectrum to statistical characteristics of the turbulent velocity fields

THE ASTROPHYSICAL JOURNAL, 684:395–410, 2008 September 1
© 2008. The American Astronomical Society. All rights reserved. Printed in U.S.A.

THE ASTROPHYSICAL JOURNAL, 702:1428–1442, 2009 September 10
© 2009. The American Astronomical Society. All rights reserved. Printed in the U.S.A.

doi:[10.1088/0004-637X/702/2/1428](https://doi.org/10.1088/0004-637X/702/2/1428)

ANALYTICAL THEORY FOR THE INITIAL MASS FUNCTION. II. PROPERTIES OF THE FLOW

PATRICK HENNEBELLE¹ AND GILLES CHABRIER²

¹ Laboratoire de radioastronomie, UMR CNRS 8112, École normale supérieure et Observatoire de Paris, 24 rue Lhomond, 75231 Paris cedex 05, France

² École normale supérieure de Lyon, CRAL, UMR CNRS 5574, Université de Lyon, 69364 Lyon Cedex 07, France

Received 2009 April 1; accepted 2009 July 17; published 2009 August 21



different statistical approaches

- there are different quantitative IMF based on turbulence
 - Padoan & Nordlund (2002, 2007)
 - Hennebelle & Chabrier (2008, 2009)
 - Hopkins (2012)
 - all relate the mass spectrum to statistical characteristics of the turbulent velocity fields

THE ASTROPHYSICAL JOURNAL, 684:395–410, 2008 September 1
© 2008. The American Astronomical Society. All rights reserved. Printed in U.S.A.

THE ASTROPHYSICAL JOURNAL, 702:1428–1442, 2009 September 10
© 2009. The American Astronomical Society. All rights reserved. Printed in the U.S.A.

doi:10.1088/0004-637X/702/2/1428

ANA Monthly Notices of the ROYAL ASTRONOMICAL SOCIETY
Mon. Not. R. Astron. Soc. **423**, 2037–2044 (2012) doi:10.1111/j.1365-2966.2012.20731.x

¹ Laboratoire

The stellar initial mass function, core mass function and the last-crossing distribution

Philip F. Hopkins[★]

Department of Astronomy, University of California Berkeley, Berkeley, CA 94720, USA

OW

05, France

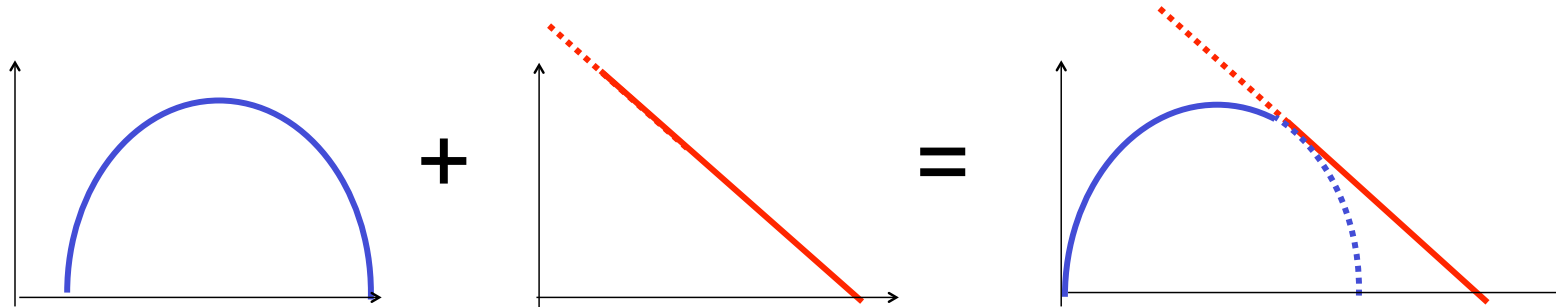


different statistical approaches

- there are different quantitative IMF based on turbulence
 - Padoan & Nordlund (2002, 2007)
 - Hennebelle & Chabrier (2008, 2009)
 - Hopkins (2012)
 - all relate the mass spectrum to statistical characteristics of the turbulent velocity fields
- there are alternative approaches
 - IMF as closest packing problem / *sampling* problem in *fractal* clouds (Larson 1992, 1995, Elmegreen 1997ab, 2000ab, 2002)
 - IMF as purely *statistical* problem (Larson 1973, Zinnecker 1984, 1990, Adams & Fatuzzo 1996)
 - IMF from (proto)stellar *feedback* (Silk 1995, Adams & Fatuzzo 1996)
 - IMF from competitive *coagulation* (Murray & Lin 1995, Bonnell et al. 2001ab, etc.)



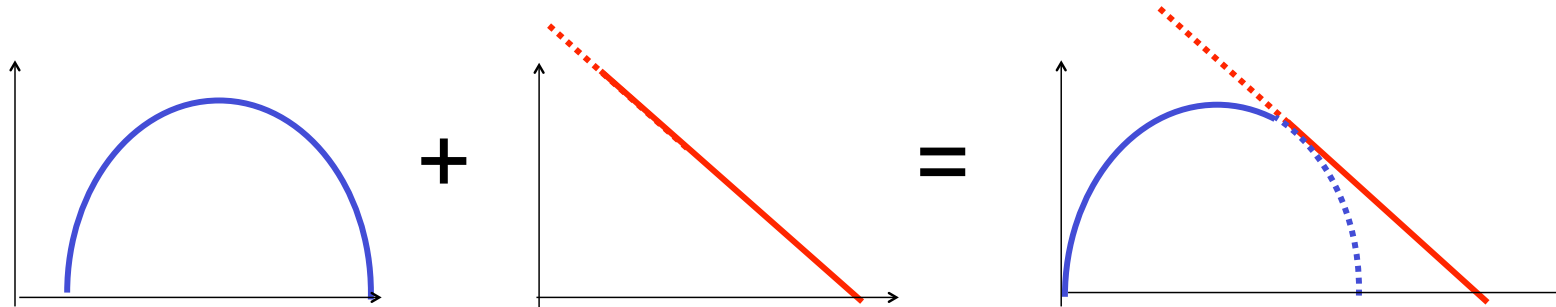
caveat: everybody gets the IMF!



- combine scale free process → **POWER LAW BEHAVIOR**
 - turbulence (Padoan & Nordlund 2002, Hennebelle & Chabrier 2008)
 - gravity in dense clusters (Bonnell & Bate 2006, Klessen 2001)
 - universality: dust-induced EOS kink insensitive to radiation field (Elmegreen et al. 2008)
- with highly stochastic processes → central limit theorem → **GAUSSIAN DISTRIBUTION**
 - basically mean thermal Jeans length (or feedback)
 - universality: insensitive to metallicity (Clark et al. 2009, submitted)



caveat: everybody gets the IMF!



“everyone” gets the right IMF
→ better look for secondary indicators

- *stellar multiplicity*
- *protostellar spin* (including disk)
- *spatial distribution + kinematics* in young clusters
- *magnetic field strength and orientation*

IMF

- distribution of stellar masses depends on
 - turbulent initial conditions
 - > mass spectrum of prestellar cloud cores
 - collapse and interaction of prestellar cores
 - > competitive mass growth and N -body effects
 - thermodynamic properties of gas
 - > balance between heating and cooling
 - > EOS (determines which cores go into collapse)
 - (proto) stellar feedback terminates star formation
 - ionizing radiation, bipolar outflows, winds, SN



example: model of Orion cloud

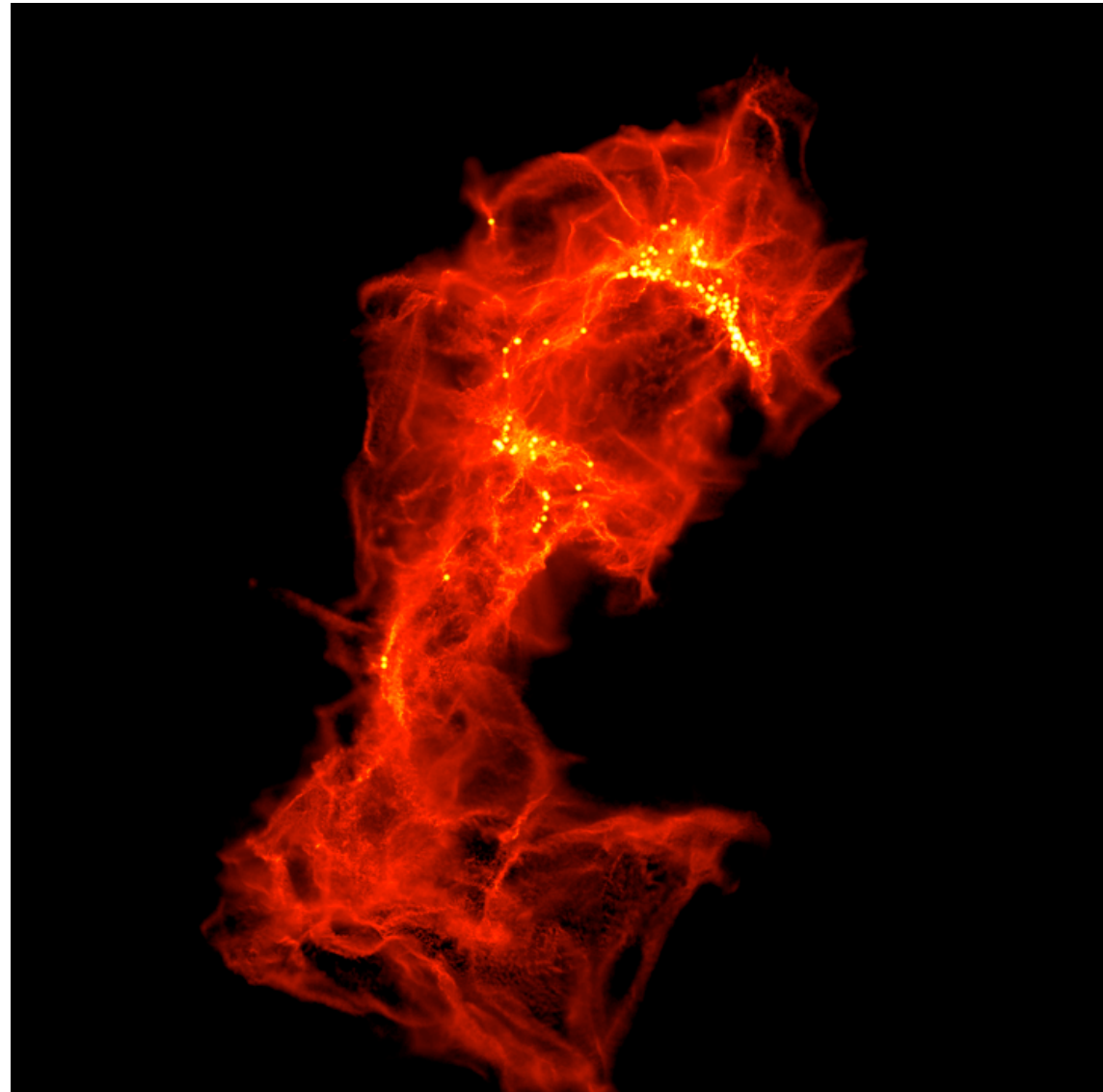
„model“ of Orion cloud:
15.000.000 SPH particles,
 $10^4 M_{\text{sun}}$ in 10 pc, mass resolution
 $0,02 M_{\text{sun}}$, forms ~ 2.500
„stars“ (sink particles)

isothermal EOS, top bound, bottom unbound

has clustered as well as distributed
„star“ formation

efficiency varies from 1% to 20%

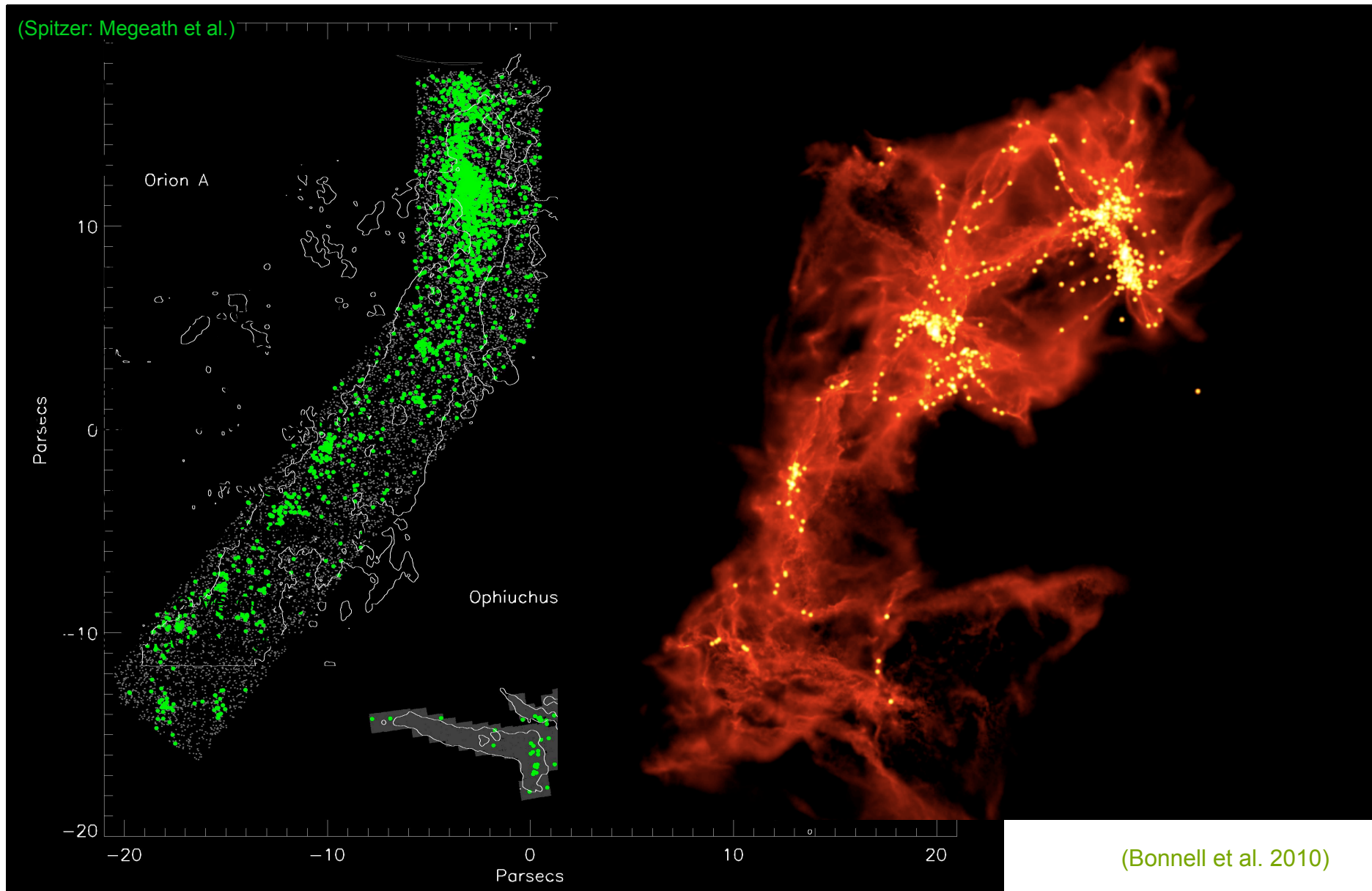
develops full IMF
(distribution of sink particle masses)



(Bonnell, Smith, Clark, & Bate 2010, MNRAS, 410, 2339)



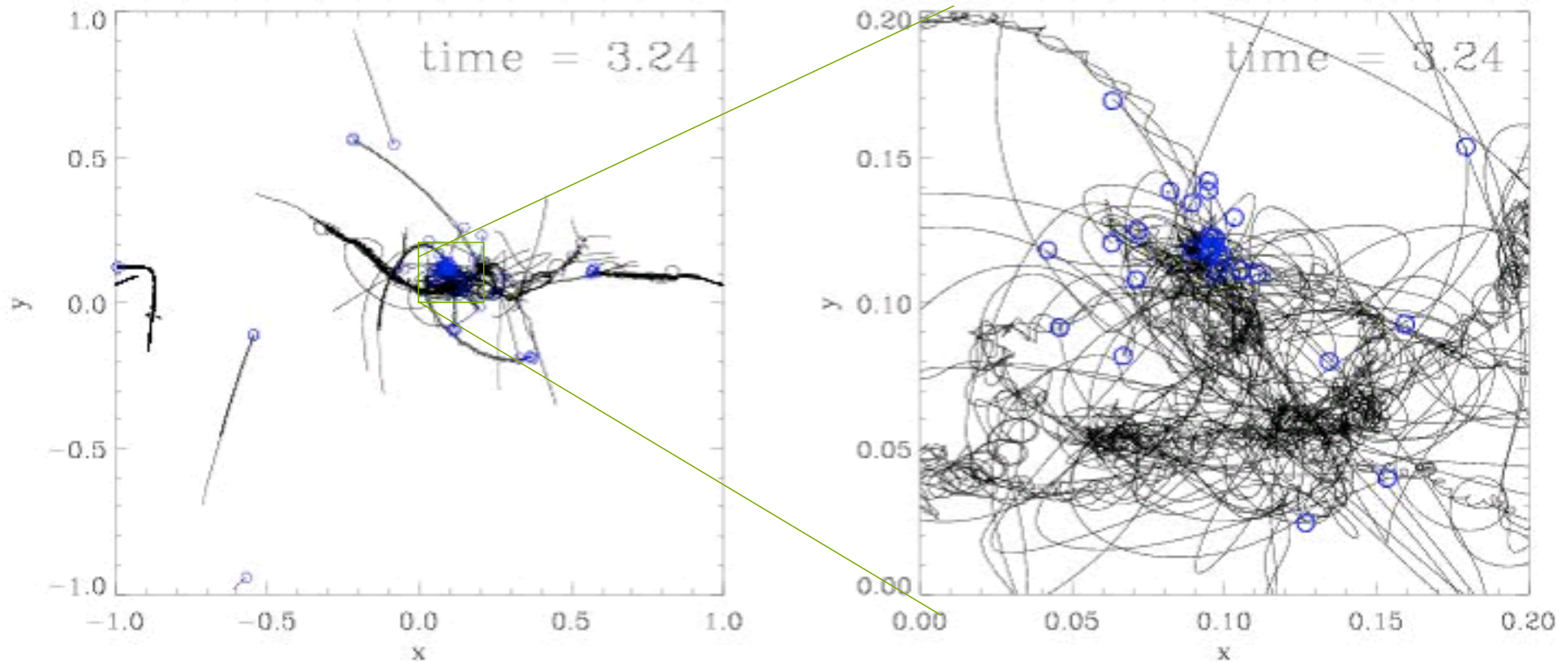
example: model of Orion cloud





dynamics of nascent star cluster

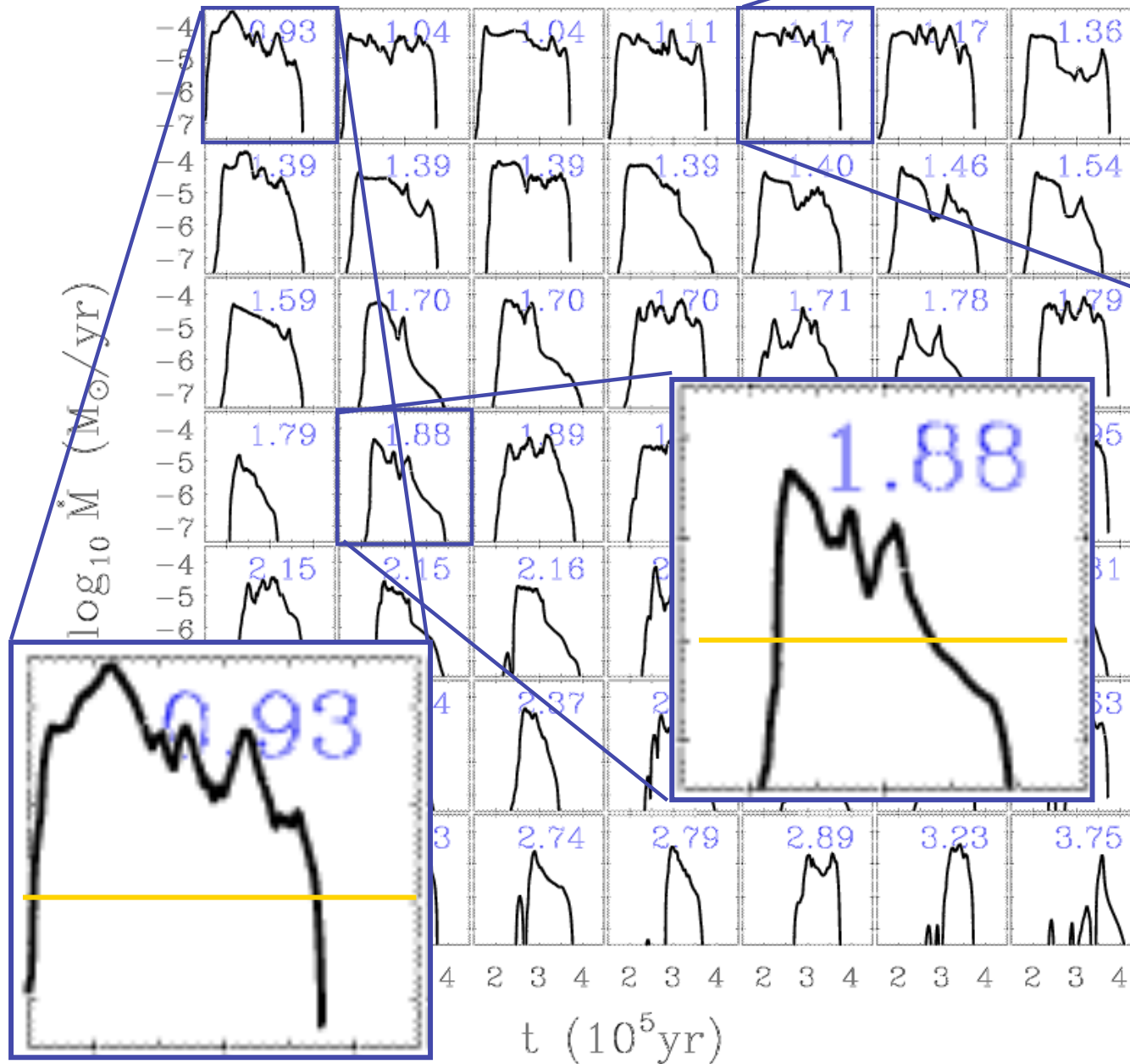
in dense clusters protostellar interaction may be come important!



Trajectories of protostars in a nascent dense cluster created by gravoturbulent fragmentation
(from Klessen & Burkert 2000, ApJS, 128, 287)



accretion rates in clust



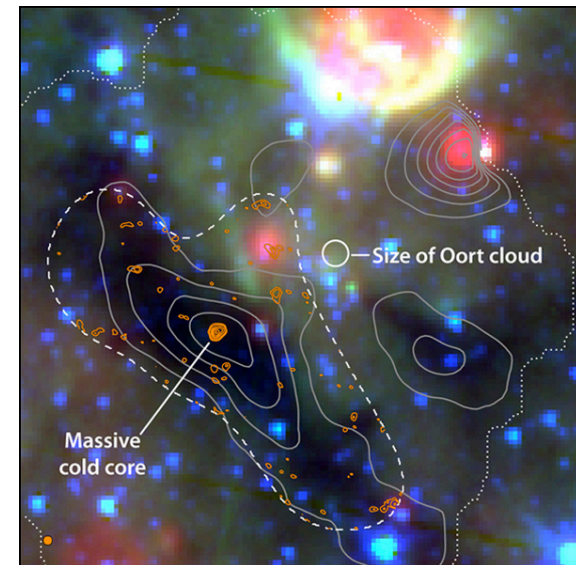
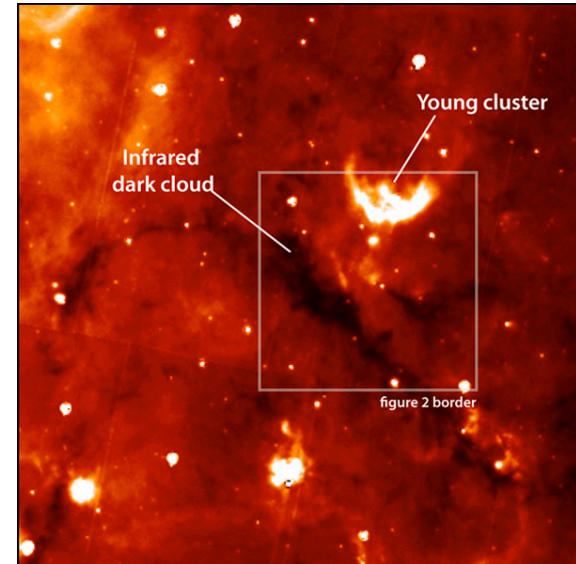
Mass accretion rates *vary with time* and are strongly *influenced* by the *cluster environment*.

(Klessen 2001, ApJ, 550, L77;
also Schmeja & Klessen,
2004, A&A, 419, 405)

initial conditions for
cluster formation

ICs of star cluster formation

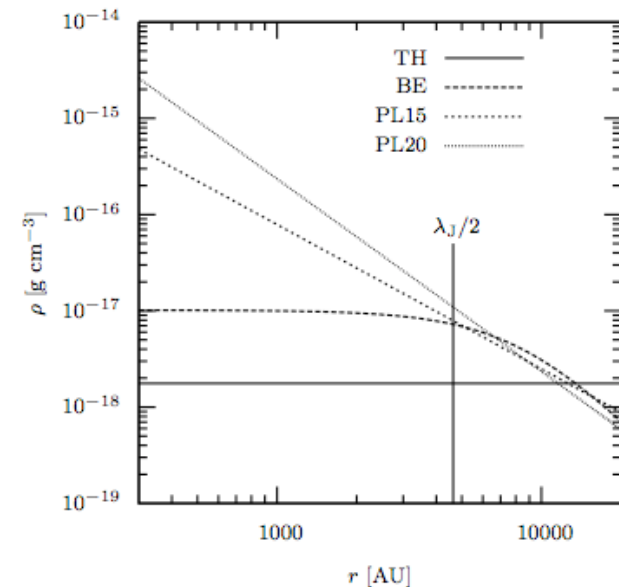
- key question:
 - what is the initial density profile of cluster forming cores? how does it compare low-mass cores?
- observers answer:
 - very difficult to determine!
 - ▶ most high-mass cores have some SF inside
 - ▶ infra-red dark clouds (IRDCs) are difficult to study
 - but, new results with Herschel



IRDC near Aquila rift, studied with the SMA: J. Swift & E. Churchwell

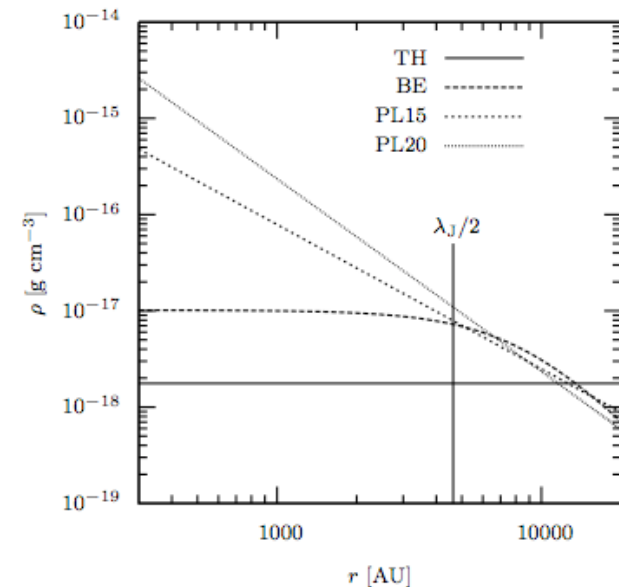
ICs of star cluster formation

- key question:
 - what is the initial density profile of cluster forming cores? how does it compare low-mass cores?
- theorists answer:
 - top hat (Larson Penston)
 - Bonnor Ebert (like low-mass cores)
 - power law $\rho \propto r^{-1}$ (logotrop)
 - power law $\rho \propto r^{-3/2}$ (Krumholz, McKee, et
 - power law $\rho \propto r^{-2}$ (Shu)
 - and many more



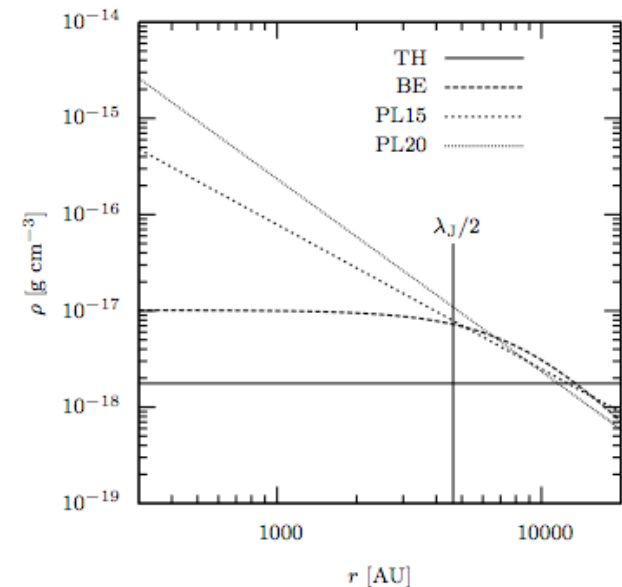
different density profiles

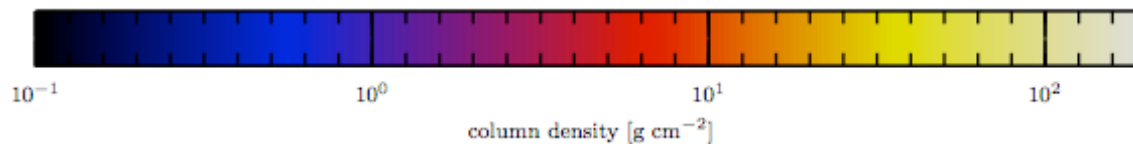
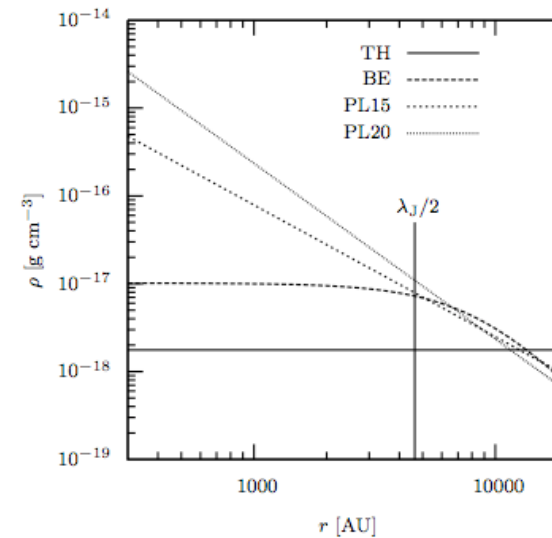
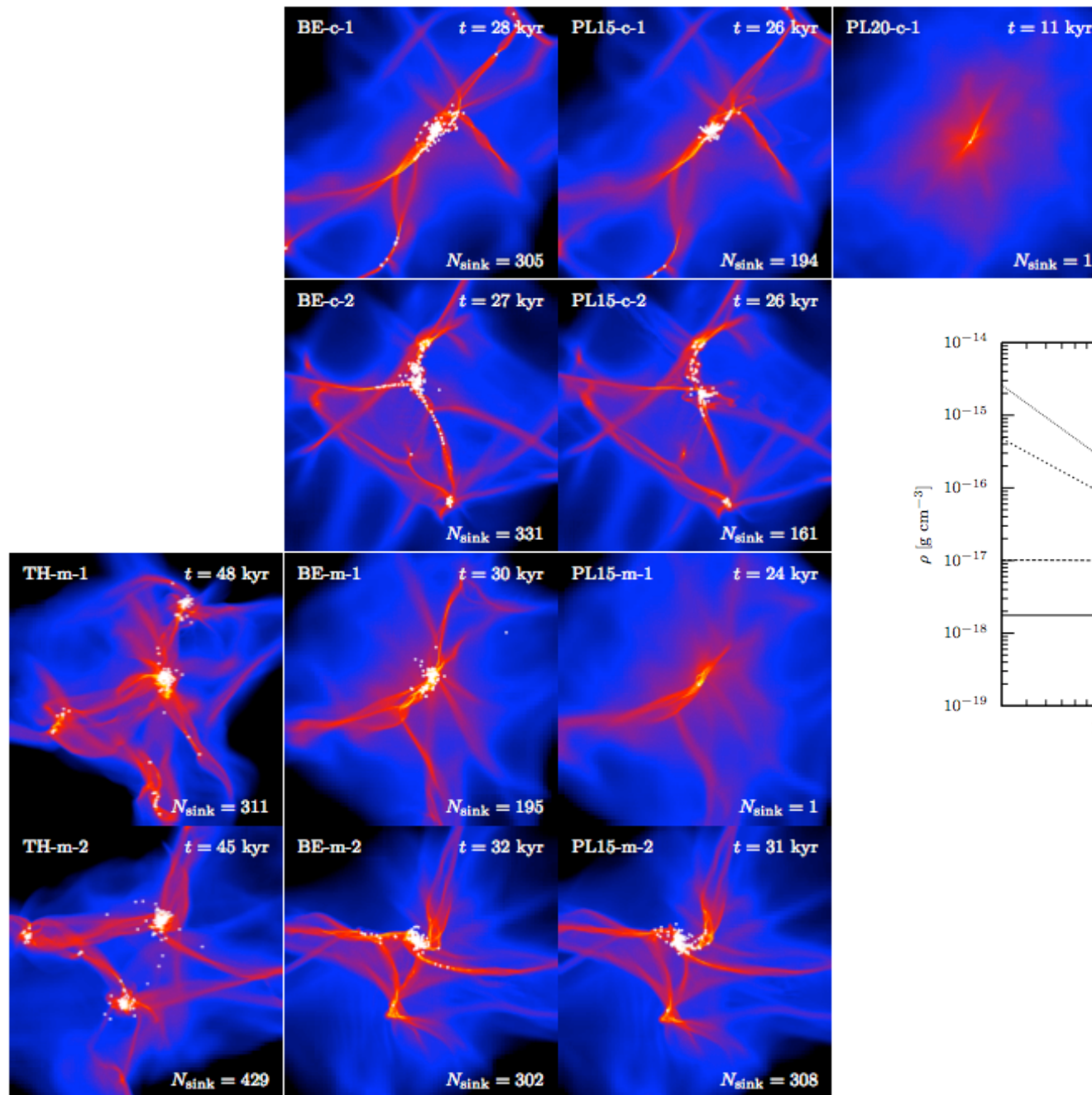
- does the density profile matter?
 -
 -
 -
- in comparison to
 - turbulence ...
 - radiative feedback ...
 - magnetic fields ...
 - thermodynamics ...

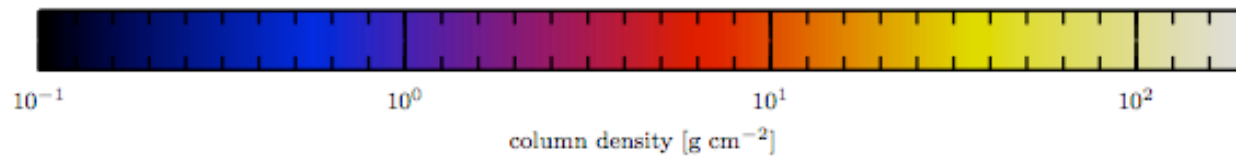
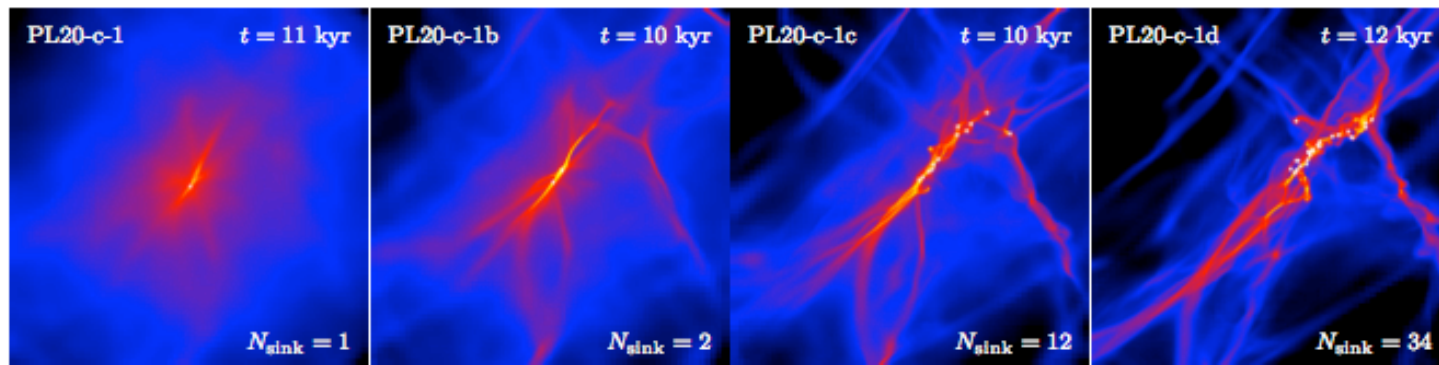


different density profiles

- address question in simple numerical experiment
- perform extensive parameter study
 - different profiles (top hat, BE, $r^{-3/2}$, r^{-3})
 - different turbulence fields
 - ▶ different realizations
 - ▶ different Mach numbers
 - ▶ solenoidal turbulence
dilatational turbulence
both modes
 - no net rotation, no B-fields
(at the moment)







M=3

M=6

M=12

M=18

for the r^{-2} profile you need to crank up turbulence a lot to get some fragmentation!

Run	t_{sim} [kyr]	$t_{\text{sim}}/t_{\text{ff}}^{\text{core}}$	$t_{\text{sim}}/t_{\text{ff}}$	N_{sinks}	$\langle M \rangle [M_{\odot}]$	M_{max}
TH-m-1	48.01	0.96	0.96	311	0.0634	0.86
TH-m-2	45.46	0.91	0.91	429	0.0461	0.74
BE-c-1	27.52	1.19	0.55	305	0.0595	0.94
BE-c-2	27.49	1.19	0.55	331	0.0571	0.97
BE-m-1	30.05	1.30	0.60	195	0.0873	1.42
BE-m-2	31.94	1.39	0.64	302	0.0616	0.54
BE-s-1	30.93	1.34	0.62	234	0.0775	1.14
BE-s-2	35.86	1.55	0.72	325	0.0587	0.51
PL15-c-1	25.67	1.54	0.51	194	0.0992	8.89
PL15-c-2	25.82	1.55	0.52	161	0.1244	12.3
PL15-m-1	23.77	1.42	0.48	1	20	20.0
PL15-m-2	31.10	1.86	0.62	308	0.0653	6.88
PL15-s-1	24.85	1.49	0.50	1	20	20.0
PL15-s-2	35.96	2.10	0.72	422	0.0478	4.50
PL20-c-1	10.67	0.92	0.21	1	20	20.0
PL20-c-1b	10.34	0.89	0.21	2	10.139	20.0
PL20-c-1c	9.63	0.83	0.19	12	1.67	17.9
PL20-c-1d	11.77	1.01	0.24	34	0.593	13.3

ICs with flat inner density profile form more fragments

number of protostars

Run	t_{sim} [kyr]	$t_{\text{sim}}/t_{\text{ff}}^{\text{core}}$	$t_{\text{sim}}/t_{\text{ff}}$	N_{sinks}	$\langle M \rangle [M_{\odot}]$	M_{max}
TH-m-1	48.01	0.96	0.96	311	0.0634	0.86
TH-m-2	45.46	0.91	0.91	429	0.0461	0.74
BE-c-1	27.52	1.19	0.55	305	0.0595	0.94
BE-c-2	27.49	1.19	0.55	331	0.0571	0.97
BE-m-1	30.05	1.30	0.60	195	0.0873	1.42
BE-m-2	31.94	1.39	0.64	302	0.0616	0.54
BE-s-1	30.93	1.34	0.62	234	0.0775	1.14
BE-s-2	35.86	1.55	0.72	325	0.0587	0.51
PL15-c-1	25.67	1.54	0.51	194	0.0992	8.89
PL15-c-2	25.82	1.55	0.52	161	0.1244	12.3
PL15-m-1	23.77	1.42	0.48	1	20	20.0
PL15-m-2	31.10	1.86	0.62	308	0.0653	6.88
PL15-s-1	24.85	1.49	0.50	1	20	20.0
PL15-s-2	35.96	2.10	0.72	422	0.0478	4.50
PL20-c-1	10.67	0.92	0.21	1	20	20.0
PL20-c-1b	10.34	0.89	0.21	2	10.139	20.0
PL20-c-1c	9.63	0.83	0.19	12	1.67	17.9
PL20-c-1d	11.77	1.01	0.24	34	0.593	13.3

however, the real situation is very complex:
 details of the initial turbulent field matter

very high Mach numbers are needed to make
 SIS fragment

number of
 protostars

different density profiles

- different density profiles lead to very different fragmentation behavior
- fragmentation is strongly suppressed for very peaked, power-law profiles
- this is *good*, because it may explain some of the theoretical controversy, we have in the field
- this is *bad*, because all current calculations are “wrong” in the sense that the formation process of the star-forming core is neglected.

IMF

- distribution of stellar masses depends on
 - turbulent initial conditions
 - > mass spectrum of prestellar cloud cores
 - collapse and interaction of prestellar cores
 - > competitive accretion and N -body effects
 - *thermodynamic properties of gas*
 - > *balance between heating and cooling*
 - > *EOS (determines which cores go into collapse)*
 - (proto) stellar feedback terminates star formation
 - ionizing radiation, bipolar outflows, winds, SN

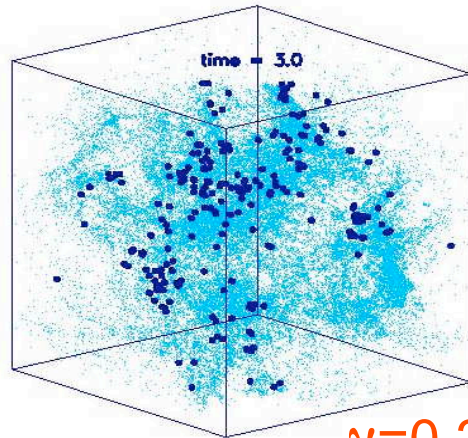


dependency on EOS

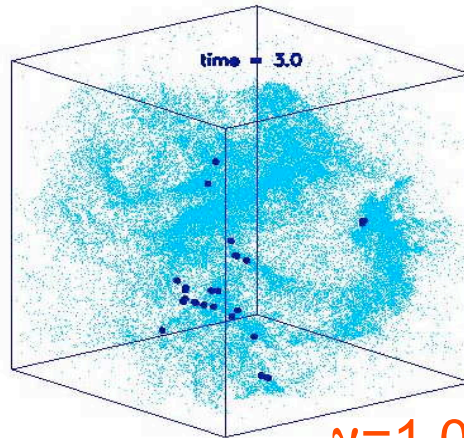
- degree of fragmentation depends on *EOS!*
- polytropic EOS: $p \propto \rho^\gamma$
- $\gamma < 1$: dense cluster of low-mass stars
- $\gamma > 1$: isolated high-mass stars
- (see Li, Klessen, & Mac Low 2003, ApJ, 592, 975; also Kawachi & Hanawa 1998, Larson 2003)



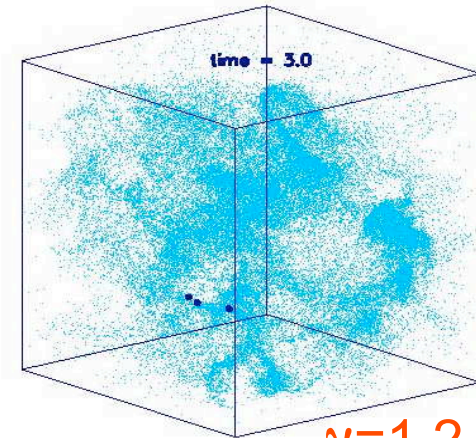
dependency on EOS



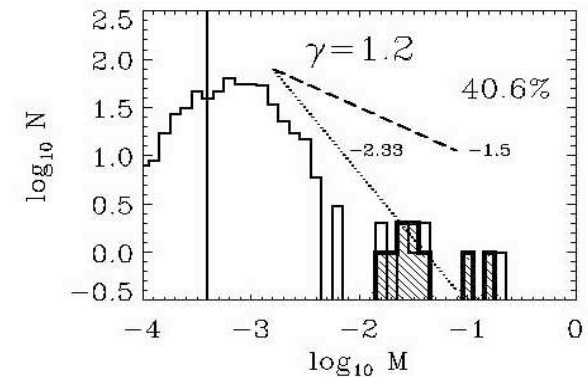
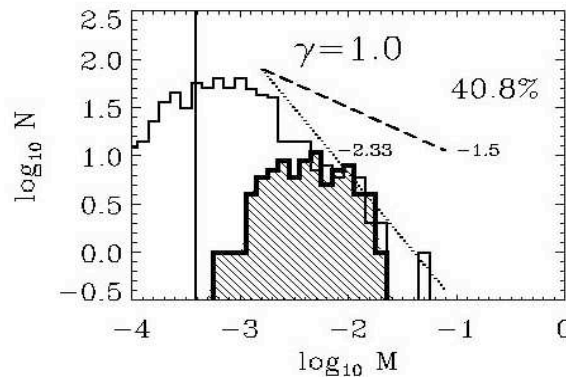
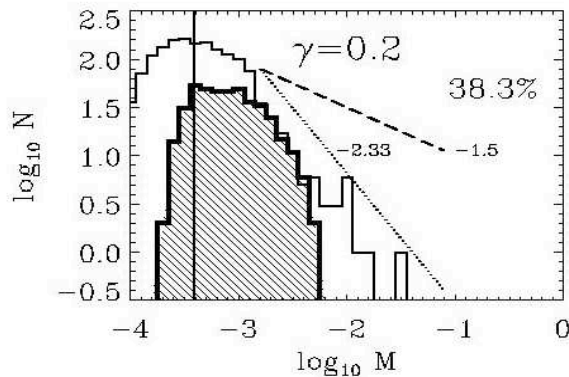
$\gamma=0.2$



$\gamma=1.0$



$\gamma=1.2$



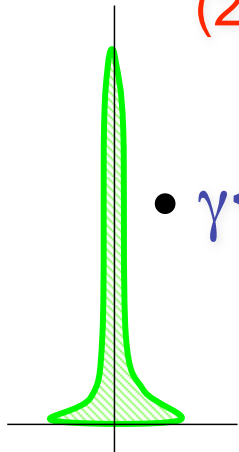
for $\gamma < 1$ fragmentation is enhanced \rightarrow *cluster of low-mass stars*
for $\gamma > 1$ it is suppressed \rightarrow formation of *isolated massive stars*



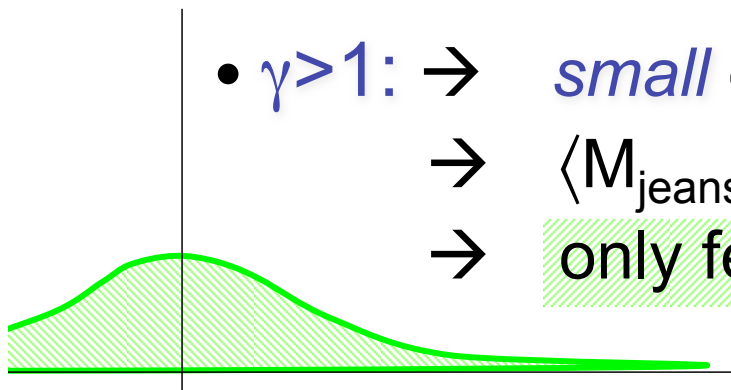
how does that work?

$$(1) \mathbf{p} \propto \rho^\gamma \rightarrow \rho \propto \mathbf{p}^{1/\gamma}$$

$$(2) \mathbf{M}_{\text{jeans}} \propto \gamma^{3/2} \rho^{(3\gamma-4)/2}$$



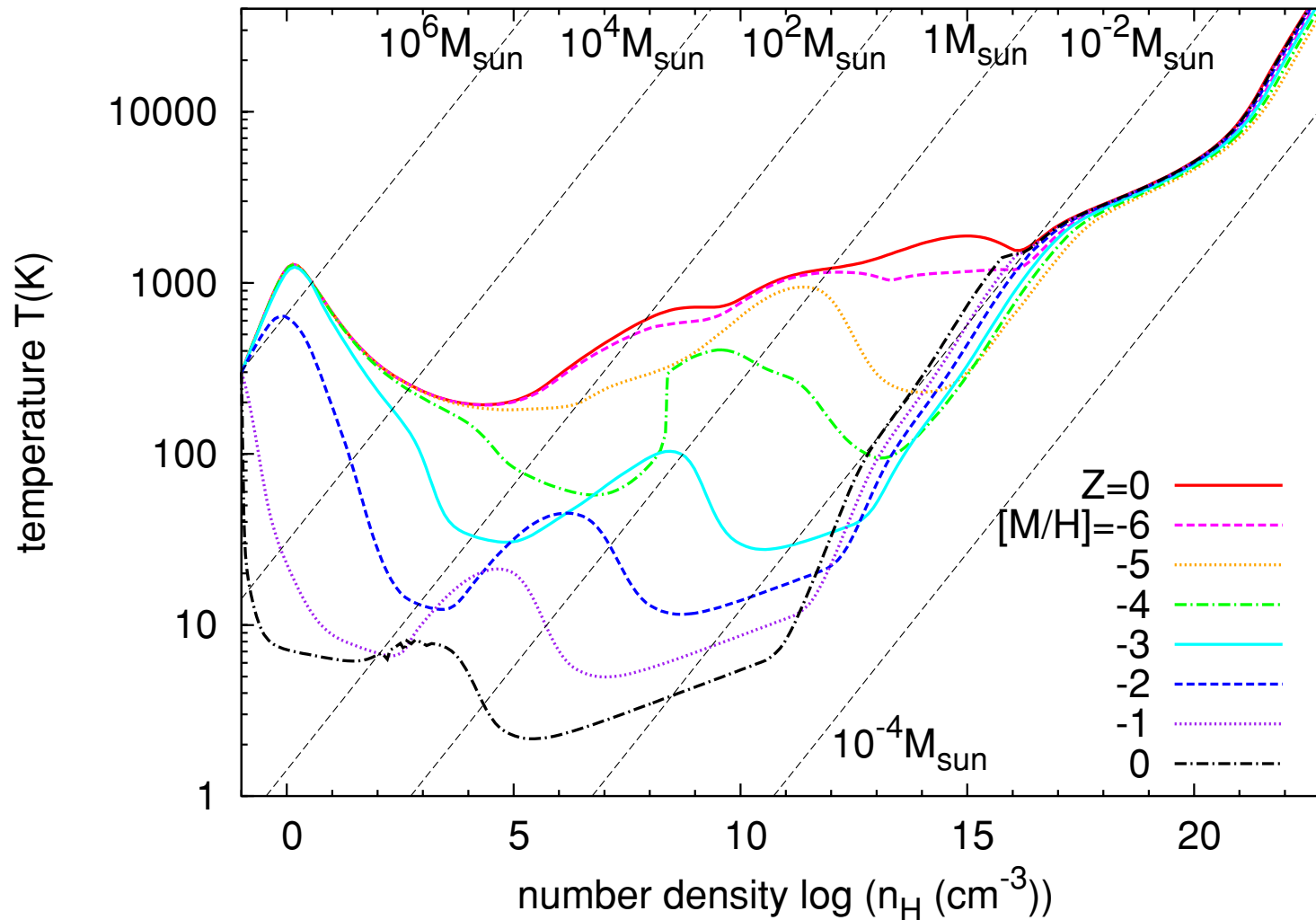
- $\gamma < 1$: \rightarrow *large* density excursion for given pressure
 - \rightarrow $\langle M_{\text{jeans}} \rangle$ becomes small
 - \rightarrow number of fluctuations with $M > M_{\text{jeans}}$ is large



- $\gamma > 1$: \rightarrow *small* density excursion for given pressure
 - \rightarrow $\langle M_{\text{jeans}} \rangle$ is large
 - \rightarrow only few and massive clumps exceed M_{jeans}

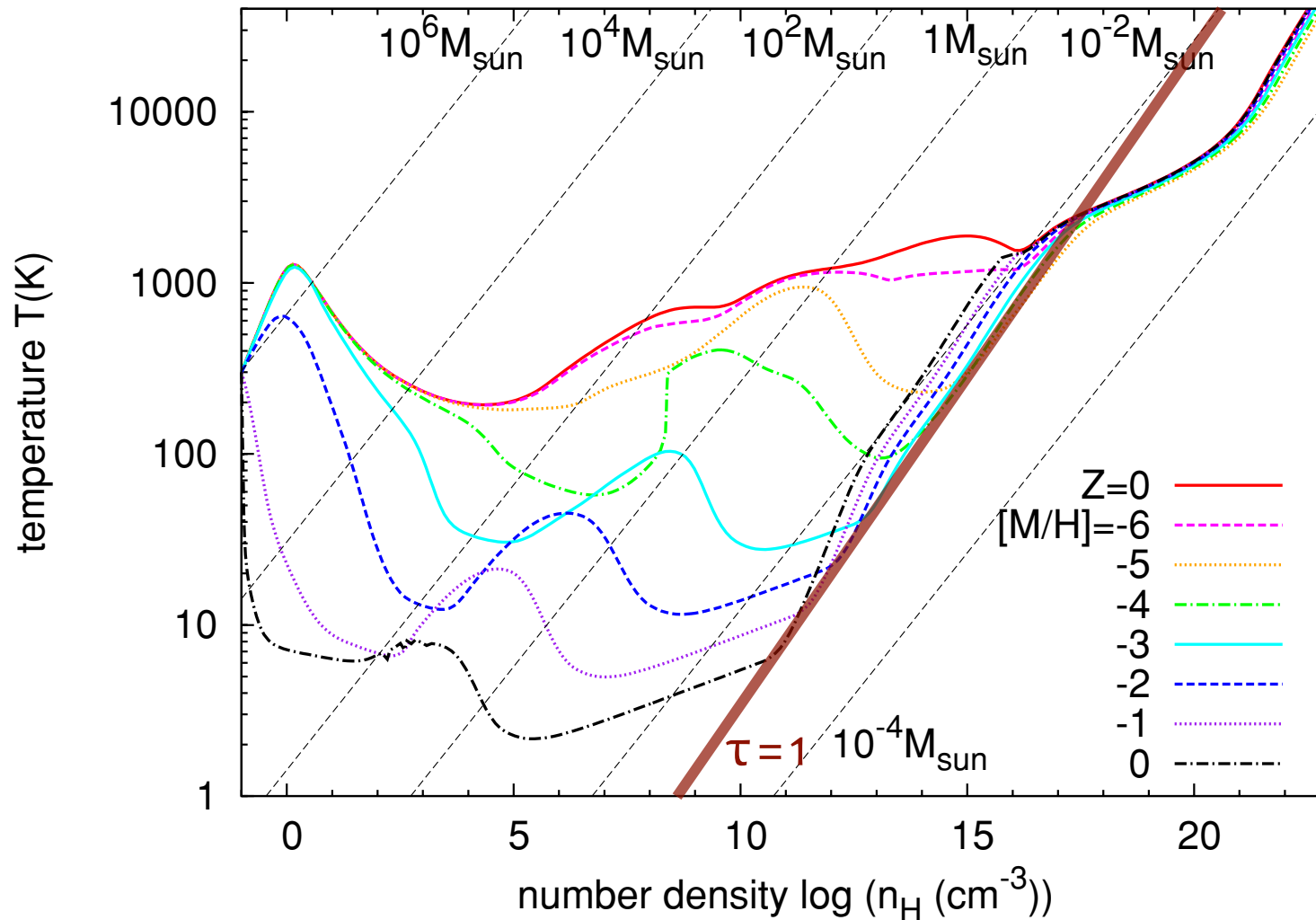
EOS in different
environments

EOS as function of metallicity



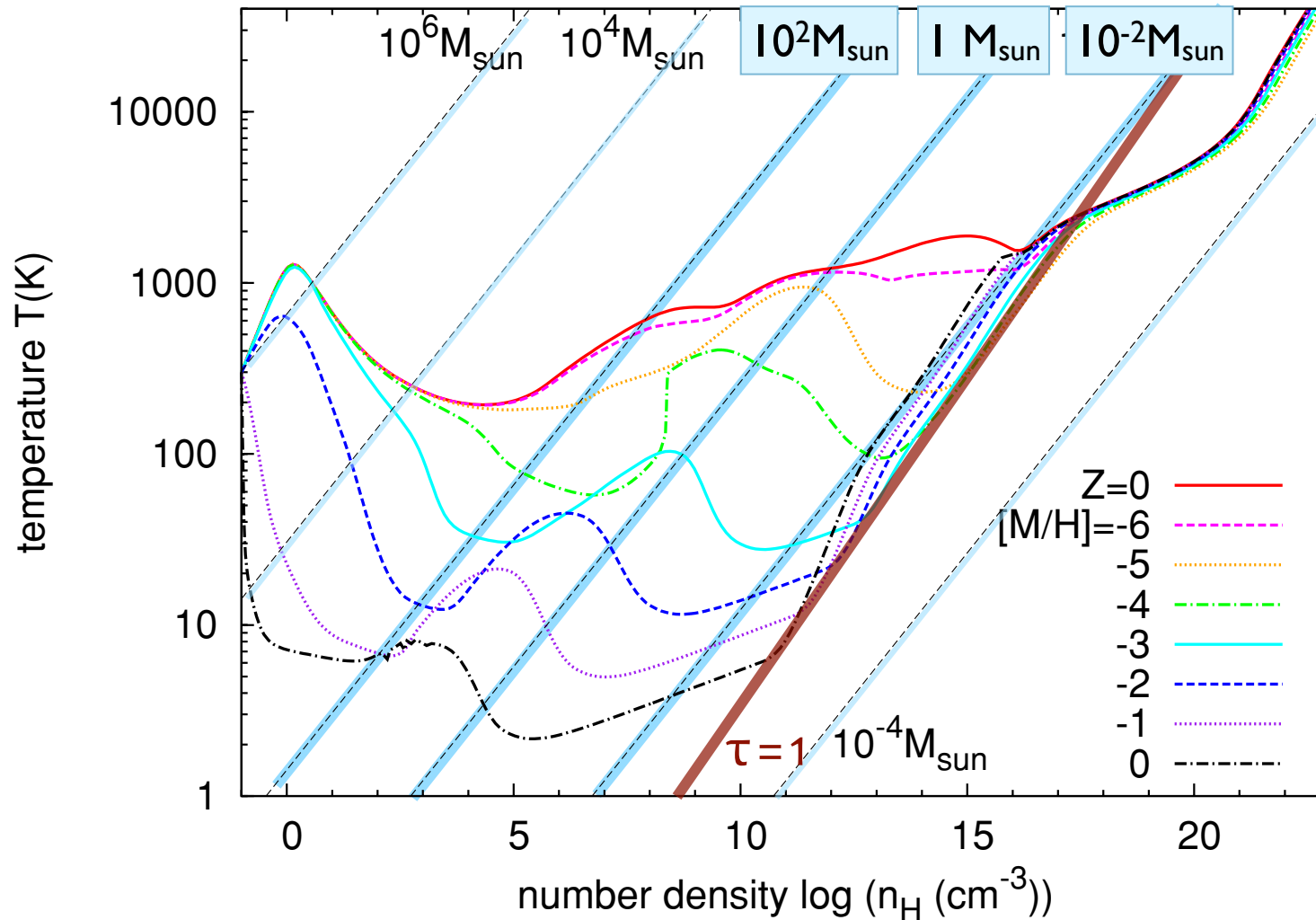
(Omukai et al. 2005, 2010)

EOS as function of metallicity



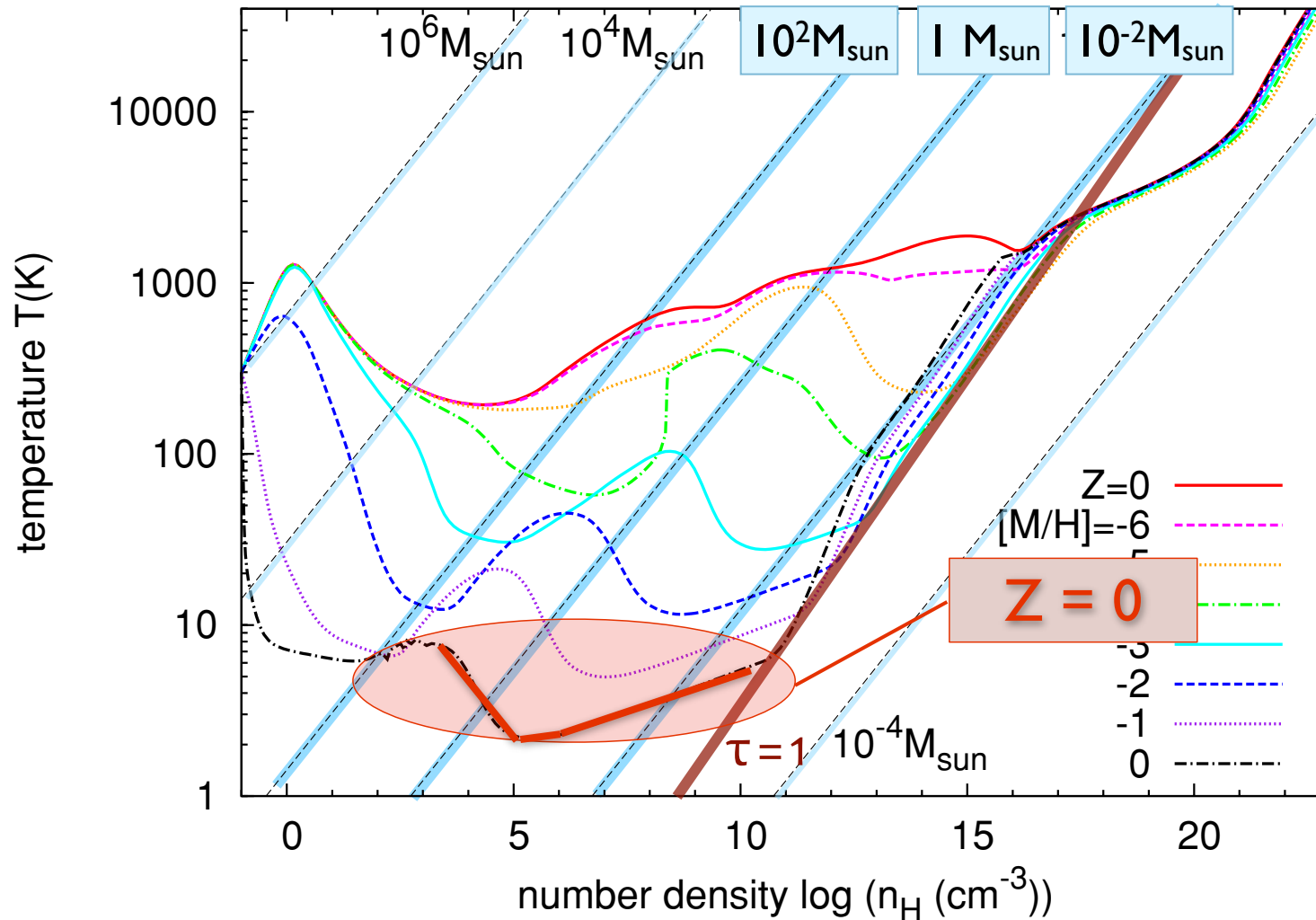
(Omukai et al. 2005, 2010)

EOS as function of metallicity



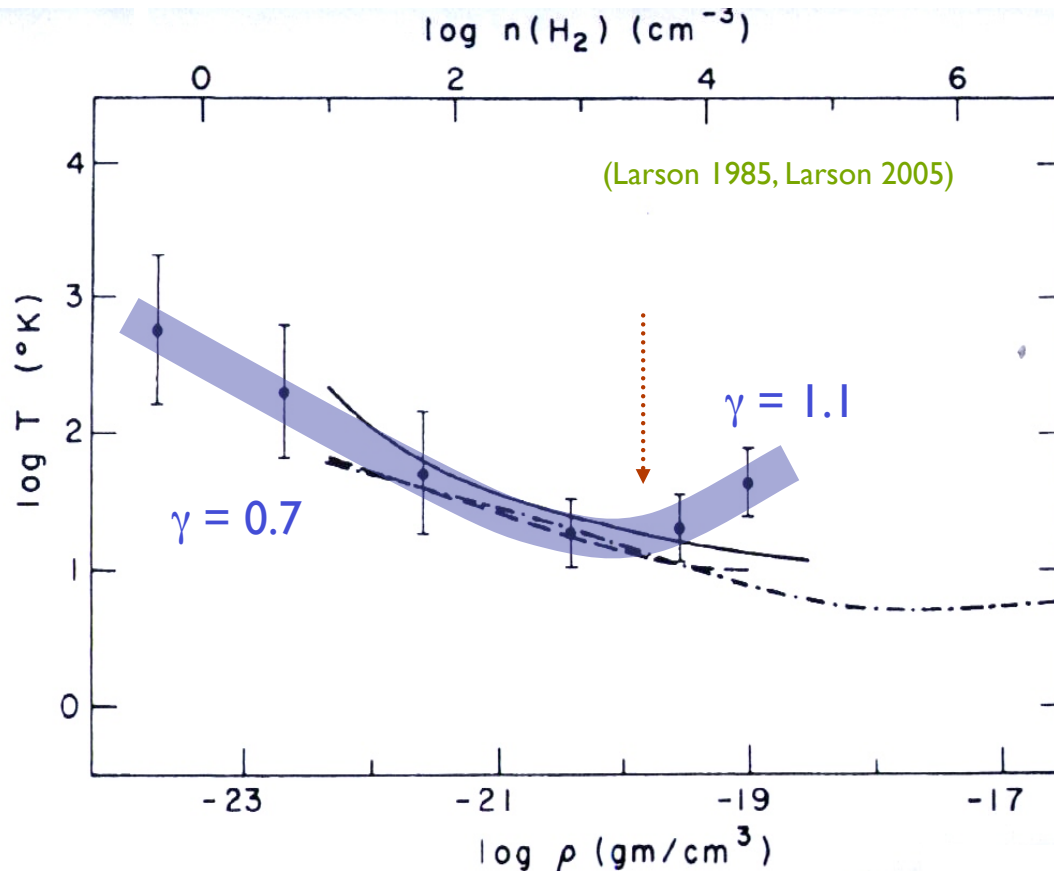
(Omukai et al. 2005, 2010)

EOS as function of metallicity

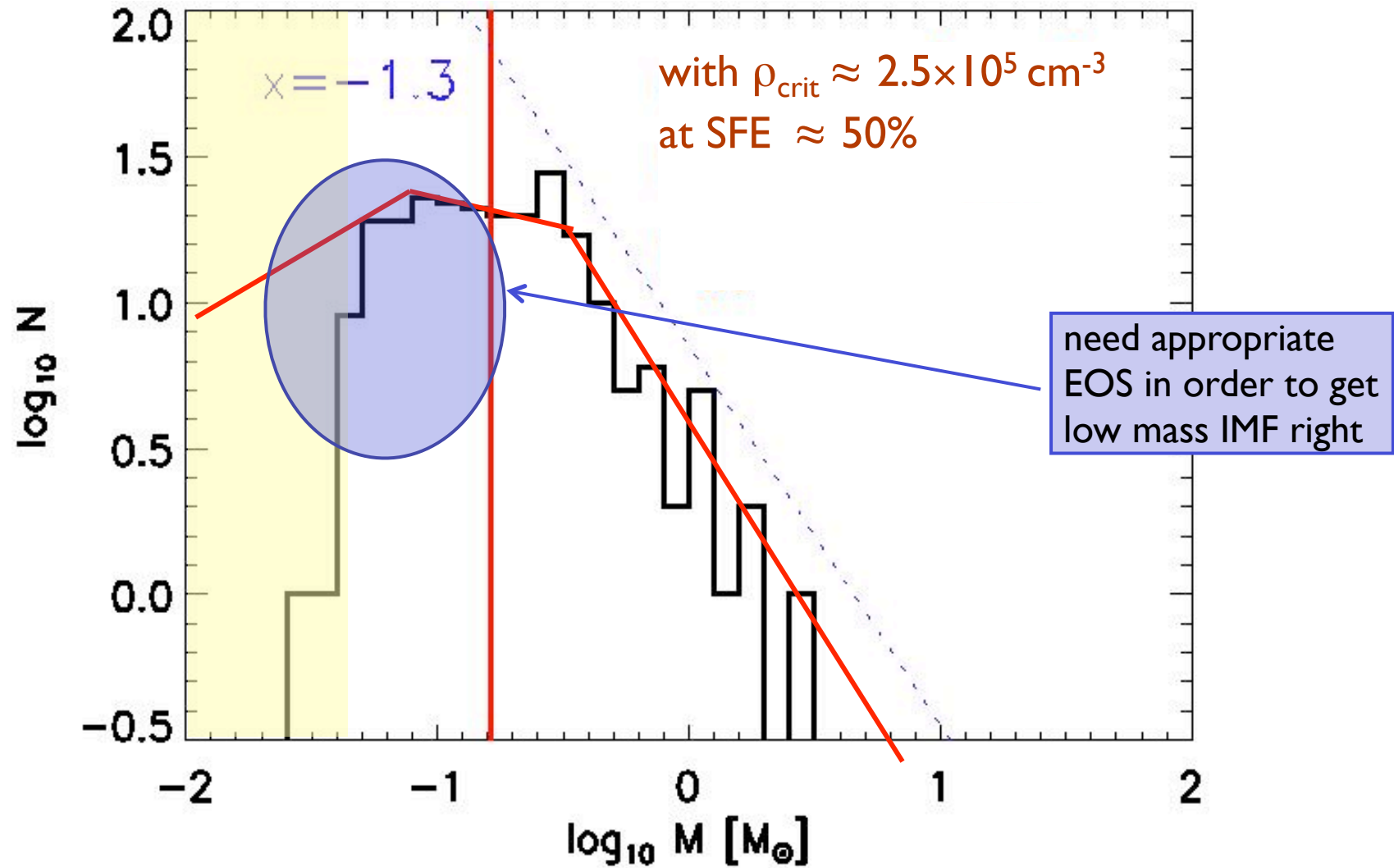


(Omukai et al. 2005, 2010)

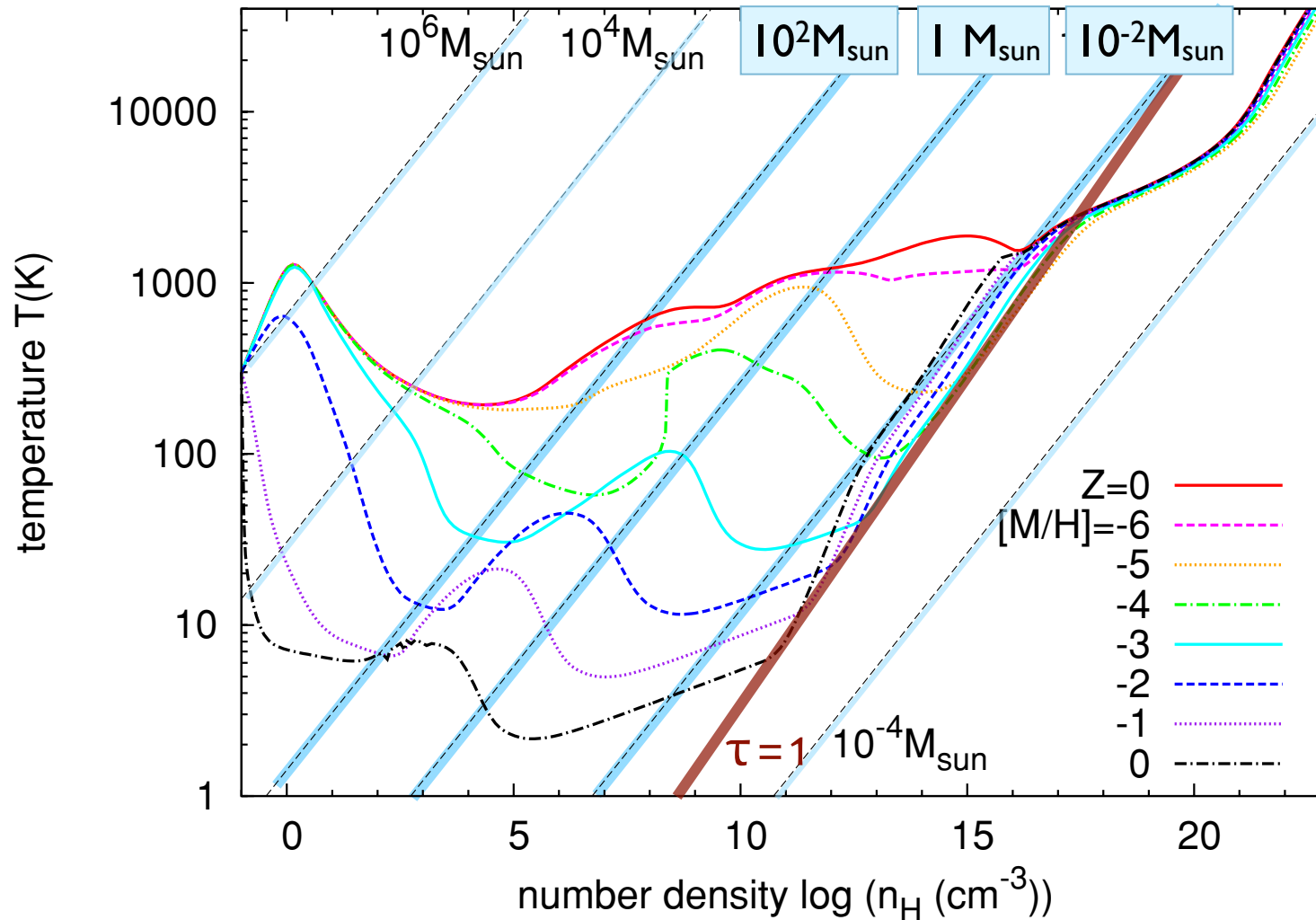
present-day star formation



IMF in nearby molecular clouds

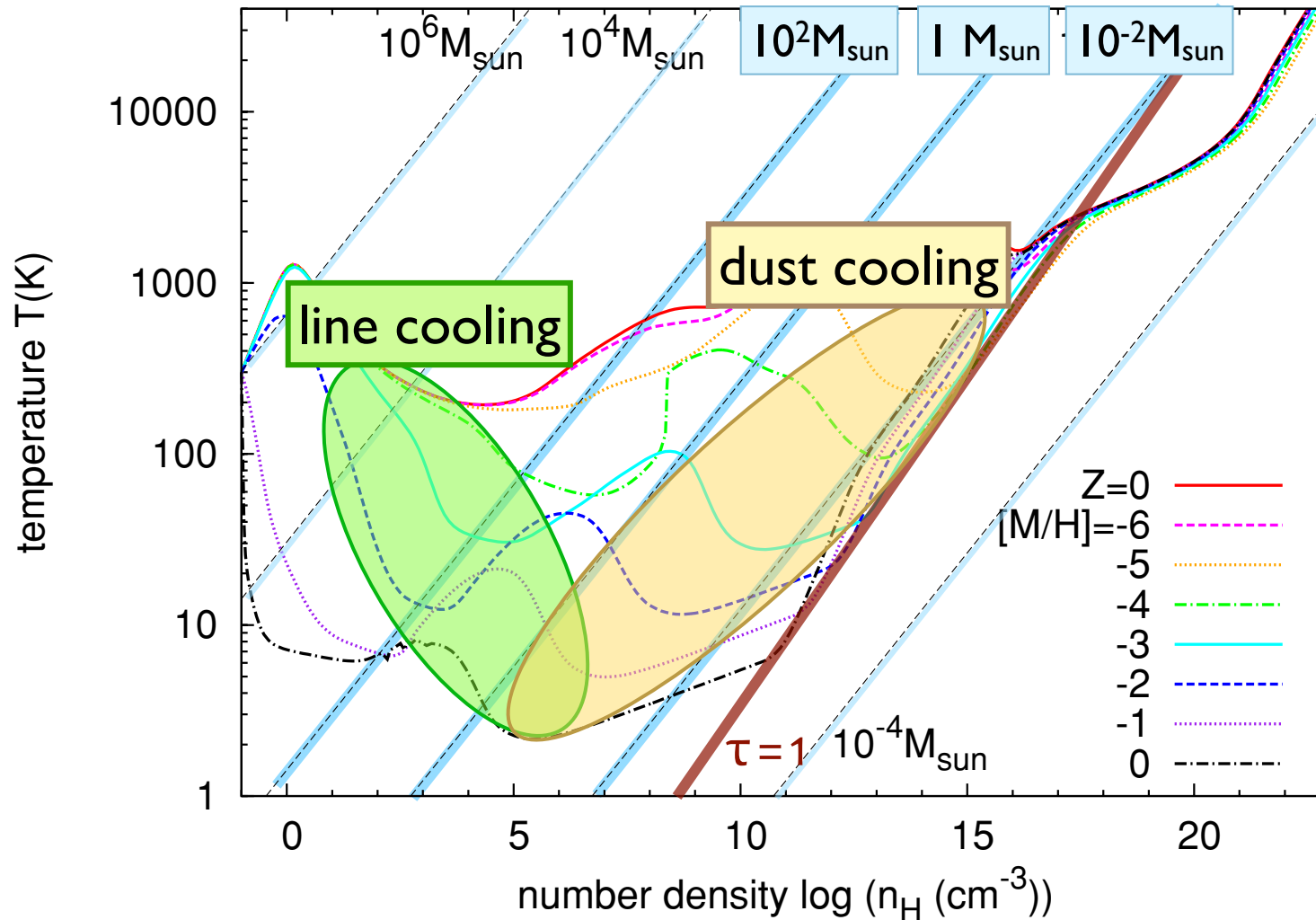


EOS as function of metallicity



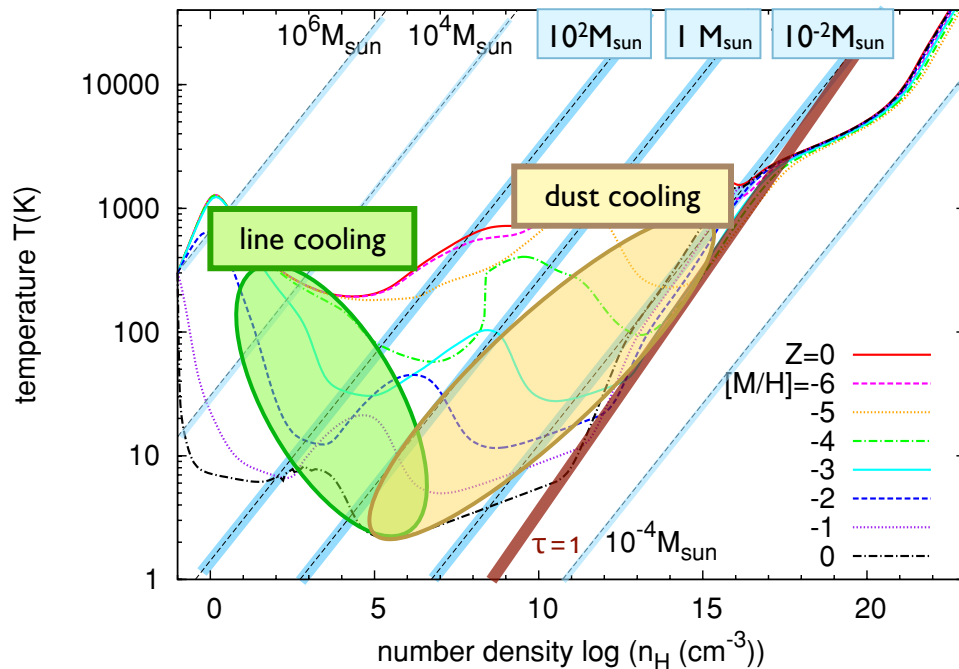
(Omukai et al. 2005, 2010)

EOS as function of metallicity



(Omukai et al. 2005, 2010)

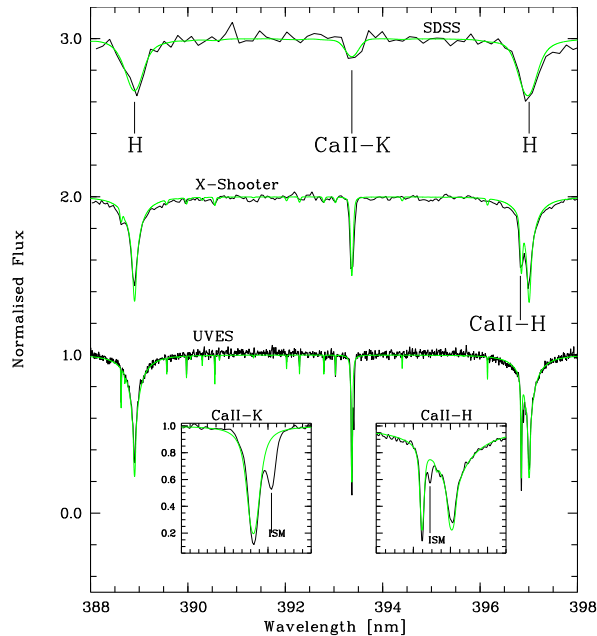
transition: Pop III to Pop II.5



two competing models:

- cooling due to atomic fine-structure lines ($Z > 10^{-3.5} Z_{\text{sun}}$)
- cooling due to coupling between gas and dust ($Z > 10^{-5 \dots -6} Z_{\text{sun}}$)
- which one explains origin of extremely metal-poor stars
NB: lines would only make very massive stars, with $M > \text{few} \times 10 M_{\text{sun}}$.

transition: Pop III to Pop II.5



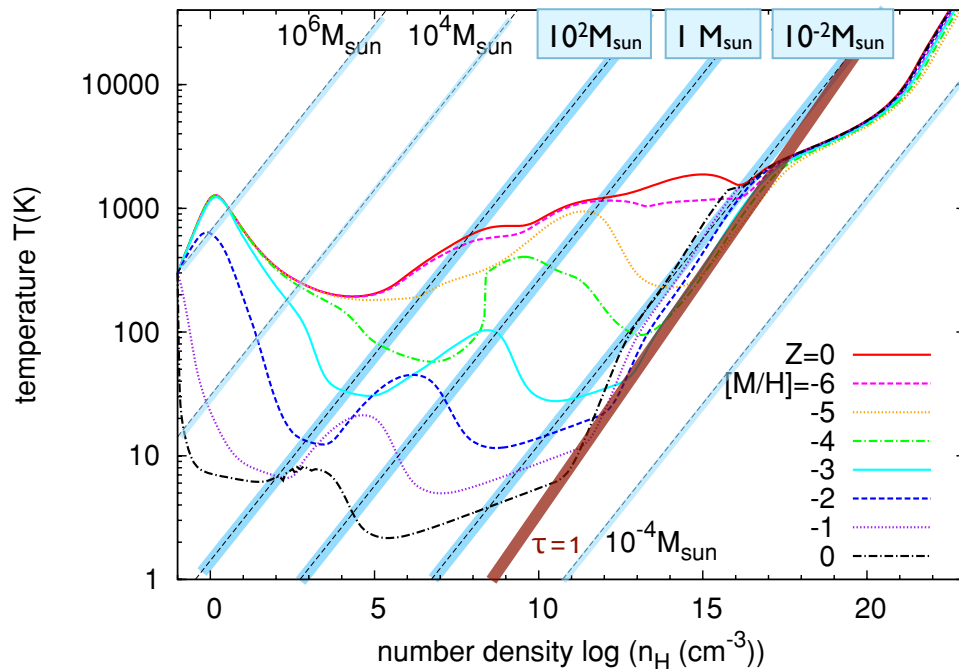
SDSS J1029151+172927

- is first ultra metal-poor star with $Z \sim 10^{-4.5} Z_{\text{sun}}$ for all metals seen (Fe, C, N, etc.)
[see Caffau et al. 2011]
- this is in regime, where metal-lines cannot provide cooling
[e.g. Schneider et al. 2011, 2012, Klessen et al. 2012]

- new ESO large program to find more of these stars (120h x-shooter, 30h UVES)
[PI E. Caffau]

Element		+3Dcor.	$[X/H]_{\text{1D}}$ +NLTE cor.	+ 3D cor + NLTE cor	N lines	S_{H}	$A(X)_{\odot}$
C	≤ -3.8	≤ -4.5			G-band		8.50
N	≤ -4.1	≤ -5.0			NH-band		7.86
Mg I	-4.71 ± 0.11	-4.68 ± 0.11	-4.52 ± 0.11	-4.49 ± 0.12	5	0.1	7.54
Si I	-4.27	-4.30	-3.93	-3.96	1	0.1	7.52
Ca I	-4.72	-4.82	-4.44	-4.54	1	0.1	6.33
Ca II	-4.81 ± 0.11	-4.93 ± 0.03	-5.02 ± 0.02	-5.15 ± 0.09	3	0.1	6.33
Ti II	-4.75 ± 0.18	-4.83 ± 0.16	-4.76 ± 0.18	-4.84 ± 0.16	6	1.0	4.90
Fe I	-4.73 ± 0.13	-5.02 ± 0.10	-4.60 ± 0.13	-4.89 ± 0.10	43	1.0	7.52
Ni I	-4.55 ± 0.14	-4.90 ± 0.11			10		6.23
Sr II	≤ -5.10	≤ -5.25	≤ -4.94	≤ -5.09	1	0.01	2.92

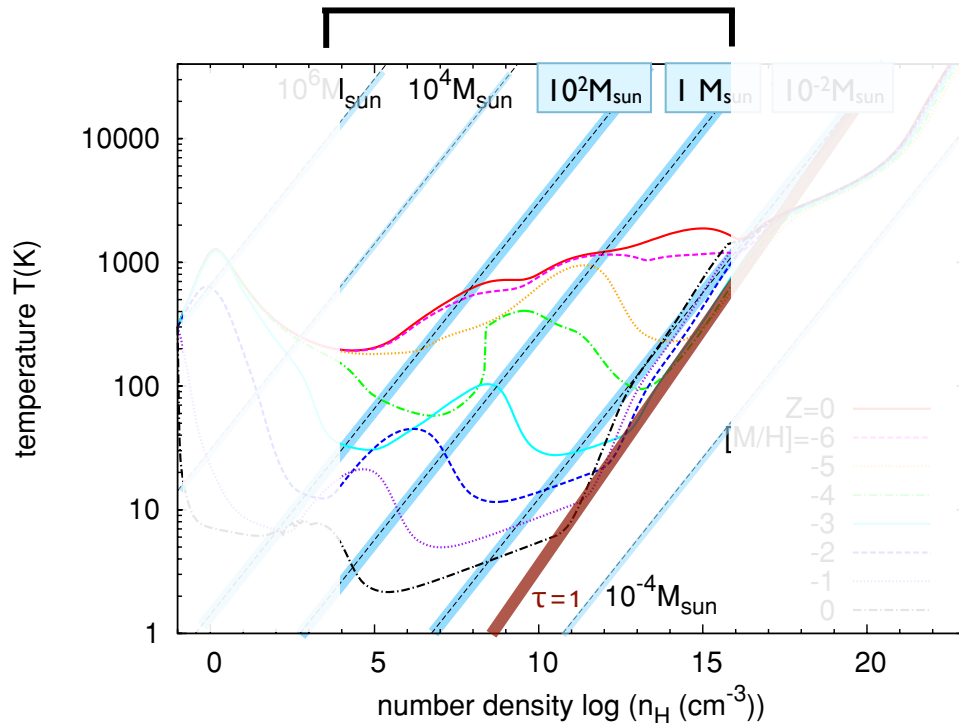
transition: Pop III to Pop II.5



approach problem with high-resolution hydrodynamic calculations of central parts of high-redshift halos

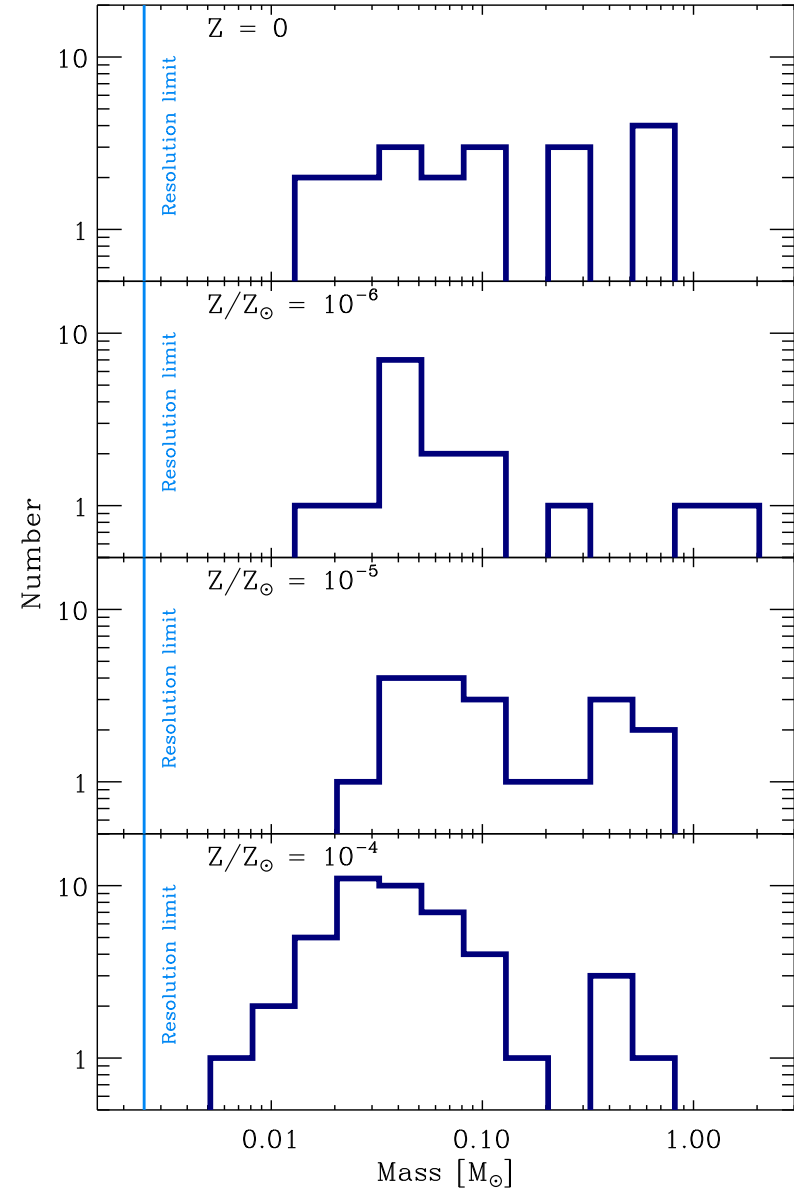
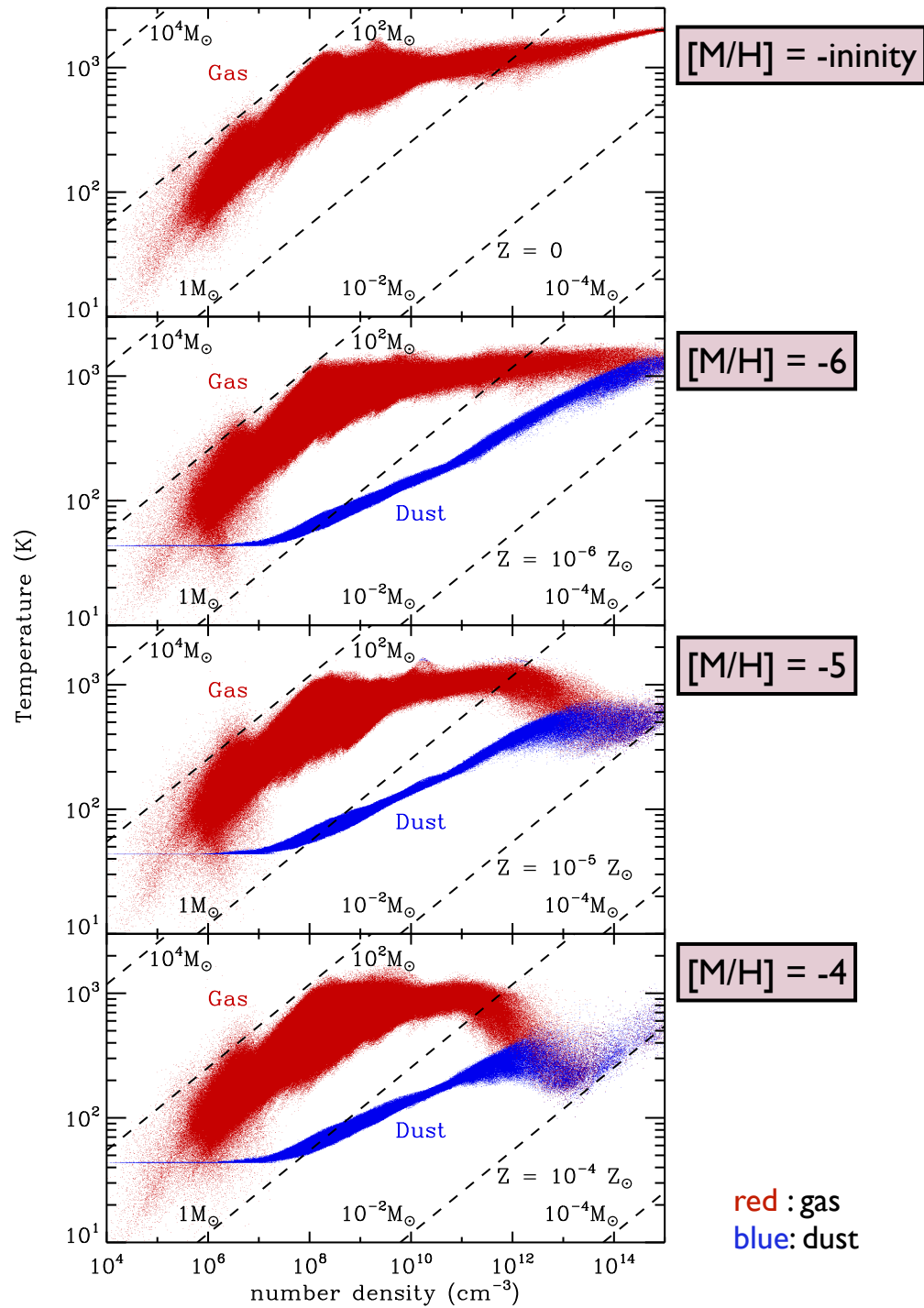
- SPH (40 million particles)
- time-dependent chemistry (with dust)
- sink particles to model star formation
- external dark-matter potential

transition: Pop III to Pop II.5



approach problem with high-resolution hydrodynamic calculations of central parts of high-redshift halos

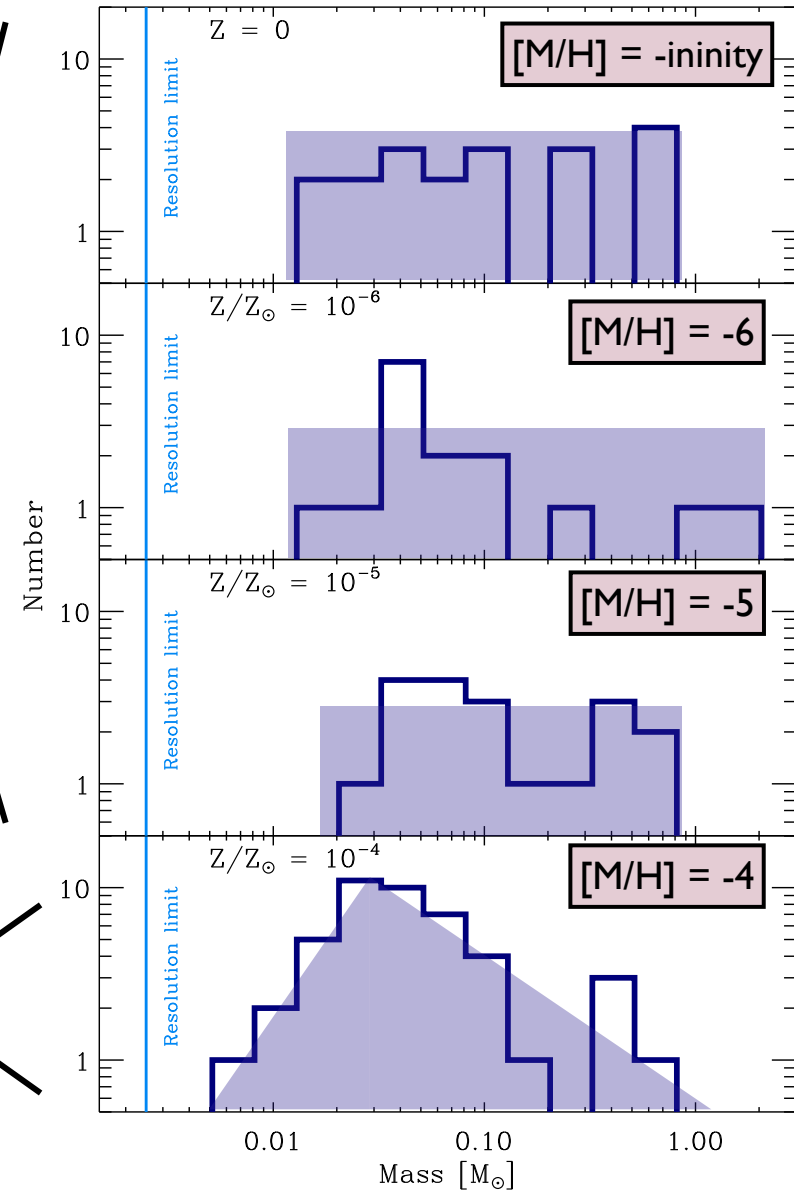
- SPH (40 million particles)
- time-dependent chemistry (with dust)
- sink particles to model star formation
- external dark-matter potential
- focus on relevant density regime (i.e. include dust dip and optically thick regime)



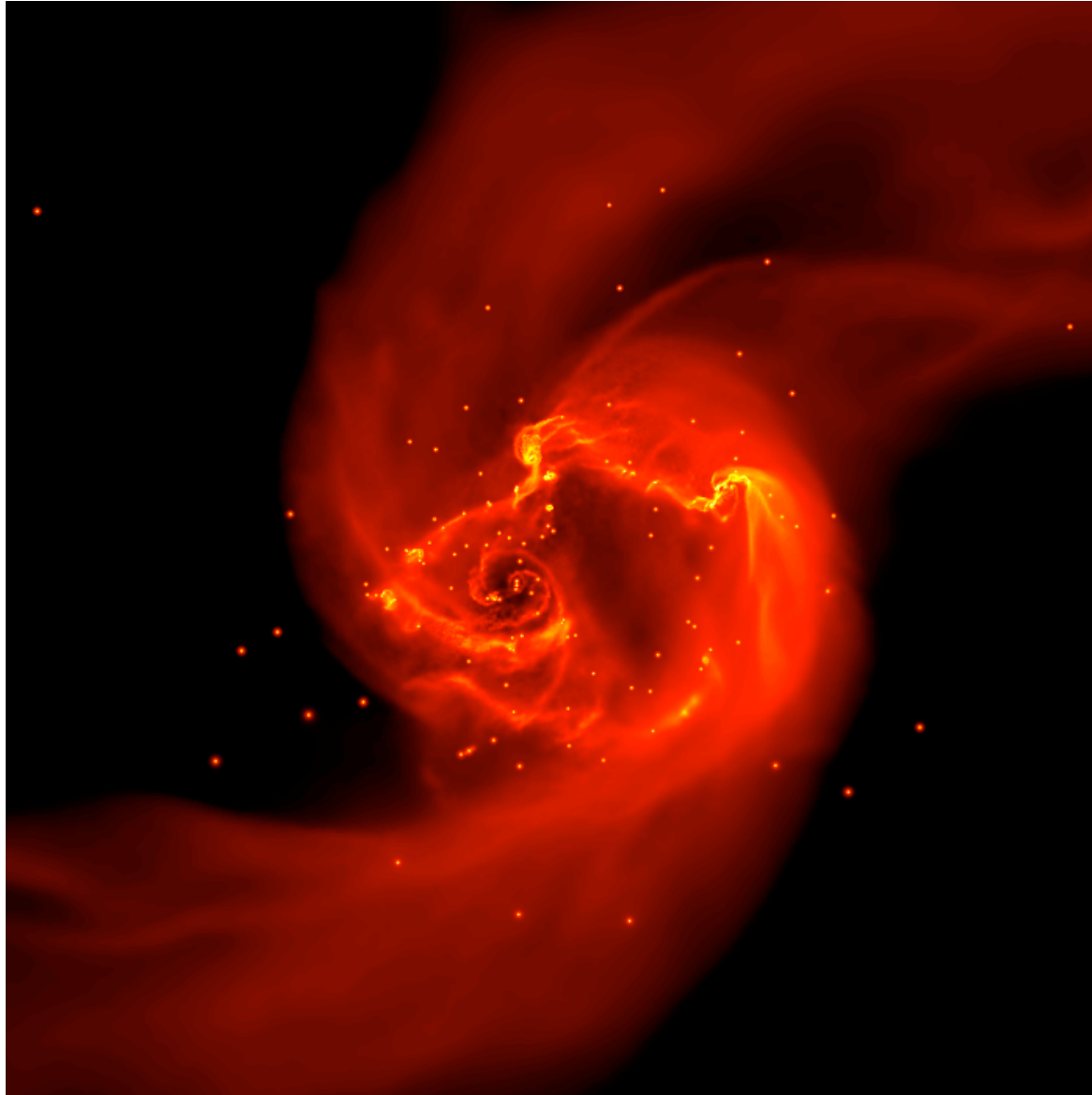
hints for differences
in mass spectrum

disk fragmentation mode

gravoturbulent fragmentation mode



dust induced fragmentation at $Z=10^{-5}$

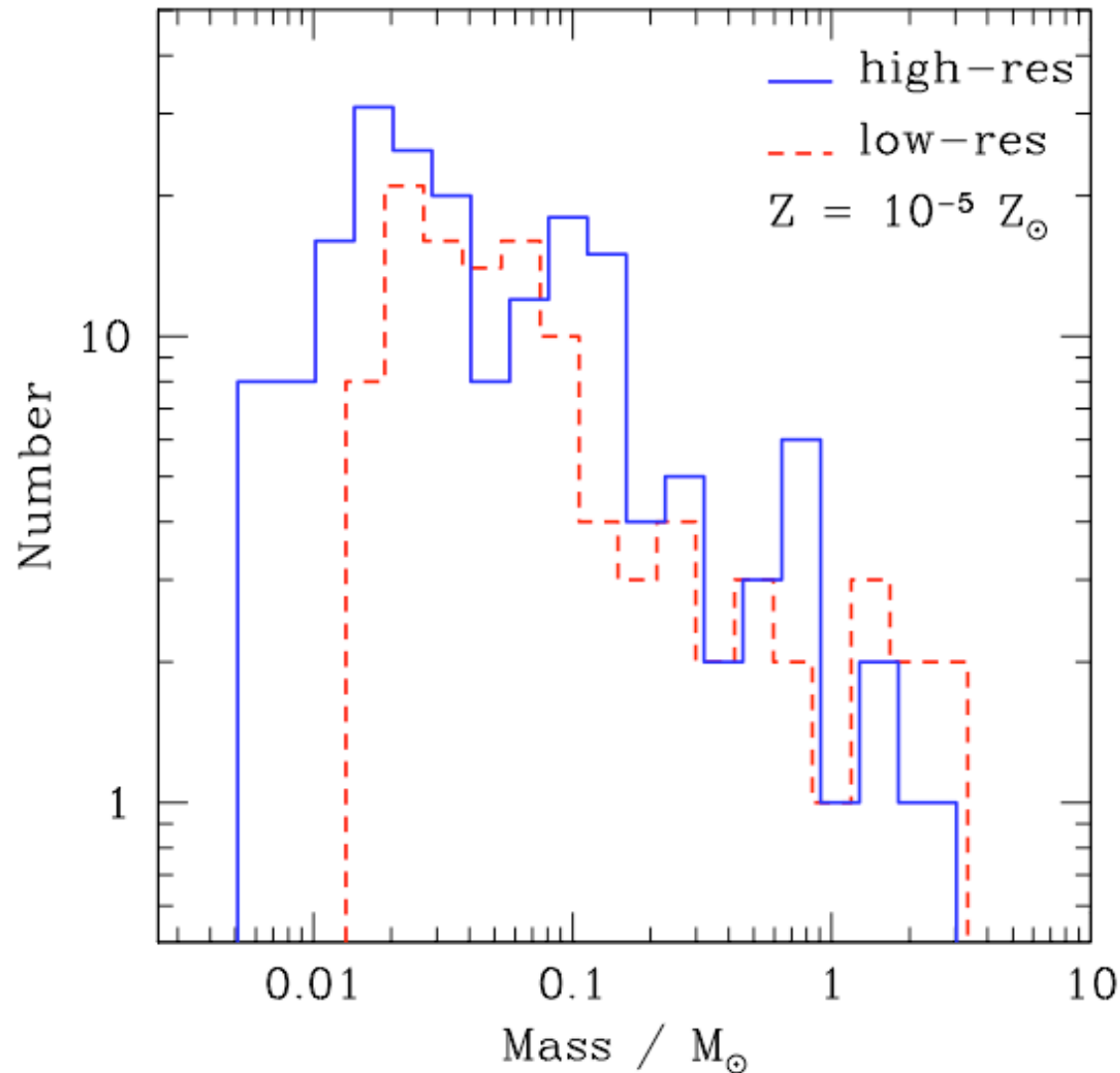


dense cluster of low-mass protostars builds up:

- mass spectrum peaks *below* $1 M_{sun}$
- cluster VERY dense
 $n_{stars} = 2.5 \times 10^9 pc^3$
- fragmentation at density
 $n_{gas} = 10^{12} - 10^{13} cm^{-3}$

(Clark et al. 2008, ApJ 672, 757)

dust induced fragmentation at $Z=10^{-5}$



dense cluster of low-mass protostars builds up:

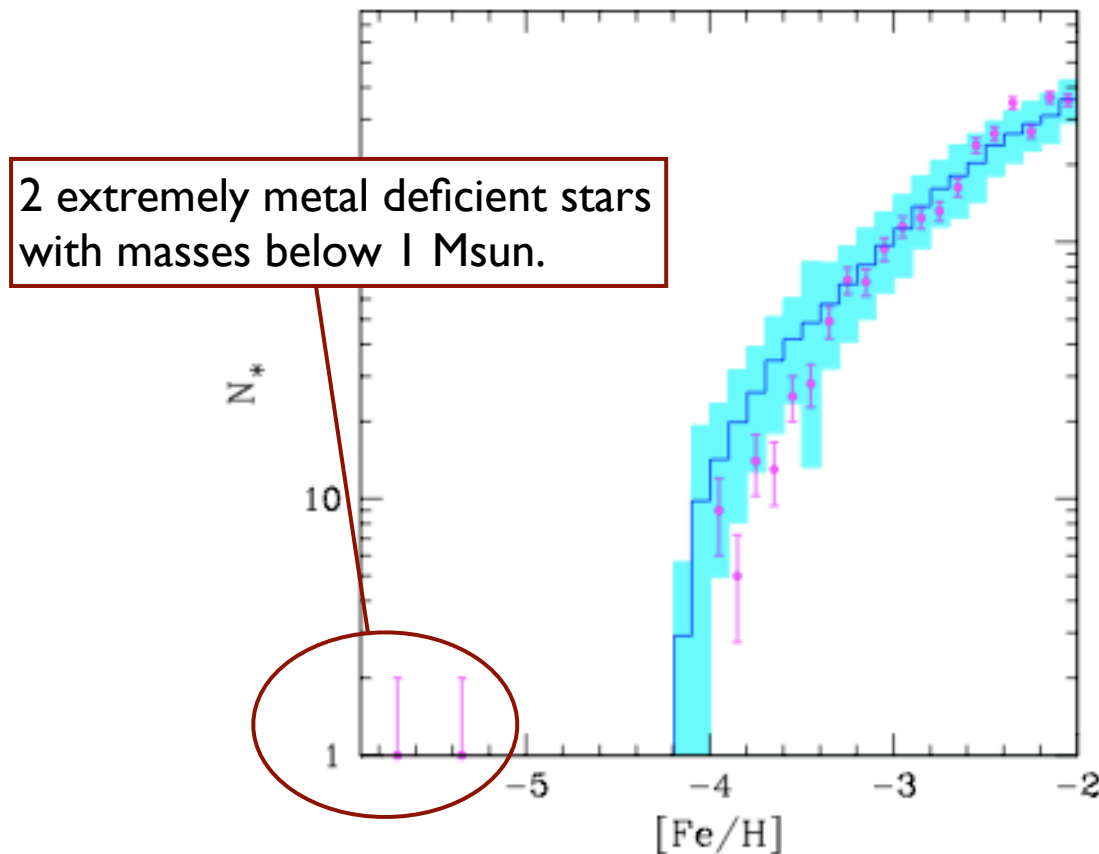
- mass spectrum peaks below $1 M_{\text{sun}}$
- cluster VERY dense
 $n_{\text{stars}} = 2.5 \times 10^9 \text{ pc}^{-3}$

- *predictions:*

- * low-mass stars with $[\text{Fe}/\text{H}] \sim 10^{-5}$
- * high binary fraction

(Clark et al. 2008)

dust induced fragmentation at $Z=10^{-5}$



(plot from Salvadori et al. 2006, data from Frebel et al. 2005)

dense cluster of low-mass protostars builds up:

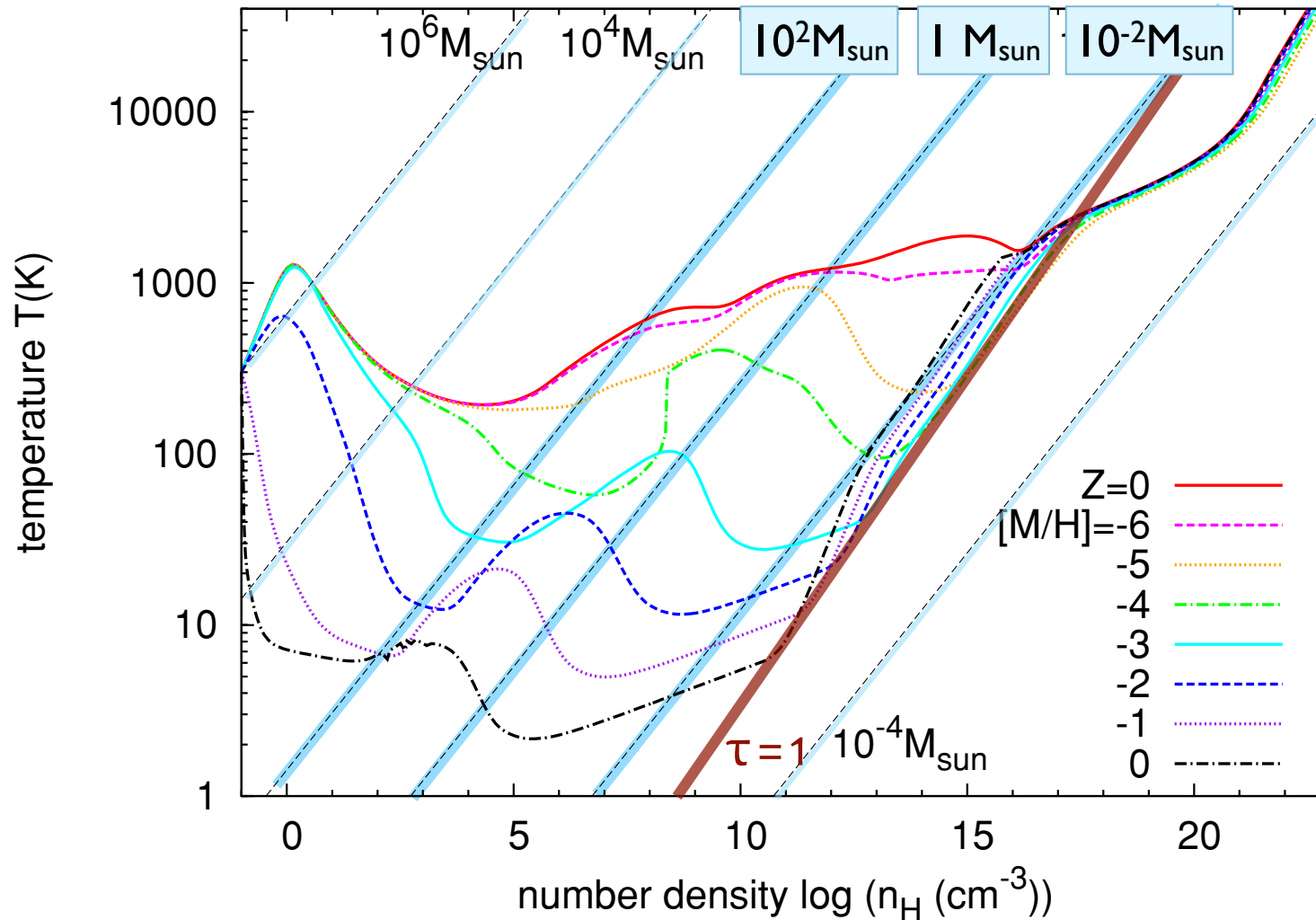
- mass spectrum peaks below 1 M_{sun}
- cluster VERY dense
 $n_{\text{stars}} = 2.5 \times 10^9 \text{ pc}^{-3}$

- *predictions:*

- * low-mass stars with $[\text{Fe}/\text{H}] \sim 10^{-5}$
- * high binary fraction

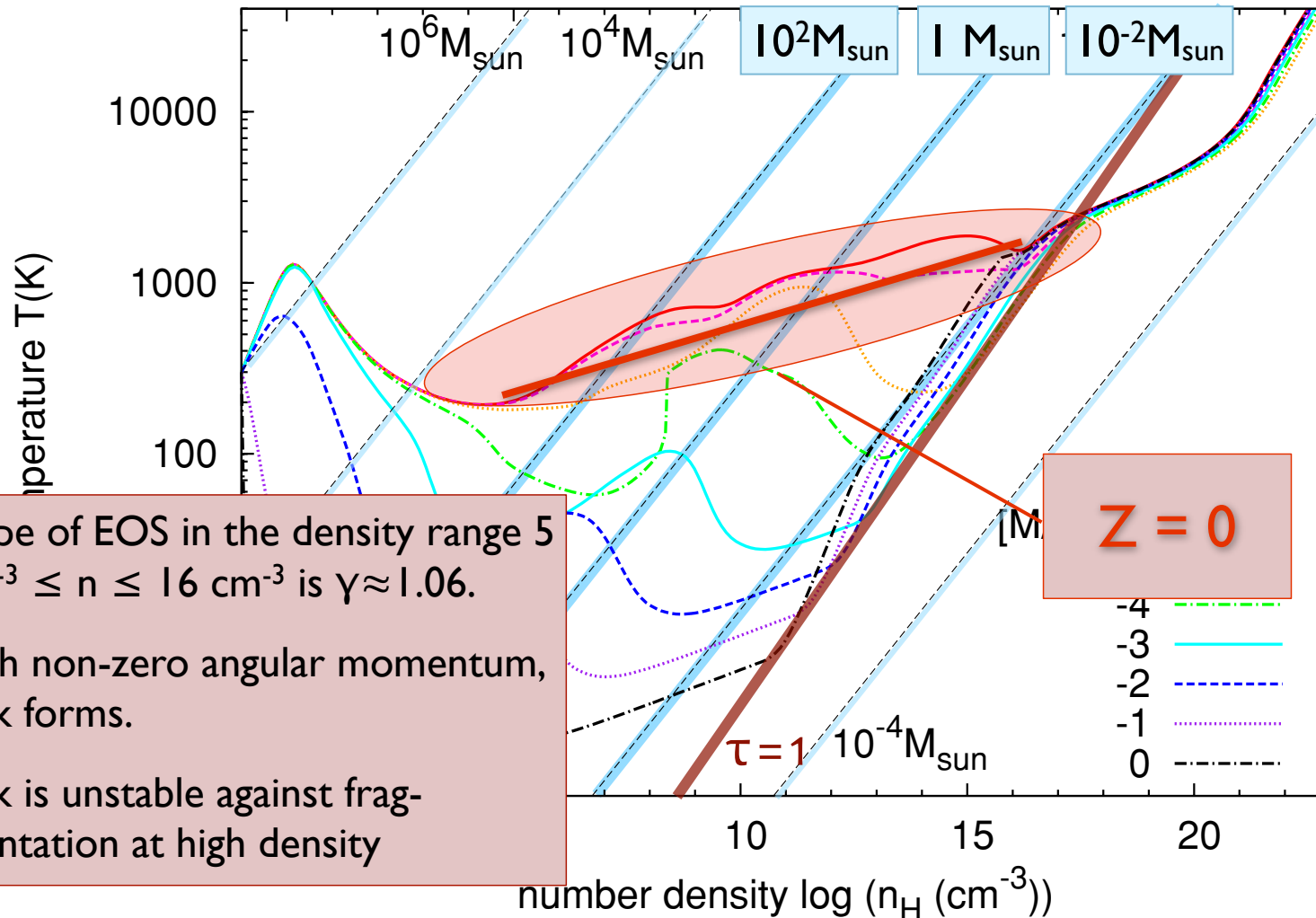
(Clark et al. 2008)

EOS as function of metallicity



(Omukai et al. 2005, 2010)

EOS as function of metallicity



- slope of EOS in the density range $5 \text{ cm}^{-3} \leq n \leq 16 \text{ cm}^{-3}$ is $\gamma \approx 1.06$.
- with non-zero angular momentum, disk forms.
- disk is unstable against fragmentation at high density

(Omukai et al. 2005, 2010)

“classical” picture

- most current numerical simulations of Pop III star formation predict very massive objects (e.g. Abel et al. 2002, Yoshida et al. 2008, Bromm et al. 2009)
- similar for theoretical models (e.g. Tan & McKee 2004)
- there are some first hints of fragmentation, however (Turk et al. 2009, Stacy et al. 2010)

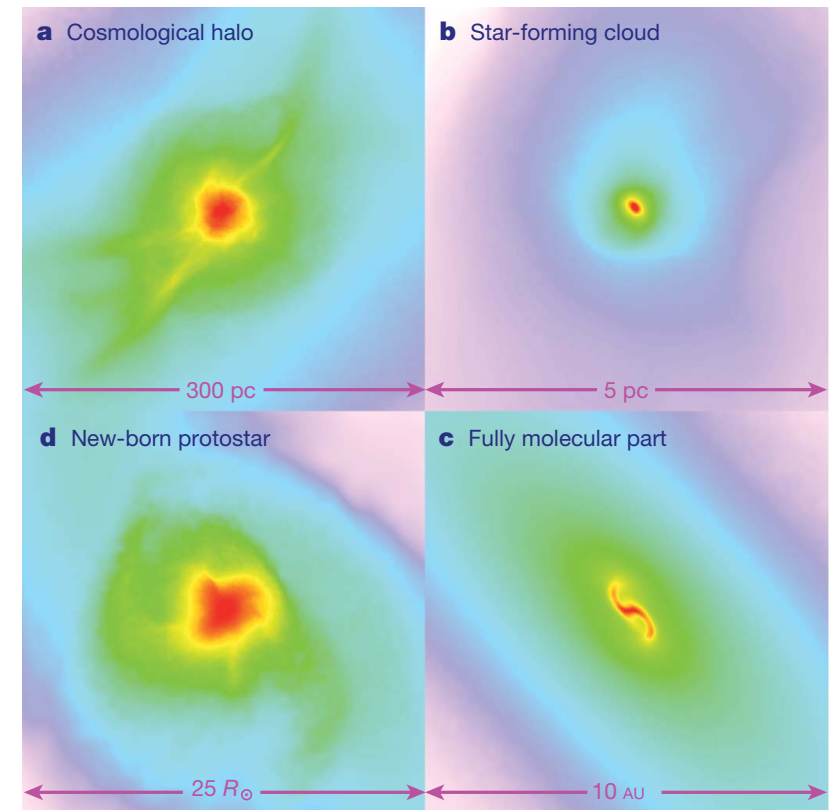
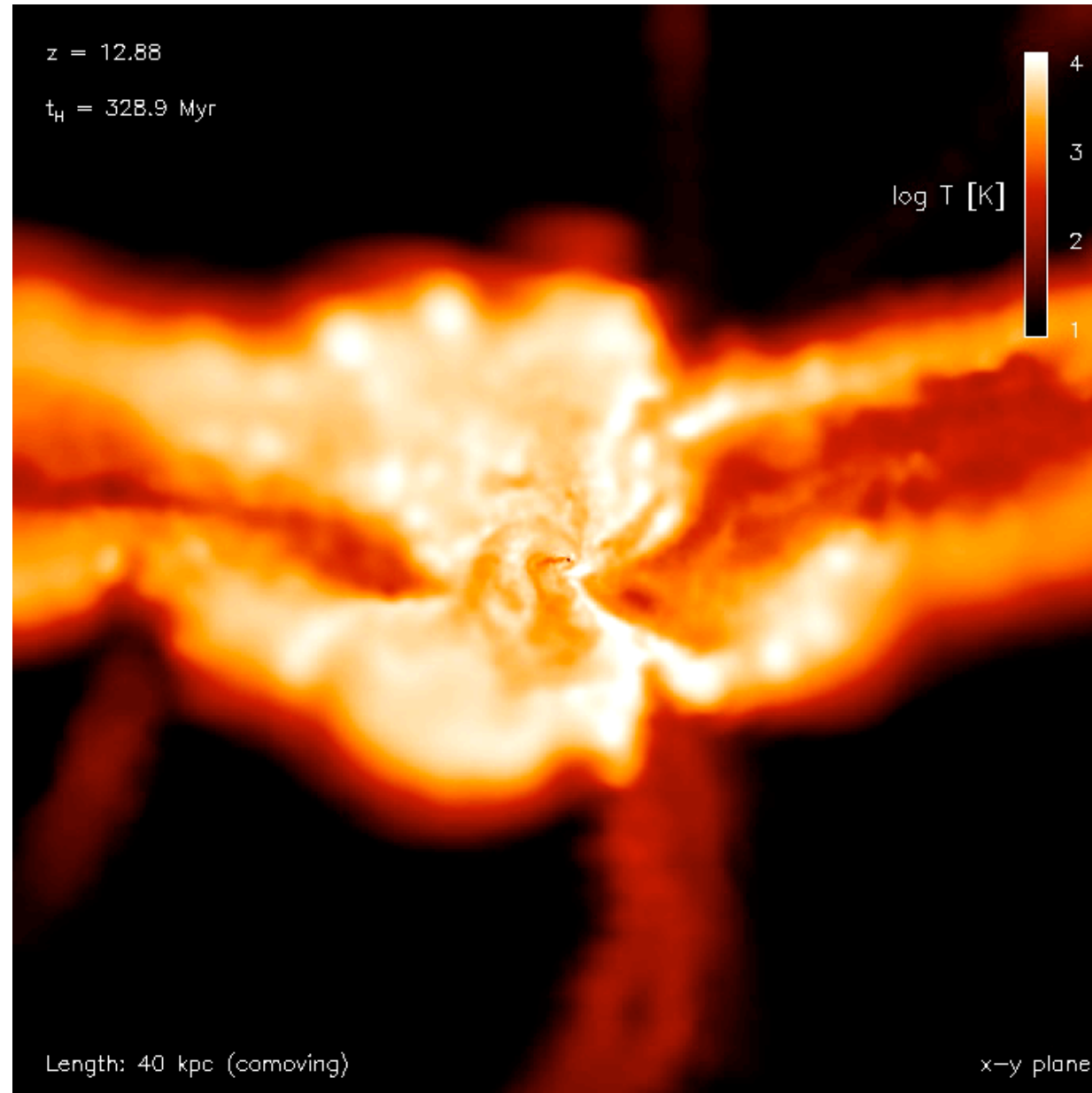


Figure 1 | Projected gas distribution around a primordial protostar. Shown is the gas density (colour-coded so that red denotes highest density) of a single object on different spatial scales. **a**, The large-scale gas distribution around the cosmological minihalo; **b**, a self-gravitating, star-forming cloud; **c**, the central part of the fully molecular core; and **d**, the final protostar. Reproduced by permission of the AAAS (from ref. 20).

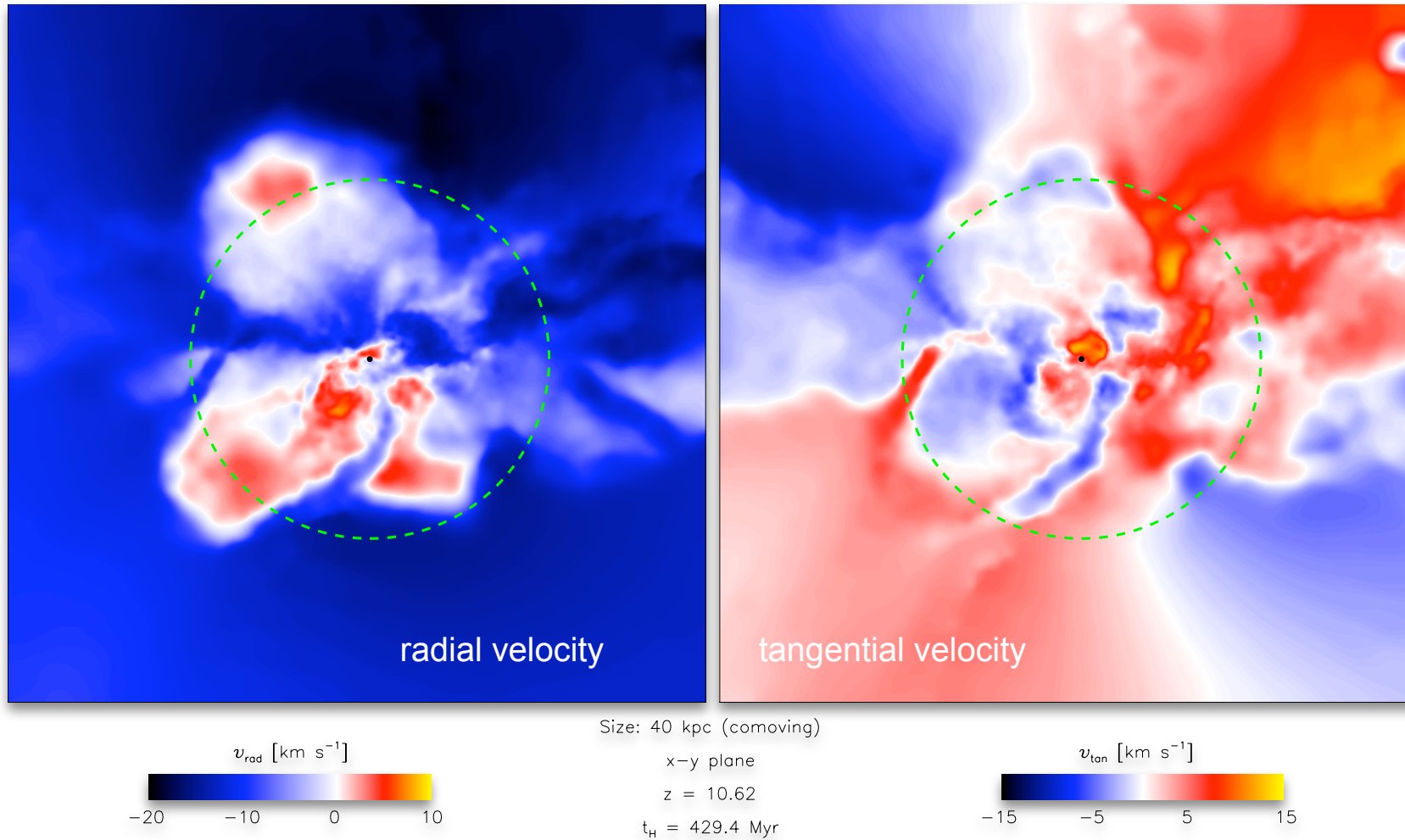
(Yoshida et al. 2008, *Science*, 321, 669)



turbulence developing in an atomic cooling halo



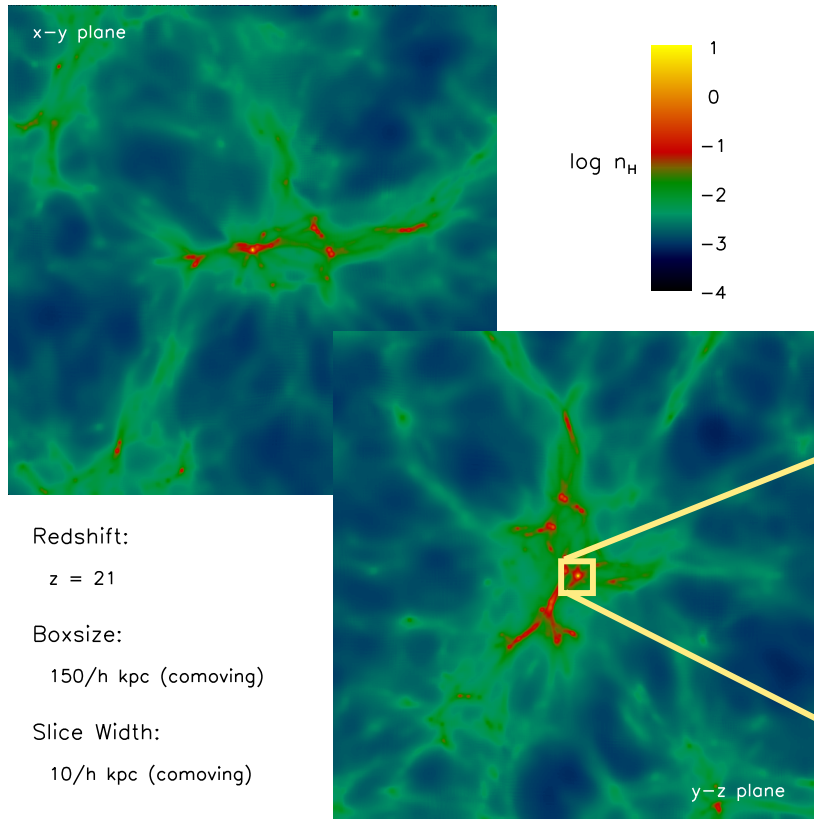
(Greif et al. 2008, see also Wise & Abel 2007)



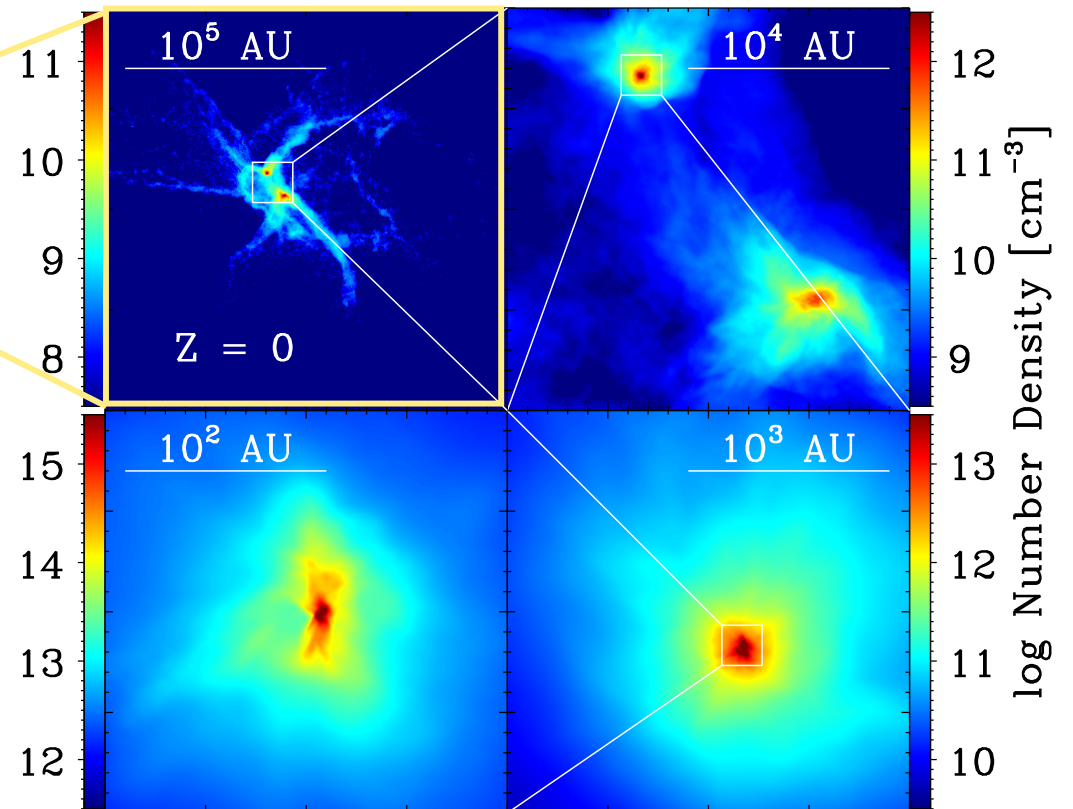
turbulence developing in an atomic cooling halo

(Greif et al. 2008)

detailed look at accretion disk around first star



successive zoom-in calculation from cosmological initial conditions (using SPH and new grid-code AREPO)

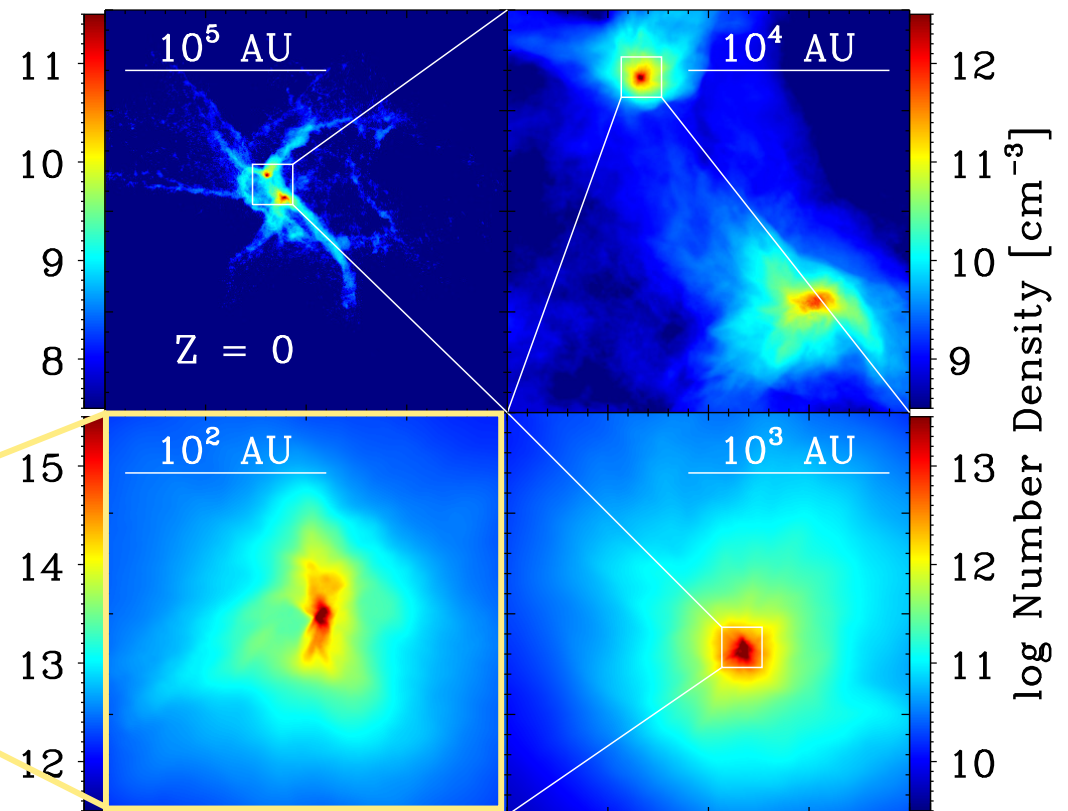


(Greif et al., 2007, ApJ, 670, 1)

(Greif et al. 2011, ApJ, 737, 75, Greif et al. 2012, MNRAS, 424, 399, Dopcke et al. 2012, ApJ submitted, arXiv/1203.6842)

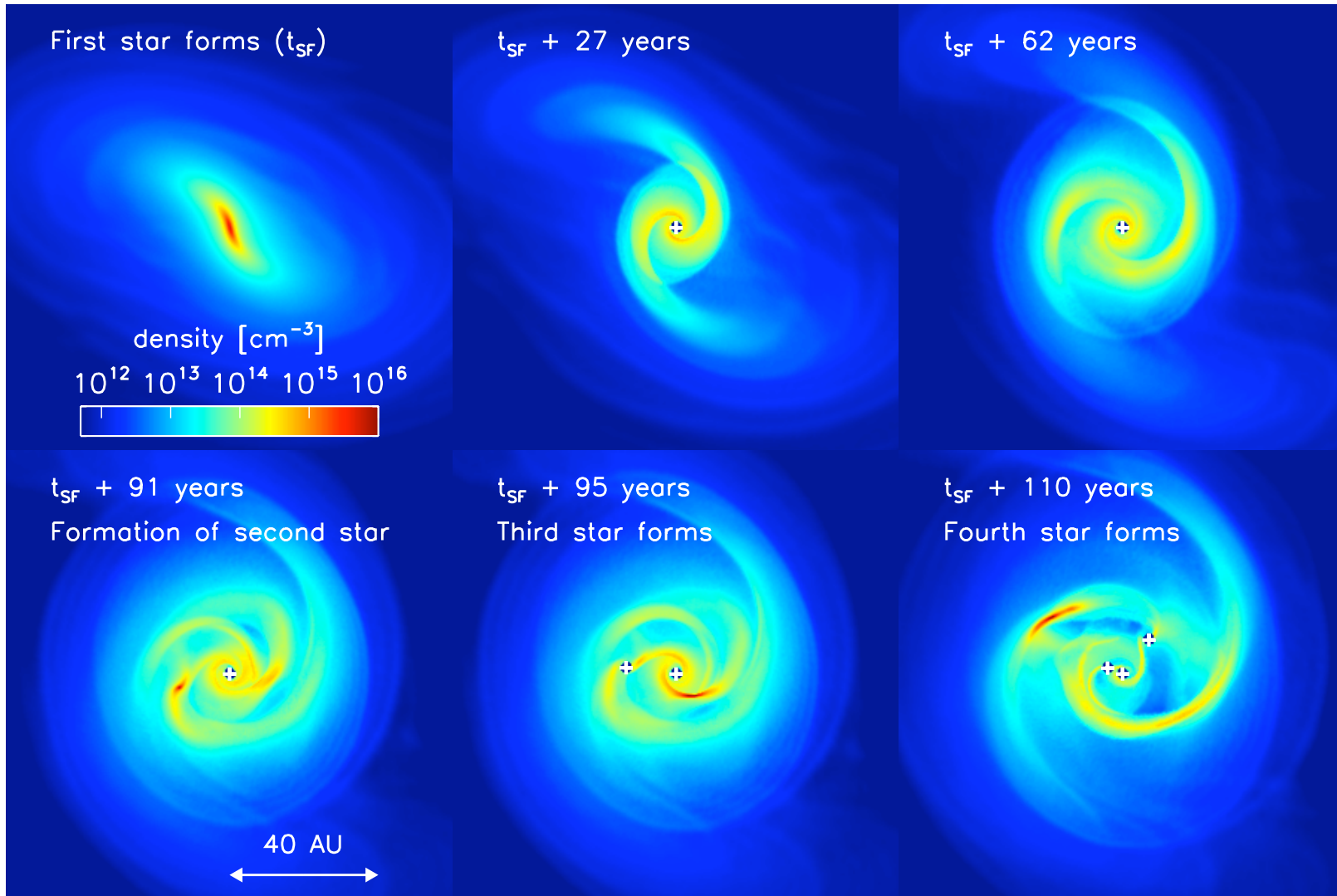
detailed look at accretion disk around first star

successive zoom-in calculation from
cosmological initial conditions (using
SPH and new grid-code AREPO)



what is the time
evolution of
accretion disk
around first star
to form?

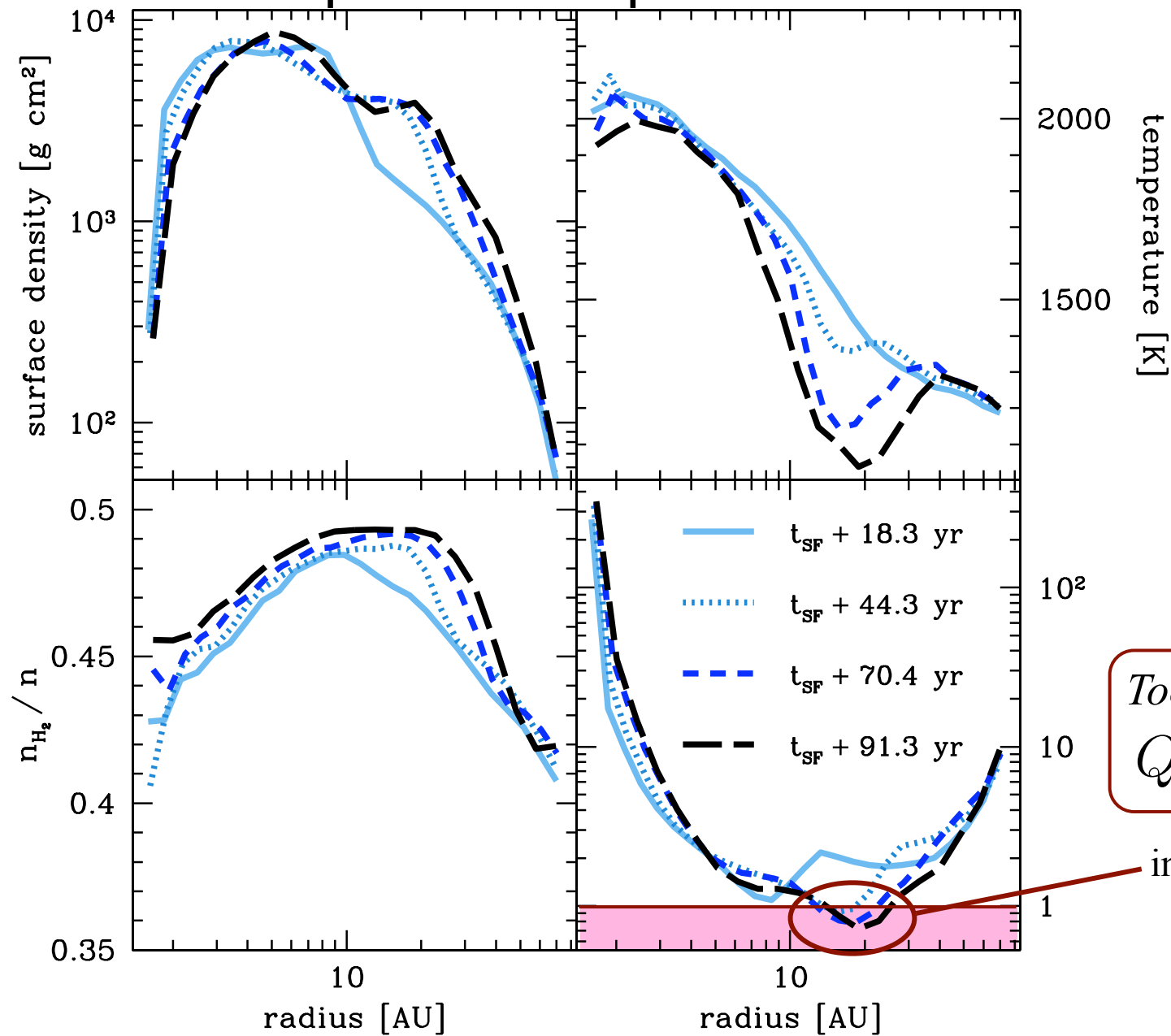
(Greif et al. 2011, ApJ, 737, 75, Greif et al. 2012, MNRAS, 424, 399,
Dopcke et al. 2012, ApJ submitted, arXiv/1203.6842)



detailed look at accretion disk

Figure 1: Density evolution in a 120 AU region around the first protostar, showing the build-up of the protostellar disk and its eventual fragmentation. We also see ‘wakes’ in the low-density regions, produced by the previous passage of the spiral arms.

important disk parameters



Toomre Q :

$$Q = c_s \kappa / \pi G \Sigma$$

instability for $Q < 1$

comparison of all relevant heating and cooling processes

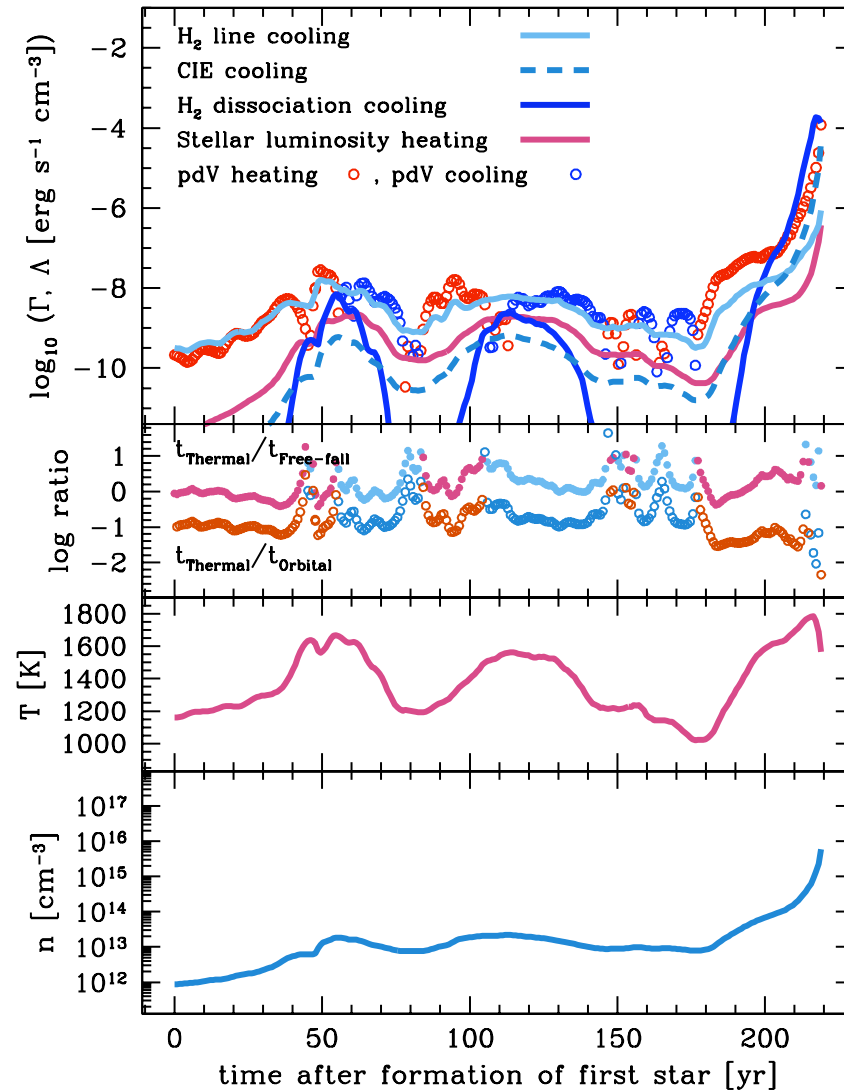
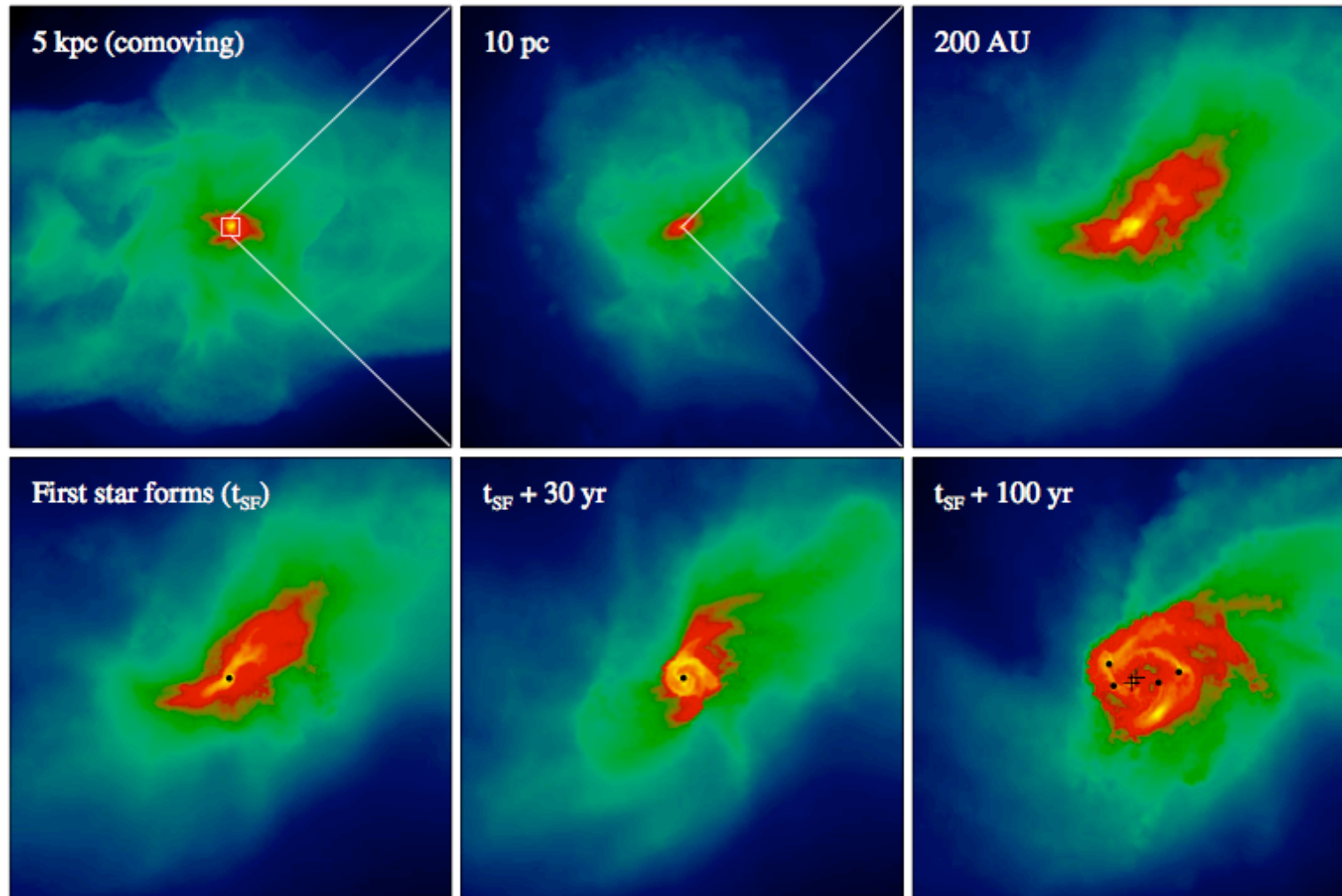


Figure 7: (a) Dominant heating and cooling processes in the gas that forms the second sink particle. (b) Upper line: ratio of the thermal timescale, t_{thermal} , to the free-fall timescale, t_{ff} , for the gas that forms the second sink particle. Periods when the gas is cooling are indicated in blue, while periods when the gas is heating are indicated in red. Lower line: ratio of t_{thermal} to the orbital timescale, t_{orbital} , for the same set of SPH particles (c) Temperature evolution of the gas that forms the second sink (d) Density evolution of the gas that forms the second sink

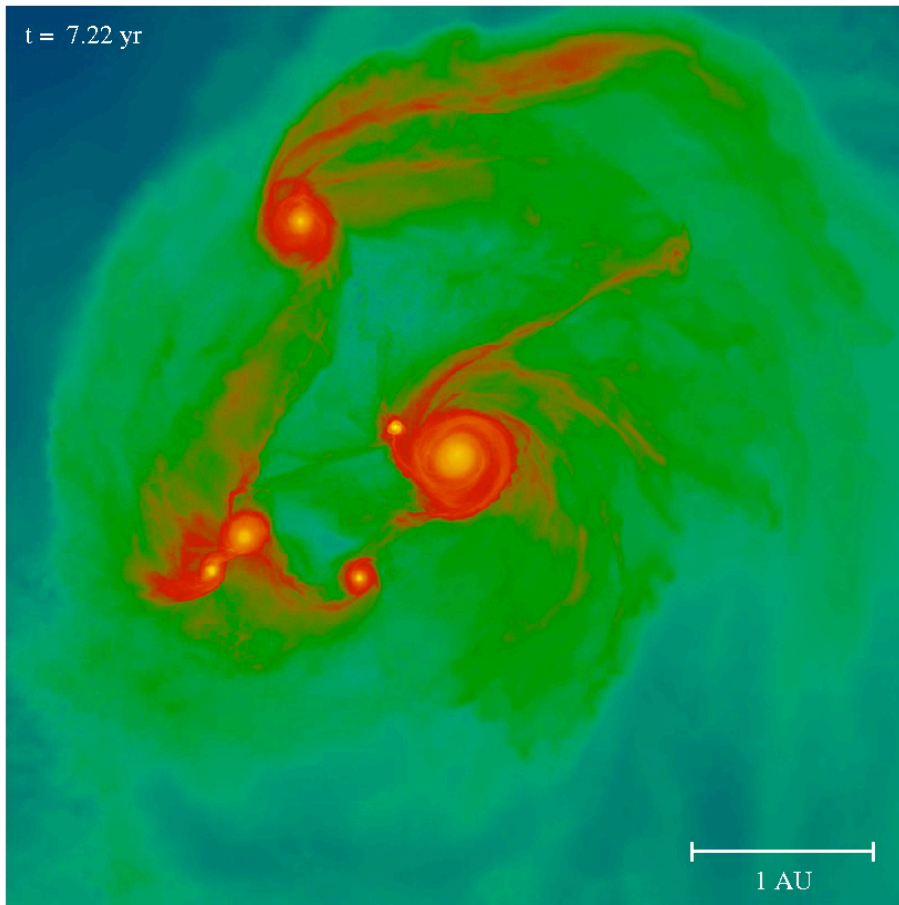
similar study with very different numerical method (AREPO)



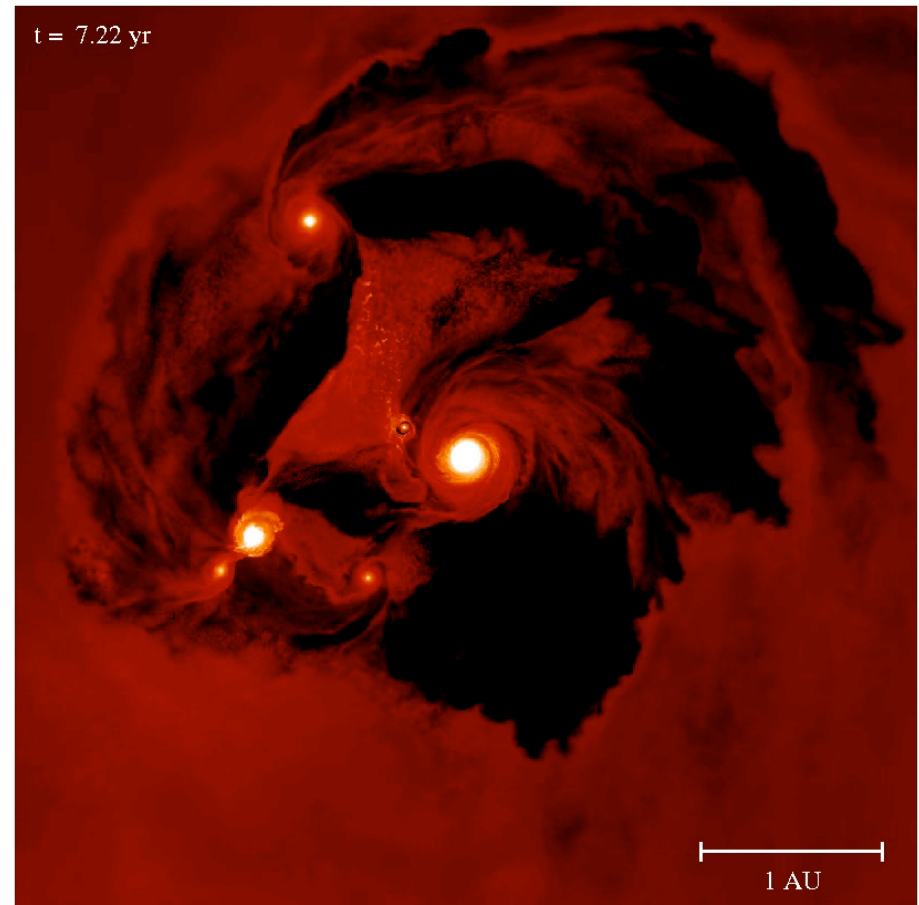
one out of five halos

Most recent calculations:

*fully sink-less simulations, following the disk build-up over ~ 10 years
(resolving the protostars - first cores - down to 10^5 km $\sim 0.01 R_{\odot}$)*

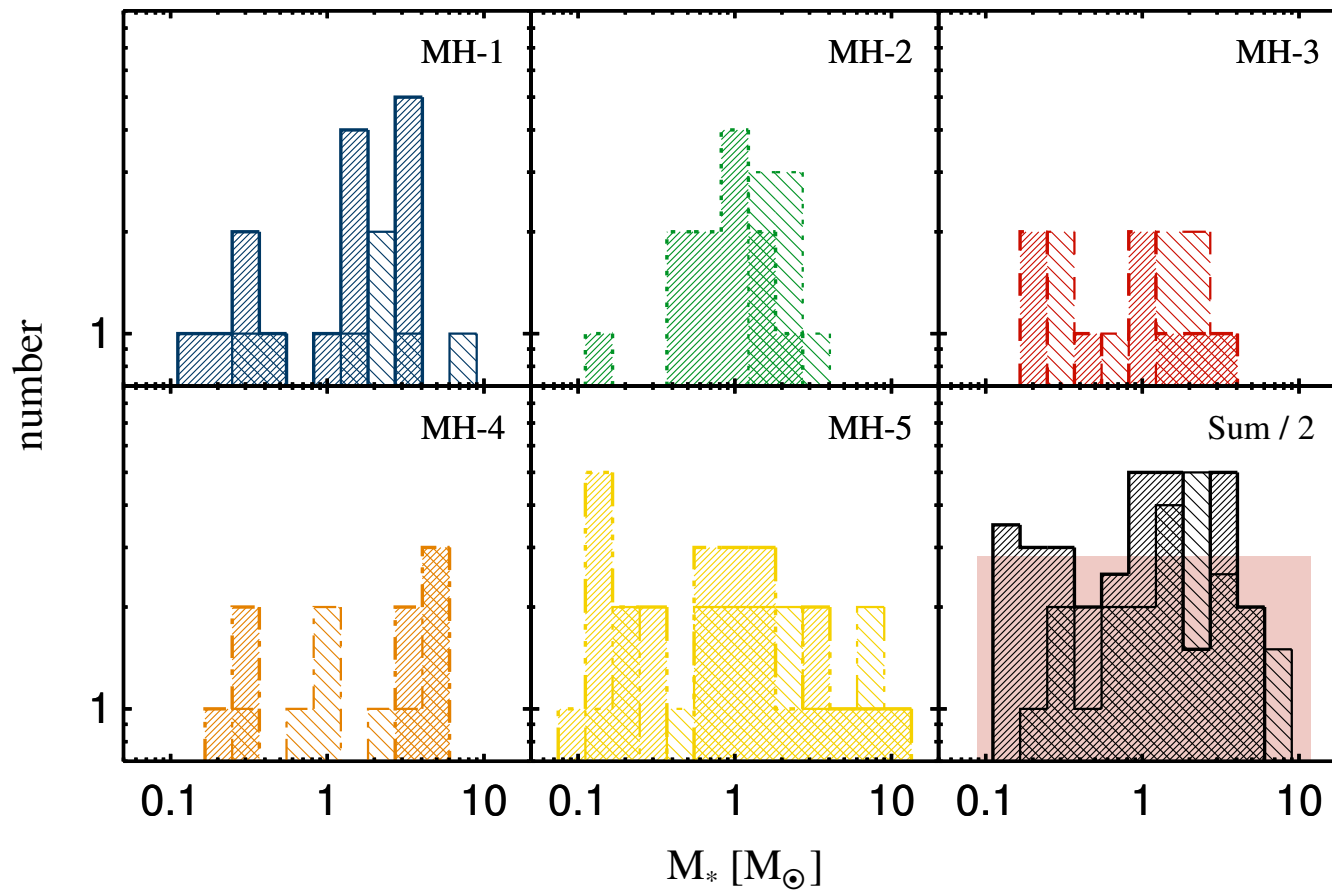


density



temperature

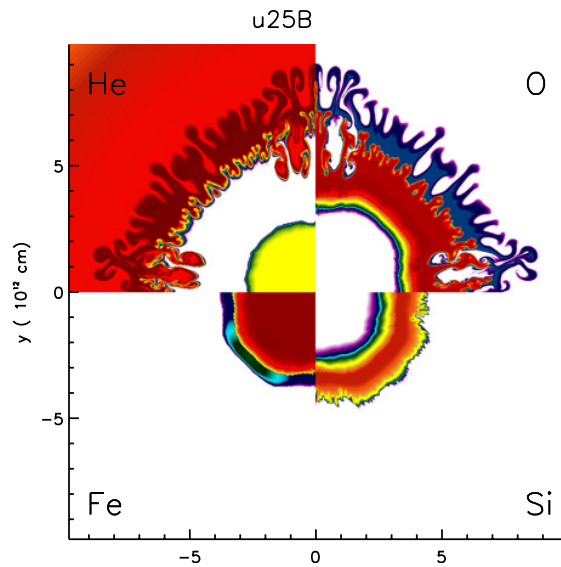
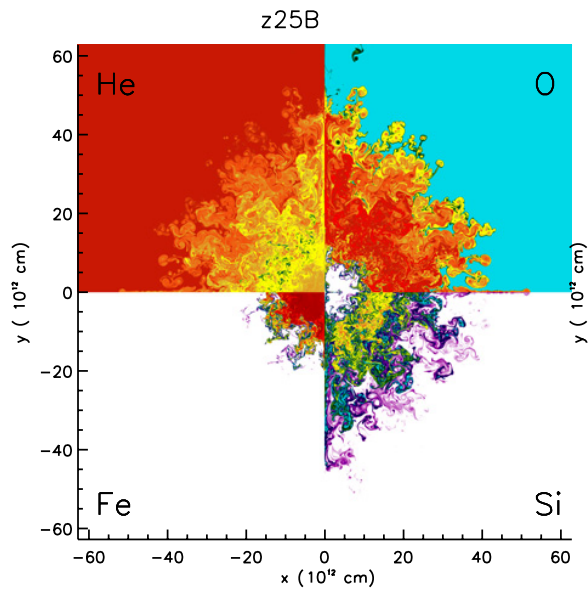
expected mass spectrum



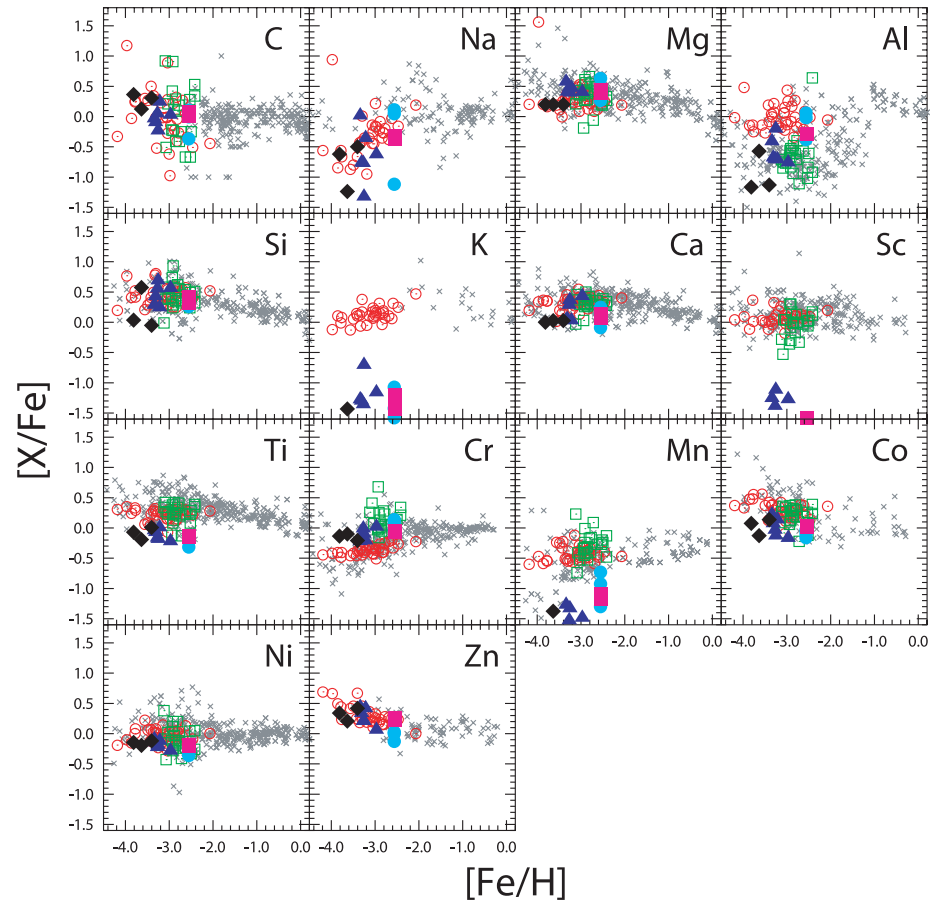
we see “flat”
mass spectrum

expected mass spectrum

- *expected IMF is flat* and covers a wide range of masses
- implications
 - because slope > -2 , most *mass is in massive objects* as predicted by most previous calculations
 - most high-mass Pop III stars should be in *binary systems* --> source of *high-redshift gamma-ray bursts*
 - because of ejection, some *low-mass objects* ($< 0.8 M_{\odot}$) might have *survived* until today and could potentially be found in the Milky Way
- consistent with abundance patterns found in second generation stars



(Joggerst et al. 2009, 2010)



(Tominaga et al. 2007)

The metallicities of extremely metal-poor stars in the halo are consistent with the yields of core-collapse supernovae, i.e. progenitor stars with 20 - 40 M_{\odot}

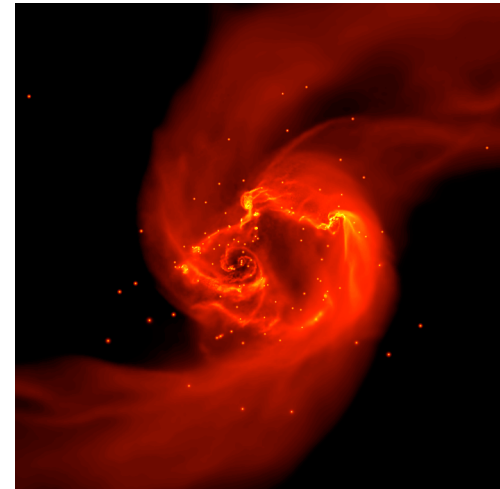
(e.g. Tominaga et al. 2007, Izutani et al. 2009, Joggerst et al. 2009, 2010)

primordial star formation

- just like in present-day SF, we expect
 - *turbulence*
 - *thermodynamics*
 - *feedback*
 - *magnetic fields*

to influence first star formation.

- masses of first stars still *uncertain* (surprises from new generation of high-resolution calculations that go beyond first collapse)
- disks unstable: first stars should be *binaries* or *part of small clusters*
- effects of feedback less important than in present-day SF



questions

- is claim of Pop III stars with $M \sim 0.5 M_{\odot}$ really justified?
 - stellar collisions
 - magnetic fields
 - radiative feedback
- how would we find them?
 - spectral features
- where should we look?
- what about magnetic fields?

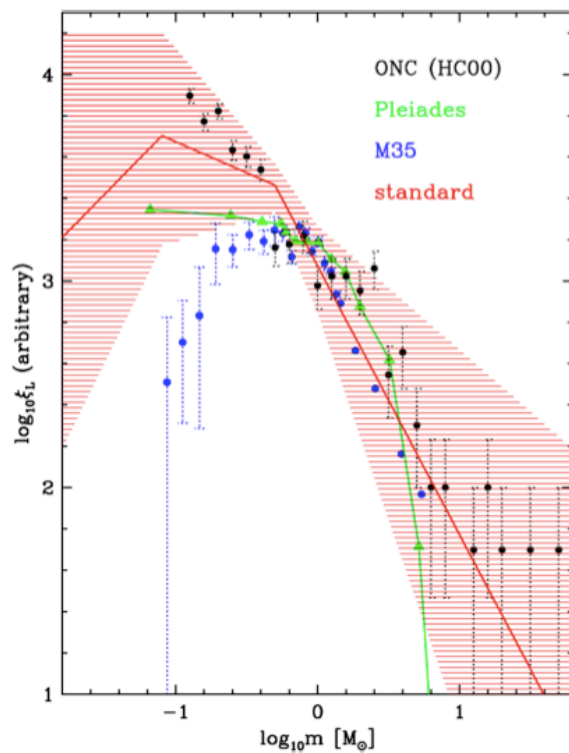
IMF

- distribution of stellar masses depends on
 - turbulent initial conditions
 - > mass spectrum of prestellar cloud cores
 - collapse and interaction of prestellar cores
 - > competitive accretion and N -body effects
 - thermodynamic properties of gas
 - > balance between heating and cooling
 - > EOS (determines which cores go into collapse)
 - *(proto) stellar feedback terminates star formation*
ionizing radiation, bipolar outflows, winds, SN

high-mass star formation

We want to address the following questions:

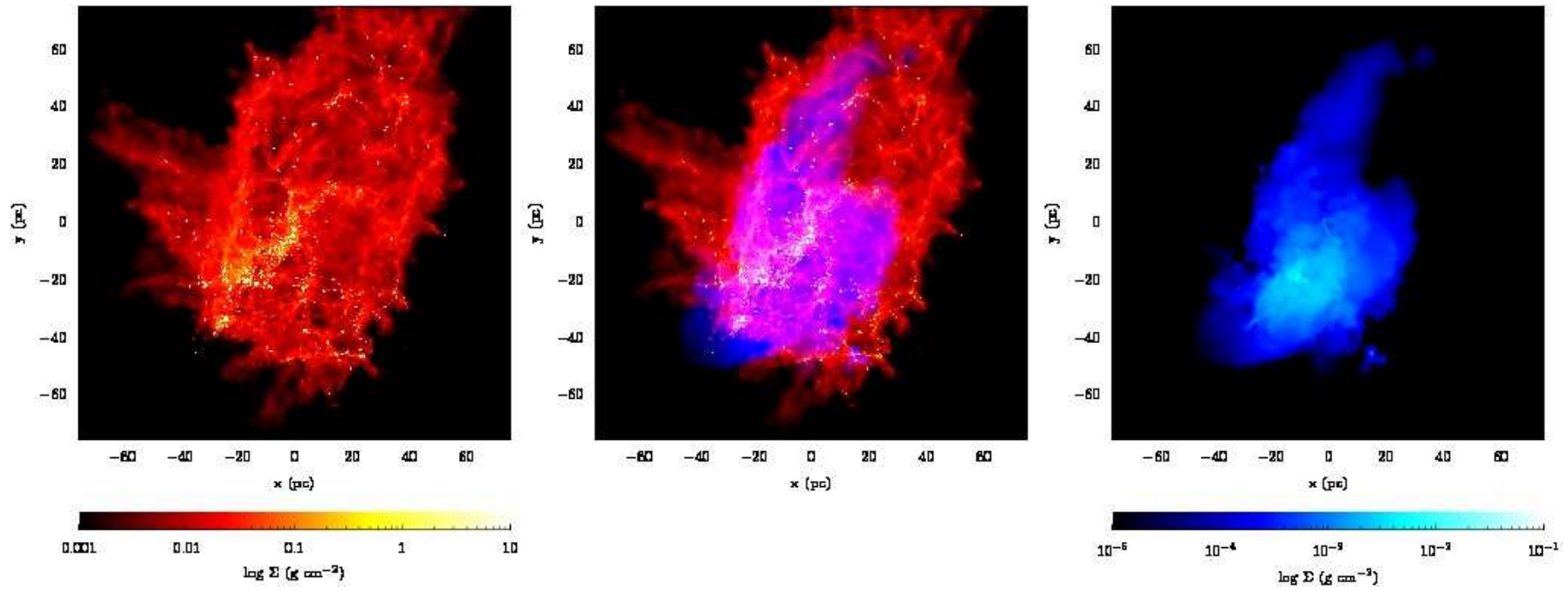
- how do massive stars (and their associated clusters) form?
- what determines the upper stellar mass limit?
- what is the physics behind observed HII regions?



IMF (Kroupa 2002)



Rosetta nebula (NGC 2237)



(c) Column density plots of cold neutral gas and stars (left panel), cold neutral gas and hot ionized gas (centre panel) and hot ionized gas alone (left panel) 2.18 Myr after ionization was turned on.

from Dale & Bonnell (2012)

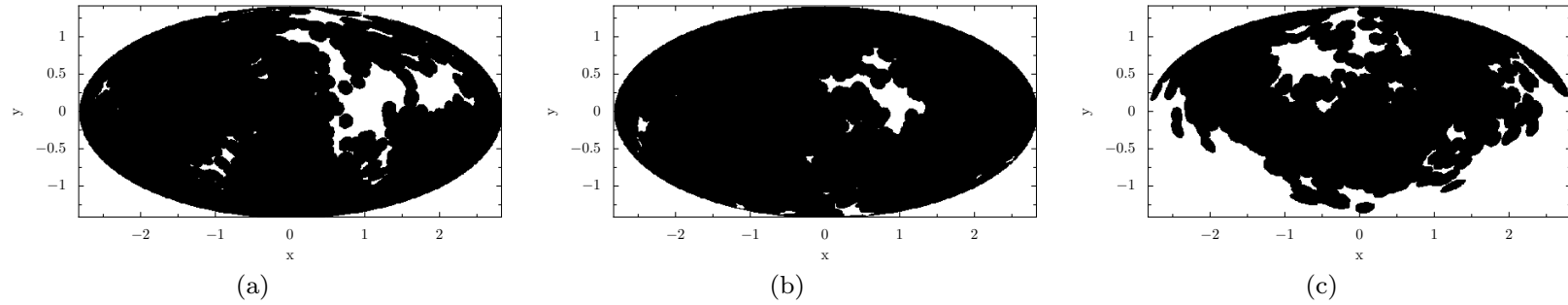


Figure 7. Hammer projections showing directions in which ionizing radiation is absorbed before reaching a radius of 5pc (black areas) from the point of view of three sources at the time when ionizing radiation was switched on.

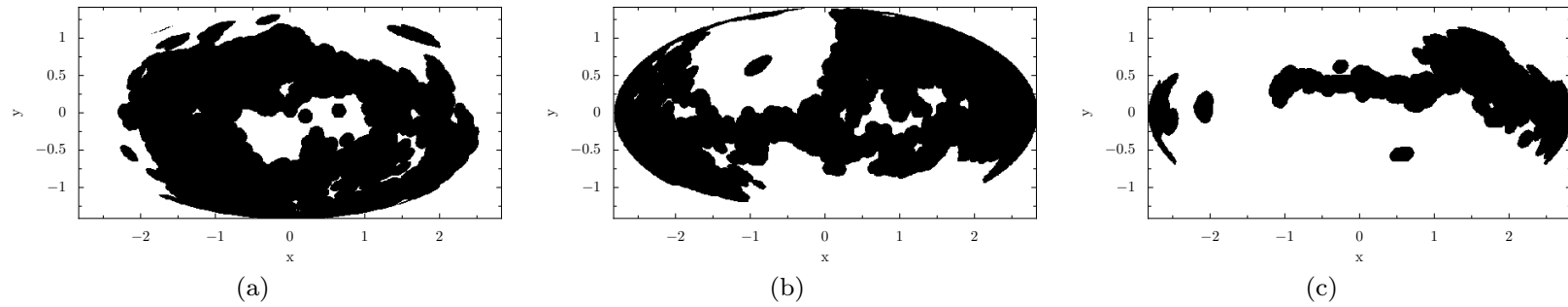
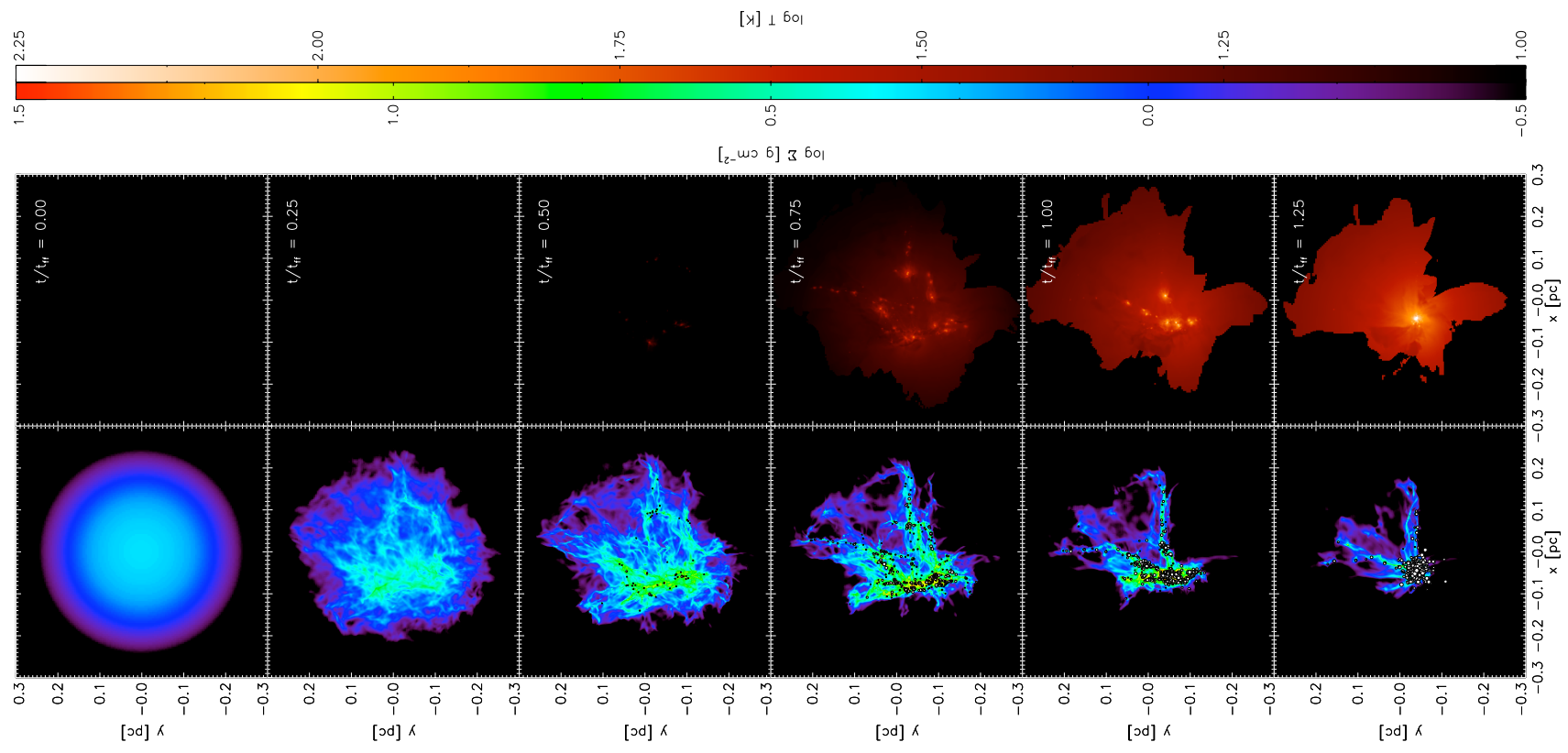


Figure 8. Hammer projections showing directions in which ionizing radiation is absorbed before reaching a radius of 5pc (black areas) from the point of view of three sources 1.62 Myr after ionizing radiation was switched on.



Krumholz et al. (2012)

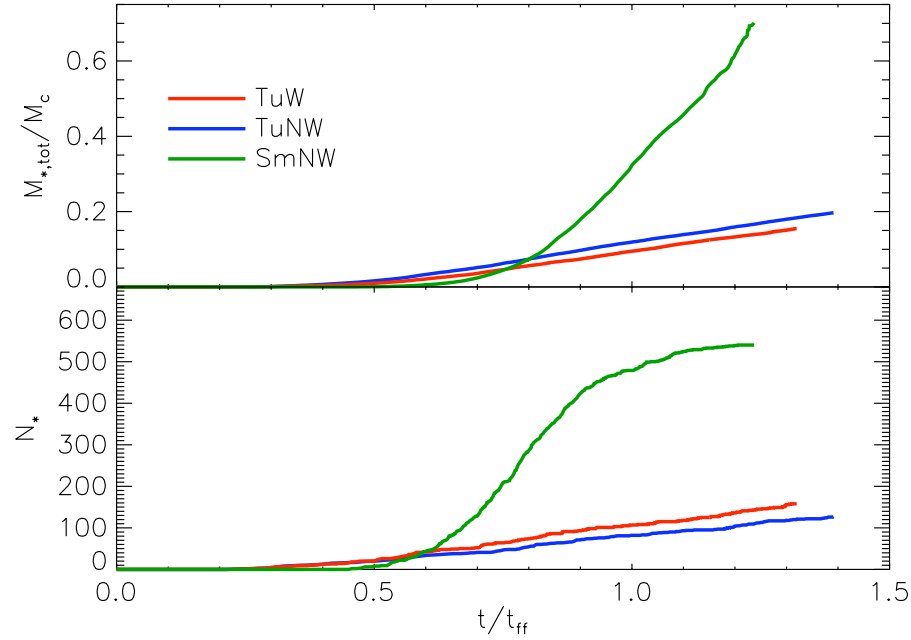


FIG. 5.— Total mass in stars (top) and total number of stars (bottom) as a function of time in runs SmNW, TuNW, and TuW.

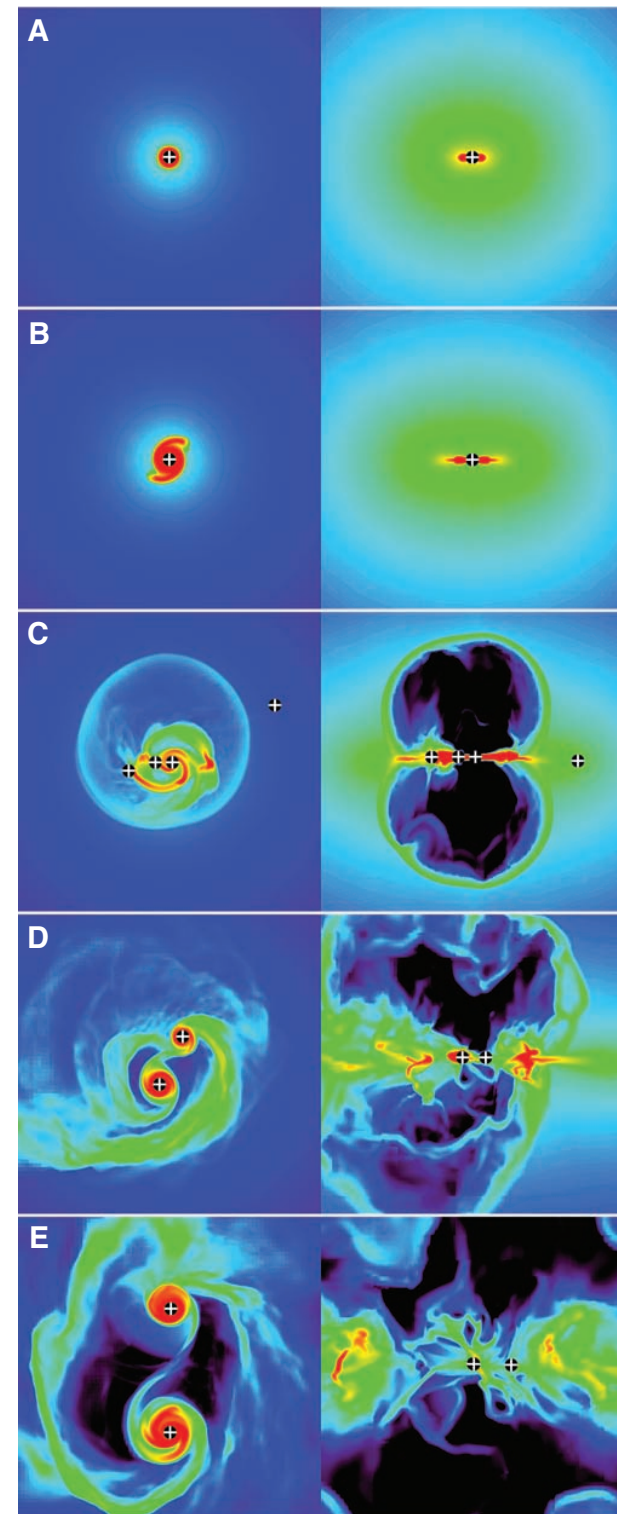
Name	Winds?	M_c (M_\odot)	ℓ_c or R_c (pc)	σ_c (km s^{-1})	$\langle \rho \rangle_M$ (g cm^{-3})	t_{ff} (kyr)	ℓ_{box} (pc)	N_0	L	Δx_L (AU)
SmNW	No	1000	0.26	2.9	1.4×10^{-18}	56	1.9	256	5	49
TuNW	No	1000	0.46	1.4	8.6×10^{-18}	23	0.46	256	4	23
TuW	Yes	1000	0.46	1.4	8.6×10^{-18}	23	0.46	256	4	23

NOTE. — Col. 3: cloud mass. Col. 4: cloud radius (for run SmNW) or box size (for runs TuNW and TuW). Col. 6: mass weighted-mean density at time $t = 0$. Col. 7: free-fall time computed using $\langle \rho \rangle_M$. Col. 8: size of computational box. Col. 9: number of cells per linear dimension on the coarsest AMR level. Col. 10: finest AMR level. Col. 11: grid resolution on the finest AMR level.

radiative feedback does not
limit disk accretion (radiation
modeled as radiation pressure)

Krumholz et al. (2009)

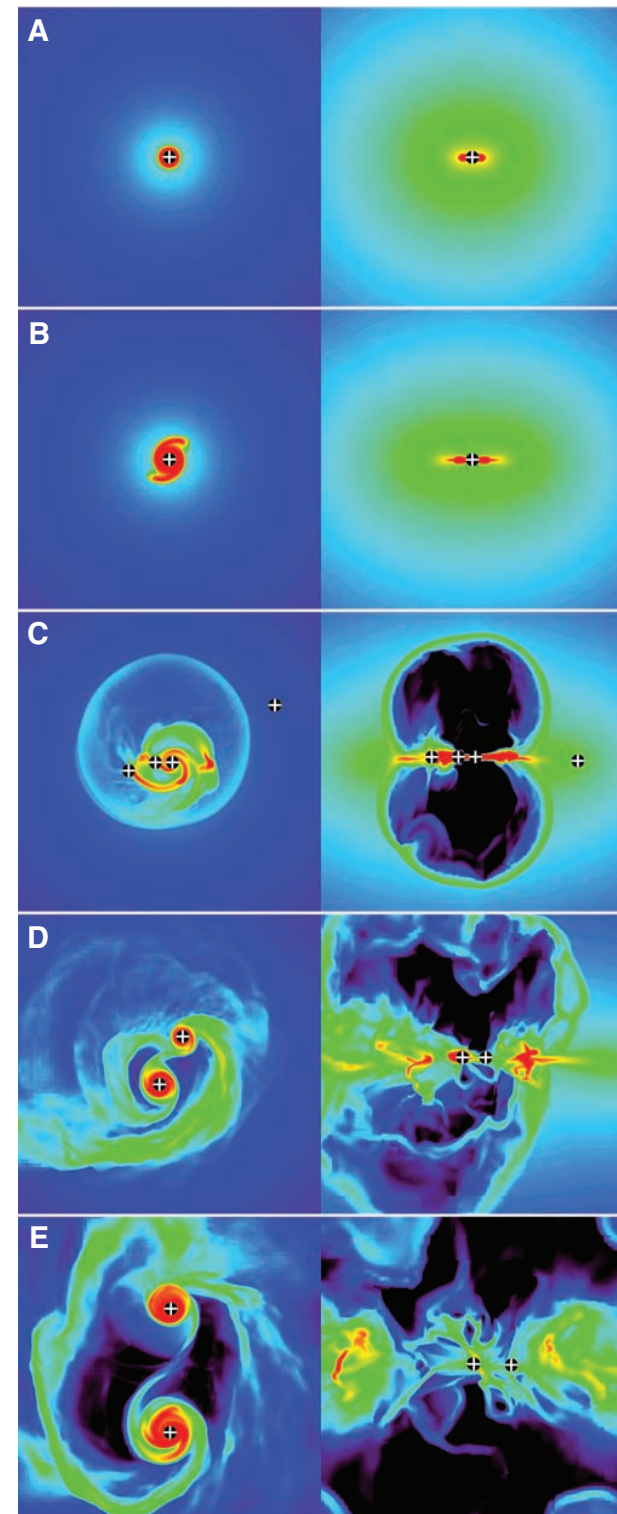
Fig. 1. Snapshots of the simulation at (A) 17,500 years, (B) 25,000 years, (C) 34,000 years, (D) 41,700 years, and (E) 55,900 years. In each panel, the left image shows column density perpendicular to the rotation axis in a $(3000 \text{ AU})^2$ region; the right image shows volume density in a $(3000 \text{ AU})^2$ slice along the rotation axis. The color scales are logarithmic (black at the minimum, red at the maximum), from 10^0 to $10^{2.5} \text{ g cm}^{-2}$ on the left and 10^{-18} to $10^{-14} \text{ g cm}^{-3}$ on the right. Plus signs indicate the projected positions of stars. See figs. S1 to S3 and movie S1 for additional images.



radiative feedback does not
limit disk accretion (radiation
modeled as radiation pressure)

Krumholz et al. (2009)

Fig. 1. Snapshots of the simulation at (A) 17,500 years, (B) 25,000 years, (C) 34,000 years, (D) 41,700 years, and (E) 55,900 years. In each panel, the left image shows column density perpendicular to the rotation axis in a $(3000 \text{ AU})^2$ region; the right image shows volume density in a $(3000 \text{ AU})^2$ slice along the rotation axis. The color scales are logarithmic (black at the minimum, red at the maximum), from 10^0 to $10^{2.5} \text{ g cm}^{-2}$ on the left and 10^{-18} to $10^{-14} \text{ g cm}^{-3}$ on the right. Plus signs indicate the projected positions of stars. See figs. S1 to S3 and movie S1 for additional images.



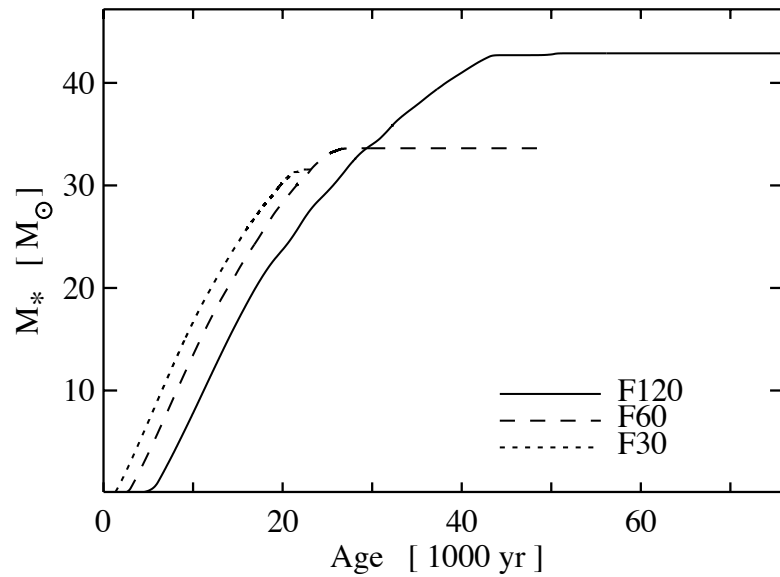
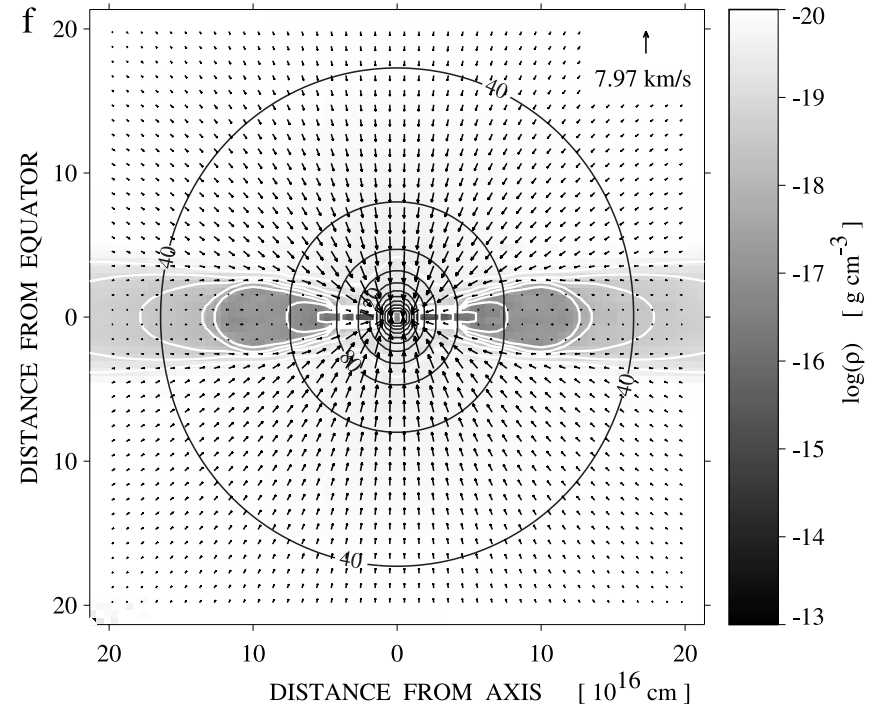


FIG. 6.—Evolution of the central (proto)stars' masses for the frequency-dependent F sequences. After an initial delay, the mass accretion rates rise rapidly to comparable values (given by the slope of the curves) and fall off rapidly as radiative effects inhibit further accretion (see also Fig. 7).



note in comparison: 2D calculations do show the termination of mass growth

(proto)stellar feedback processes

- radiation pressure on dust particles
- ionizing radiation
- stellar winds
- jets and outflows



ionization

- very few numerical studies so far, detailed collapse calculations with ionizing and non-ionizing feedback still missing
- H II regions around massive stars are directly observable
--> direct comparison between theory and observations

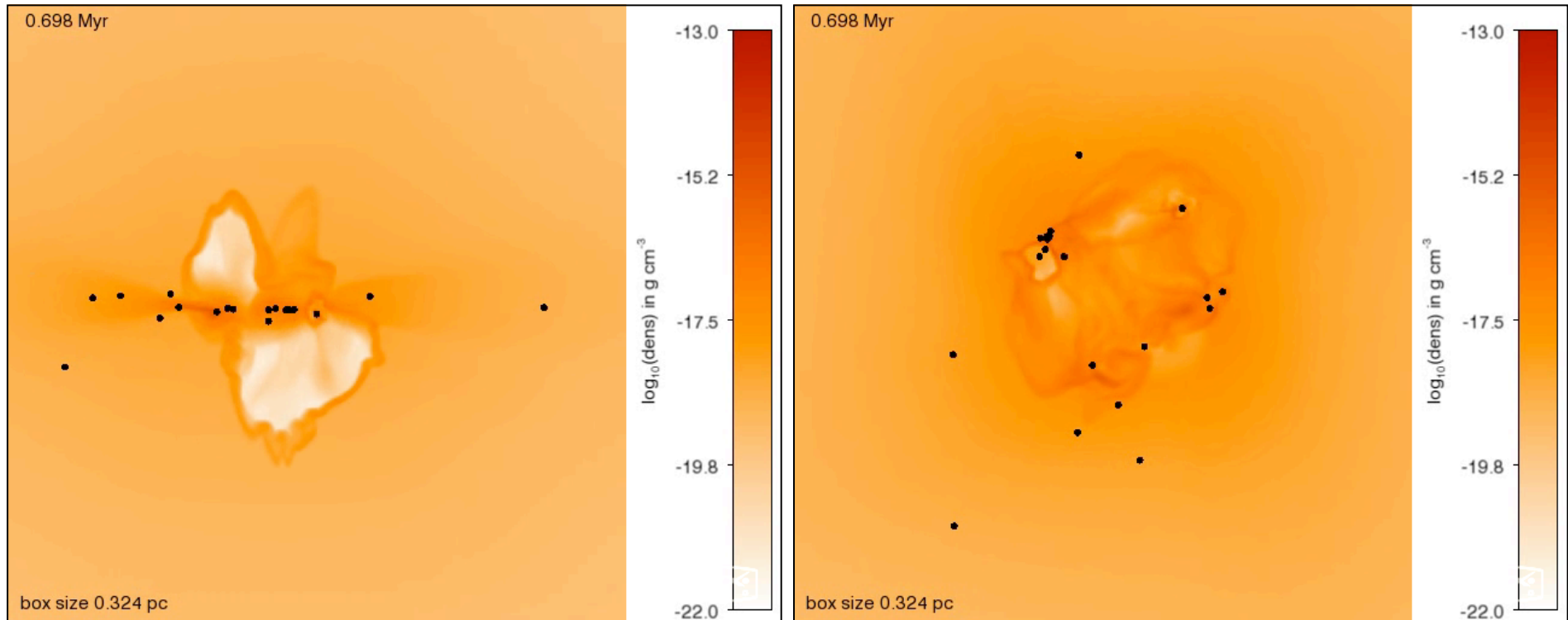
our (numerical) approach

- focus on collapse of individual high-mass cores...
 - massive core with $1,000 M_{\odot}$
 - Bonnor-Ebert type density profile
(flat inner core with 0.5 pc and $\rho \sim r^{-3/2}$ further out)
 - initial $m=2$ perturbation, rotation with $\beta = 0.05$
 - sink particle with radius 600 AU and threshold density of $7 \times 10^{-16} \text{ g cm}^{-3}$
 - cell size 100 AU

our (numerical) approach

- method:
 - FLASH with ionizing and non-ionizing radiation using raytracing based on hybrid-characteristics
 - protostellar model from Hosokawa & Omukai
 - rate equation for ionization fraction
 - relevant heating and cooling processes
 - some models include magnetic fields

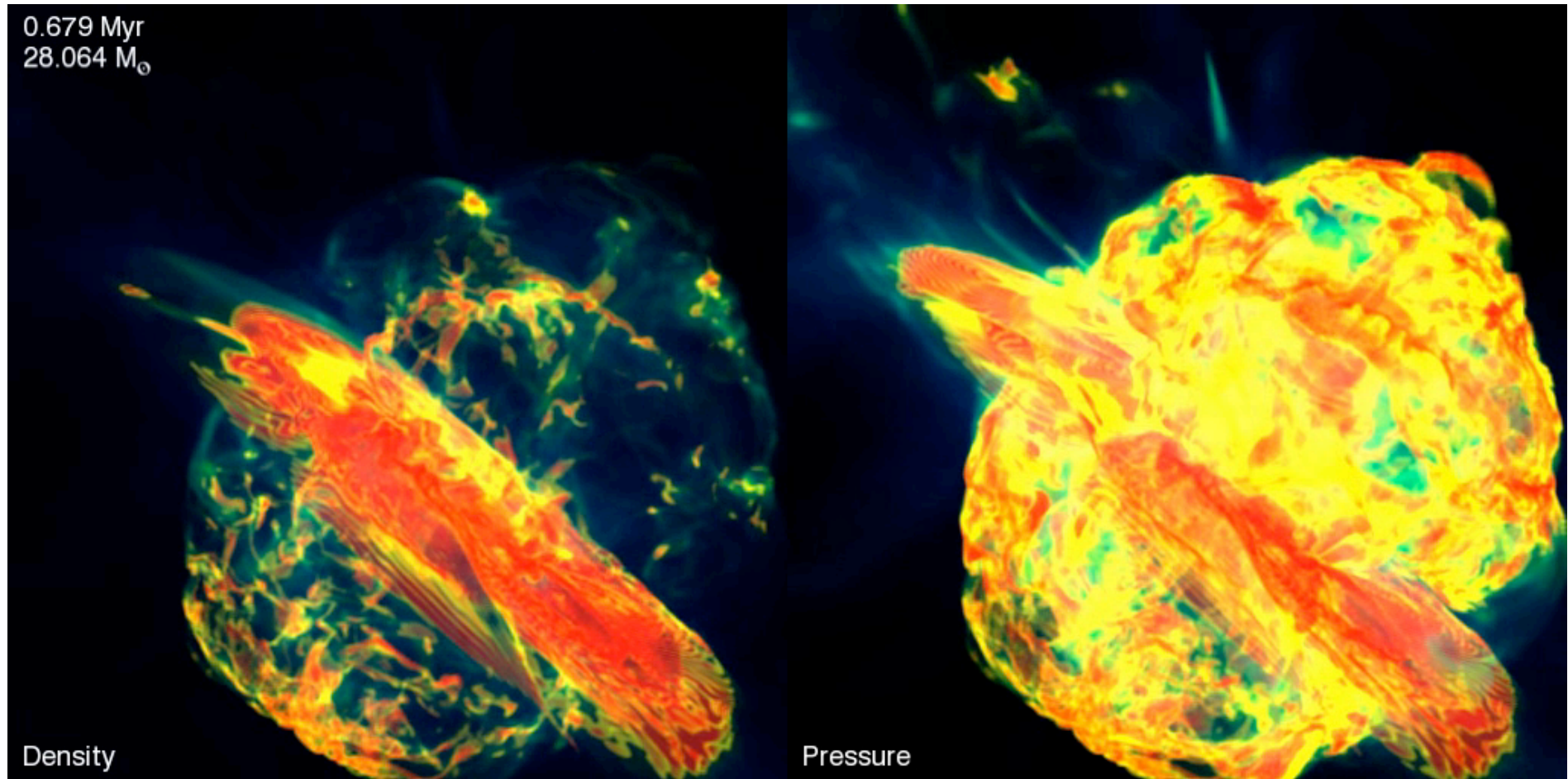
model of high mass star formation



Disk edge on

Disk plane

influence of B on disk evolution



Peters et al. (2011)

in disk around high-mass stars, fragmentation is reduced but rarely fully suppressed
see Peters et al. (2011), Hennebelle et al. (2011), Seifried et al. (2011)

interplay of ionization and B-field

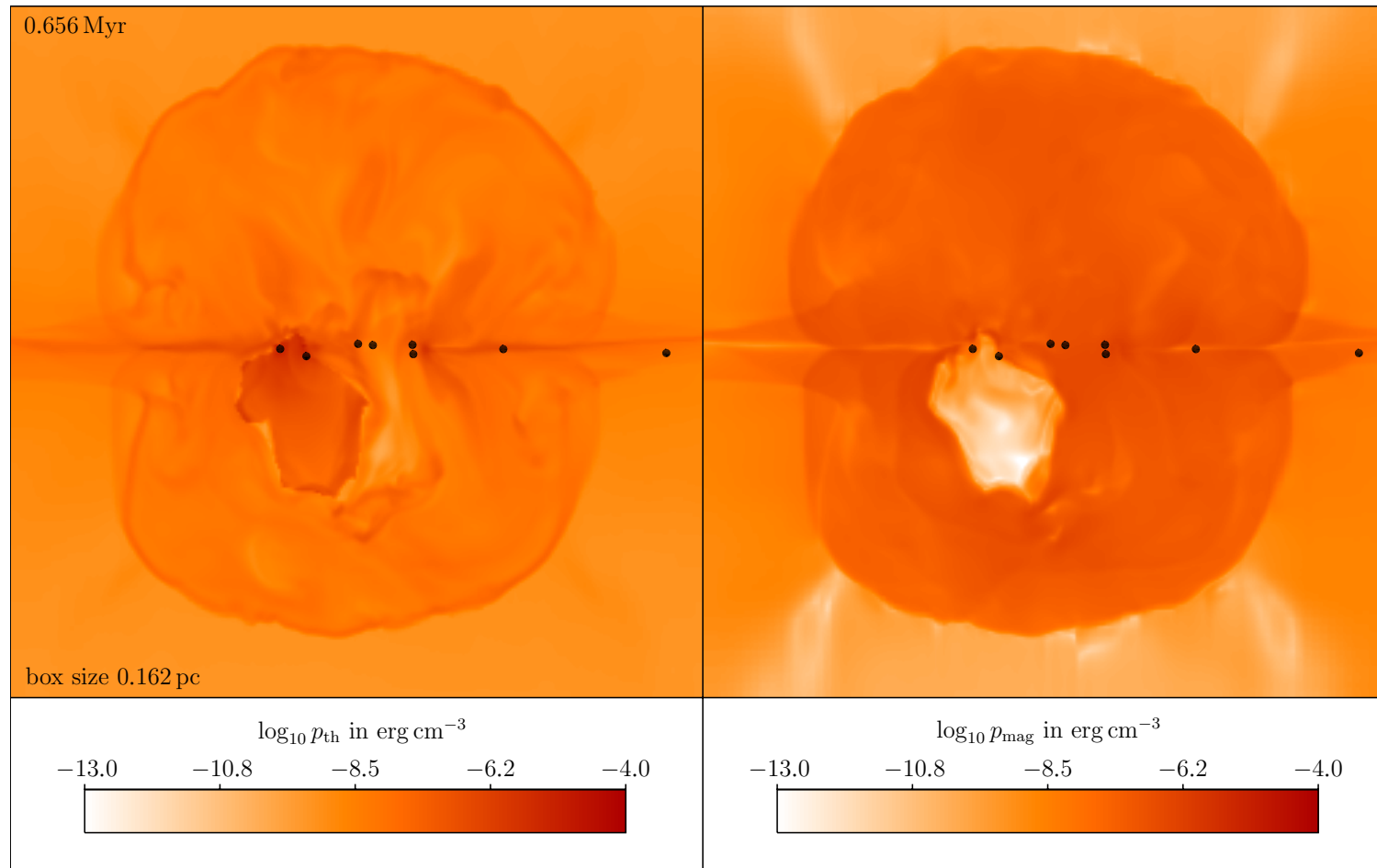
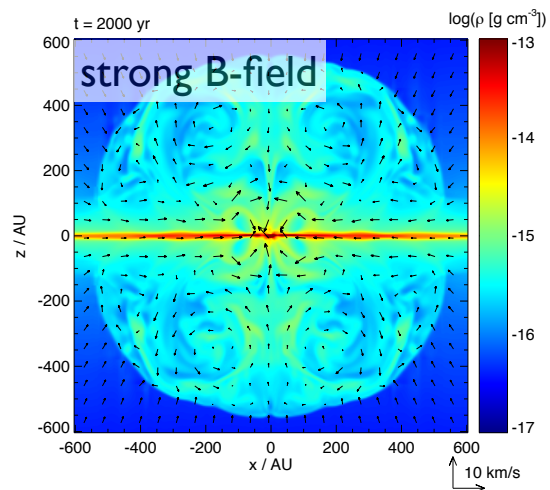
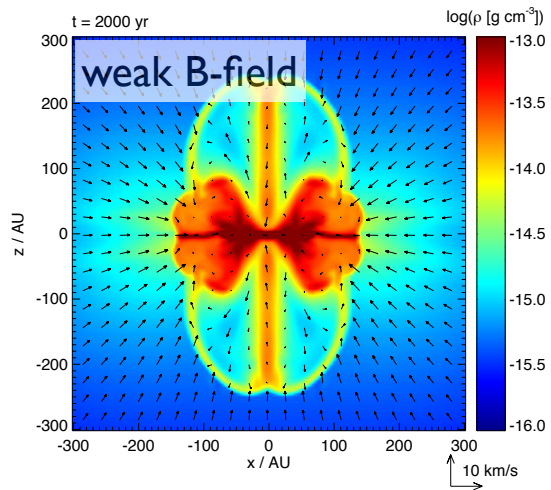
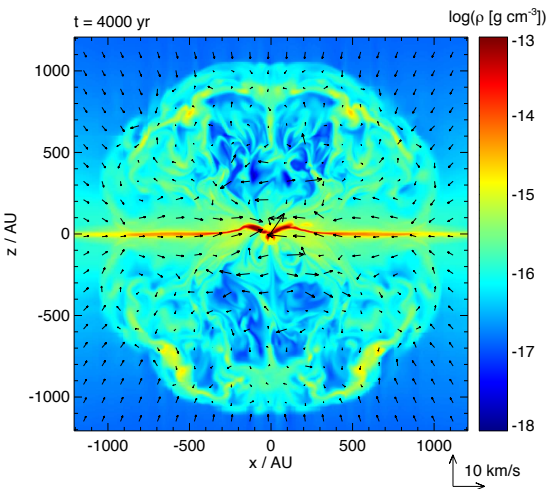
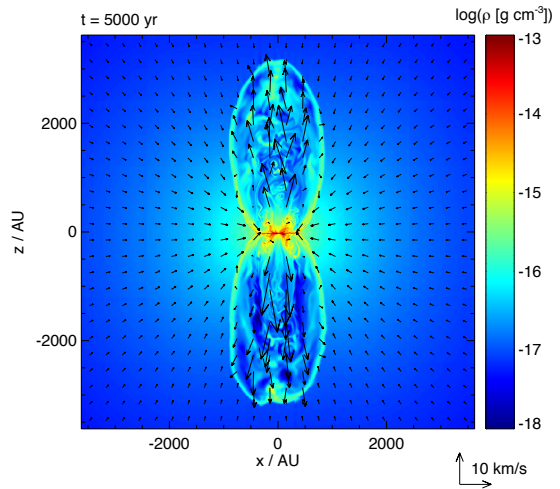


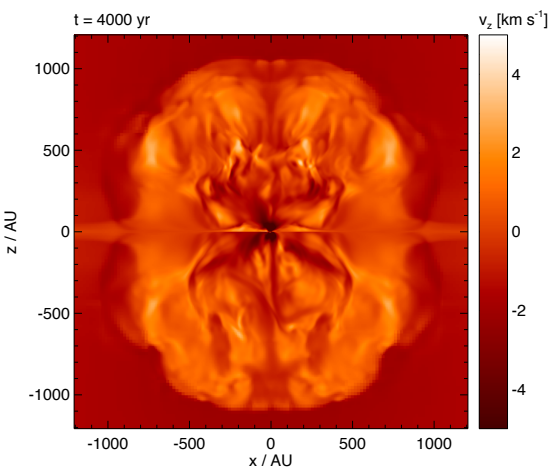
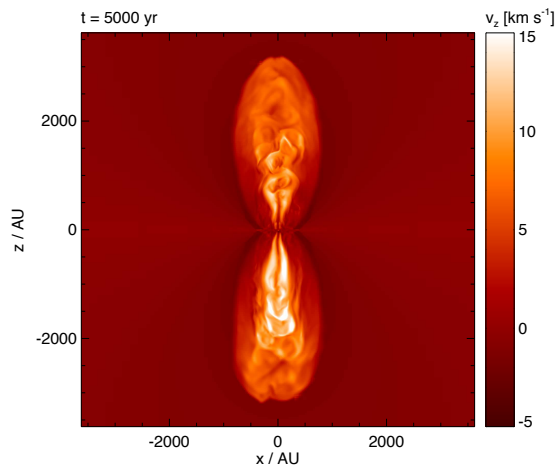
Figure 10. Comparison of thermal and magnetic pressure for the data from the lefthand panels in Figure 5. The thermal pressure p_{th} inside the H II region (left) is of comparable magnitude to the magnetic pressure p_{mag} outside the H II region (right). Thus, magnetic pressure plays a significant role in constraining the size of expanding H II regions. The black dots represent sink particles.



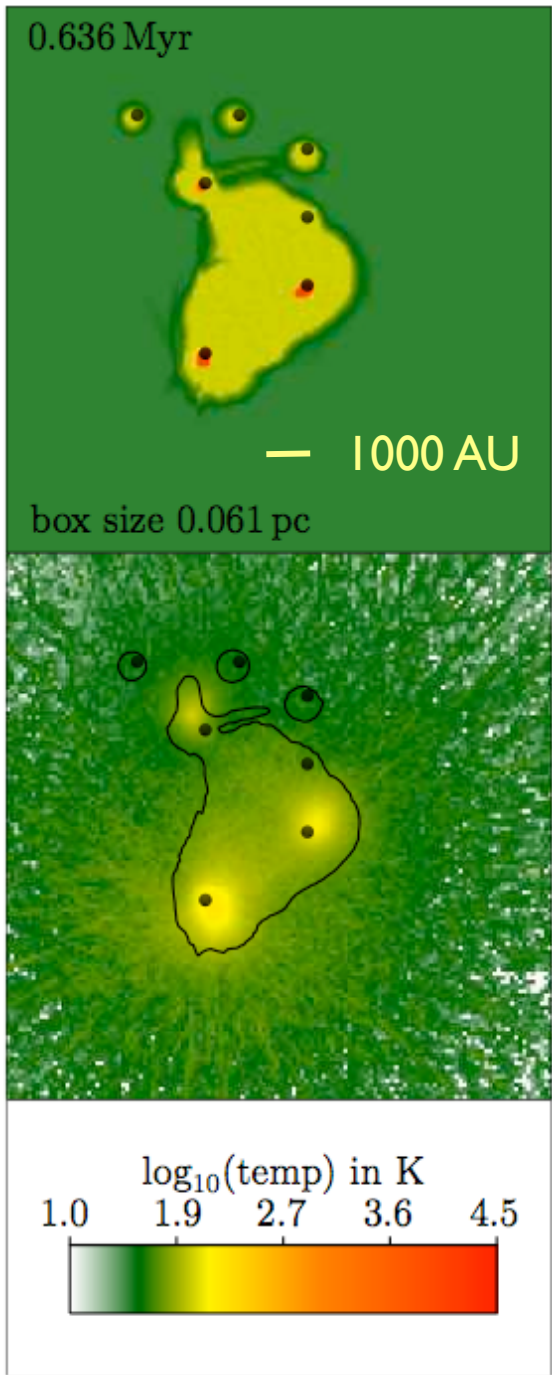
density in inner region
and early times



density on larger scales
and later times

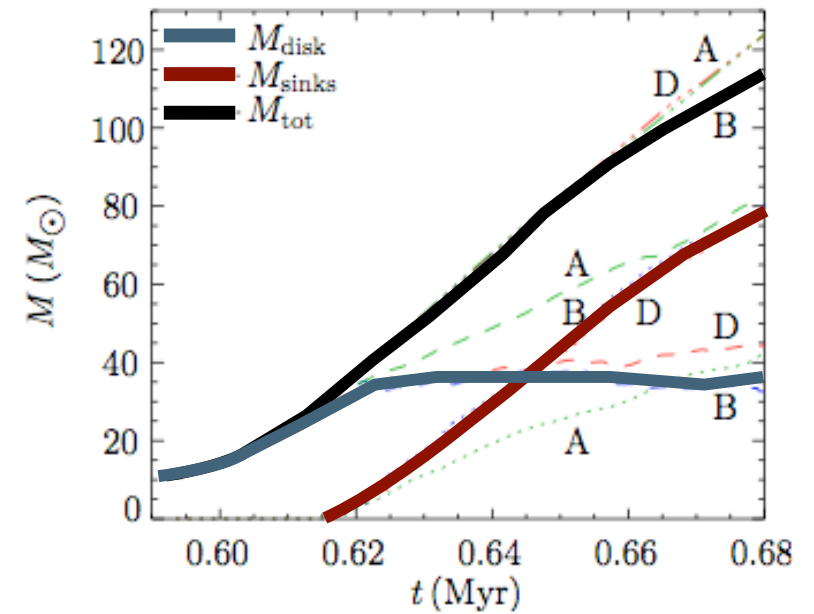
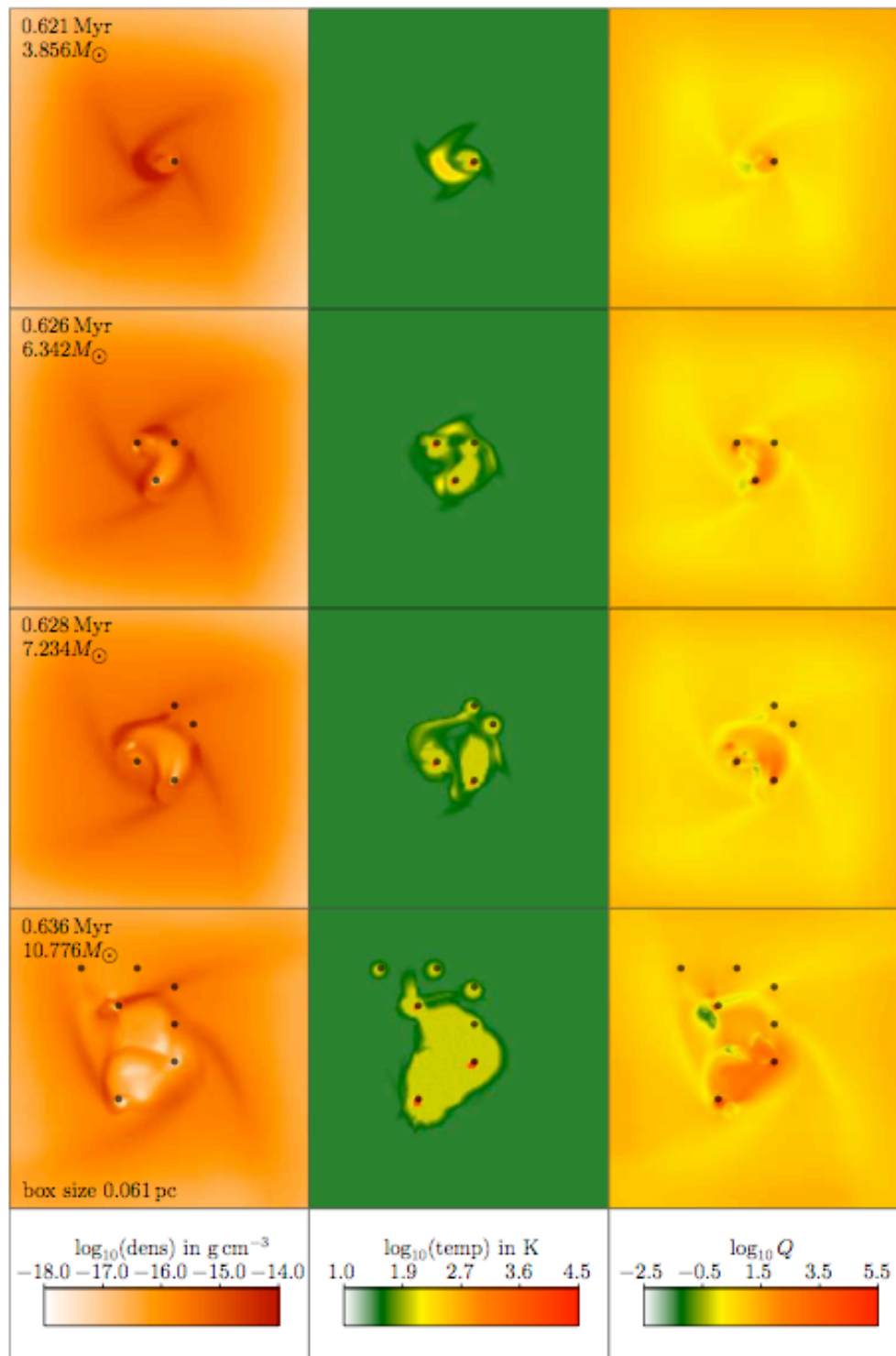


velocity on larger scales
and later times



ray tracing method
(hybrid characteristics)

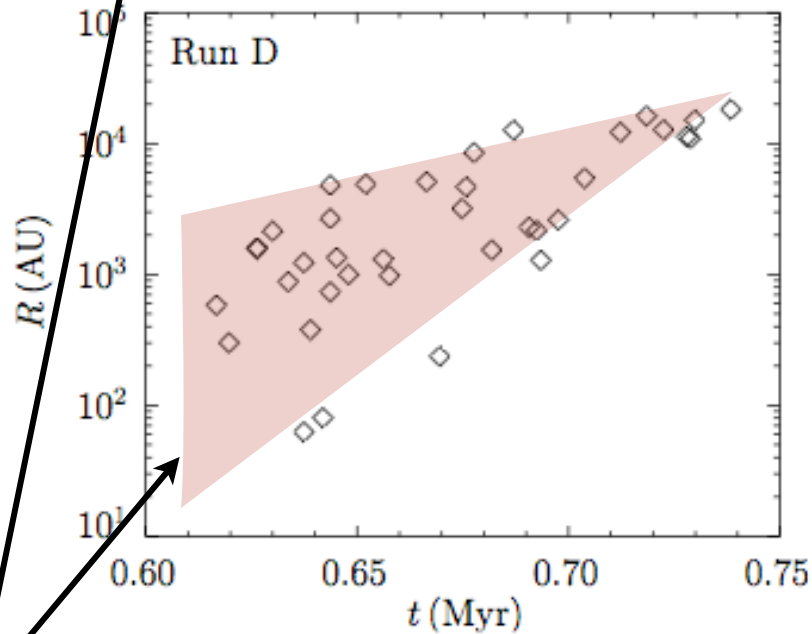
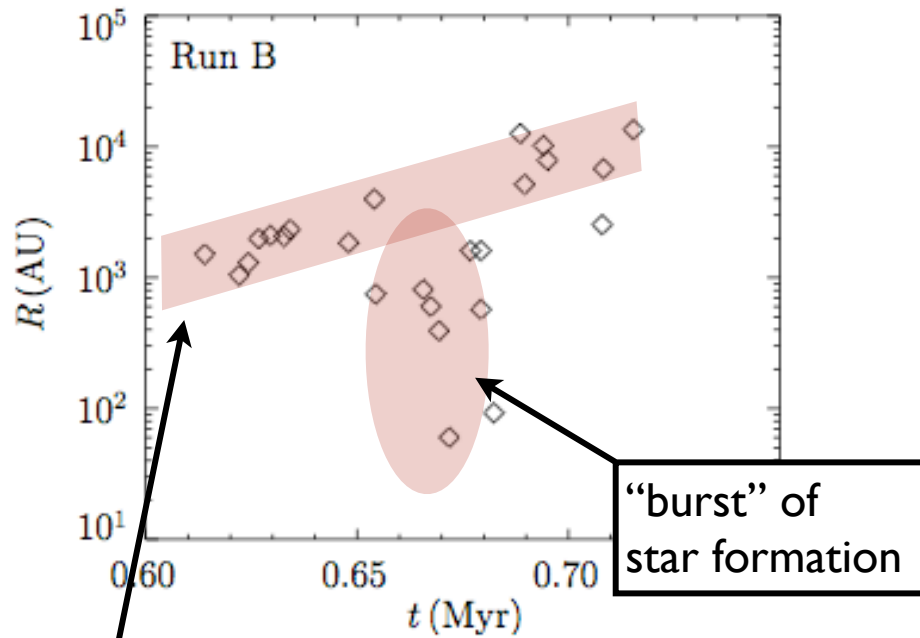
Monte Carlo: full RT
(with scattered radiation)



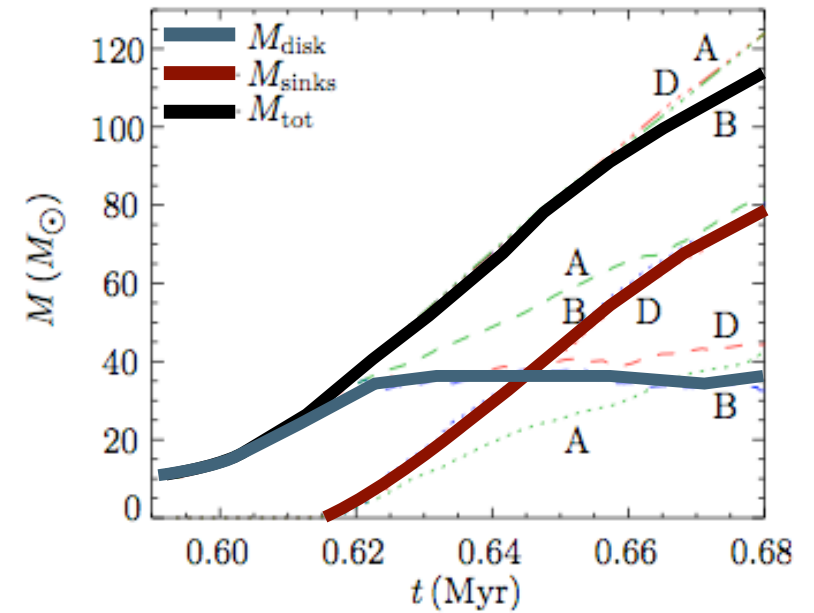
**mass load onto the disk
exceeds inward transport**
--> becomes gravitationally
unstable (see also Kratter & Matzner 2006,
Kratter et al. 2010)

fragments to form multiple
stars --> explains why high-
mass stars are seen in clusters

Peters et al. (2010a, ApJ, 711, 1017),
Peters et al. (2010b, ApJ, 719, 831),
Peters et al. (2010c, ApJ, 725, 134)



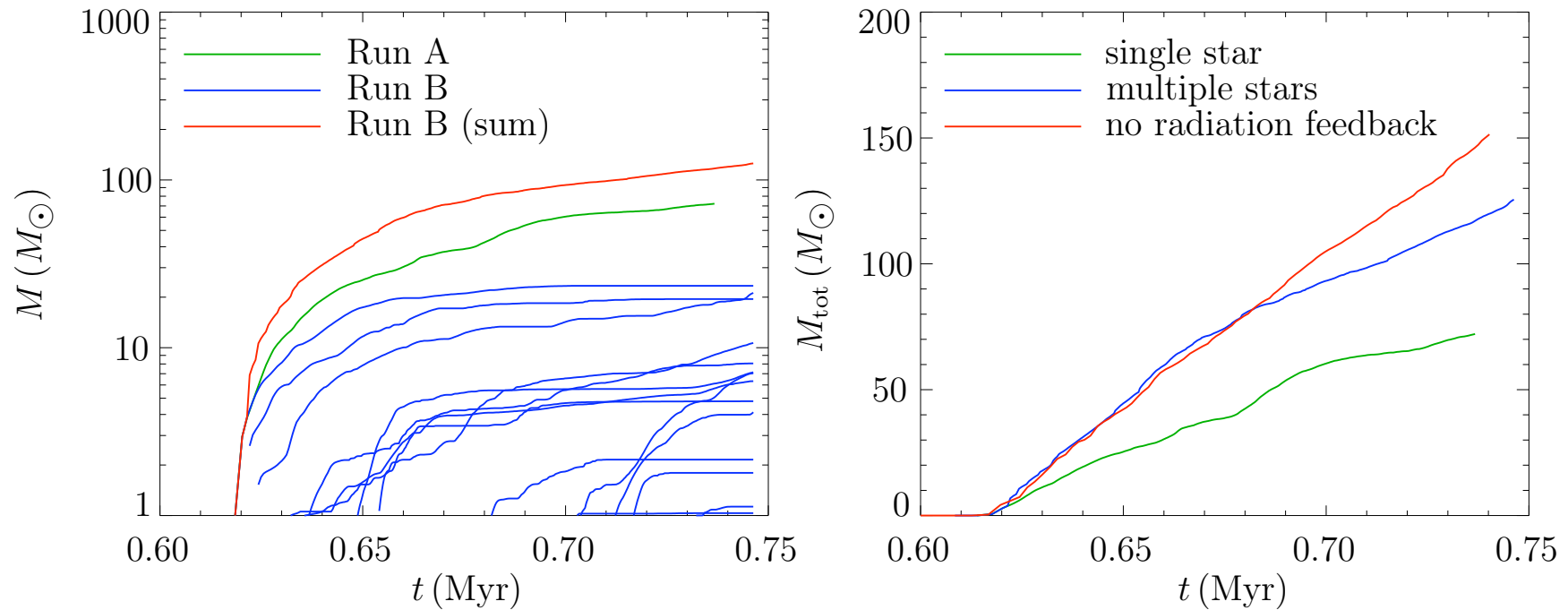
younger protostars form at larger radii



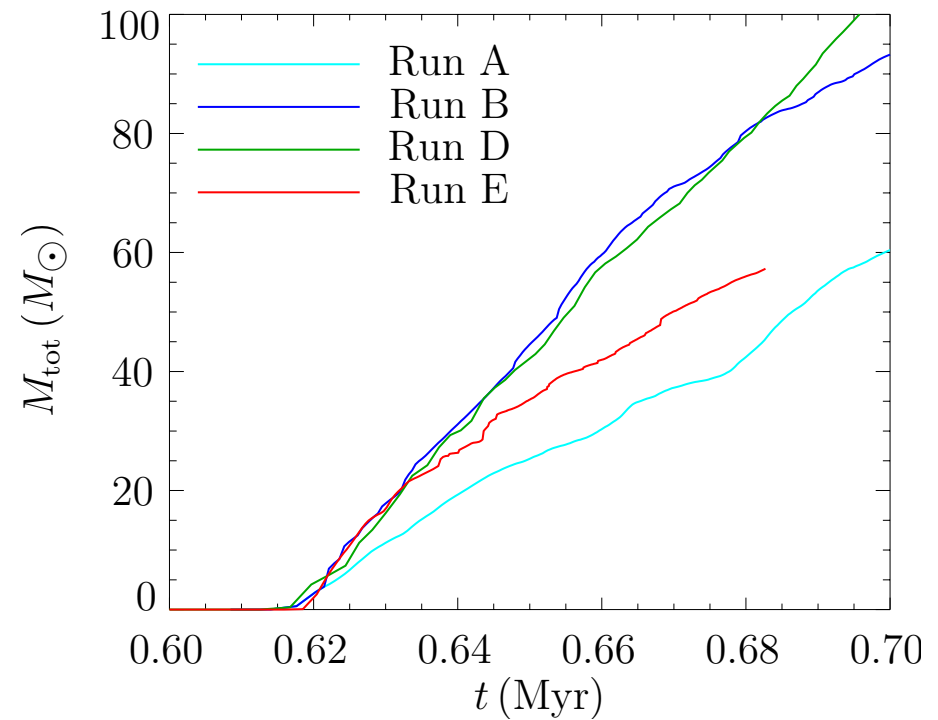
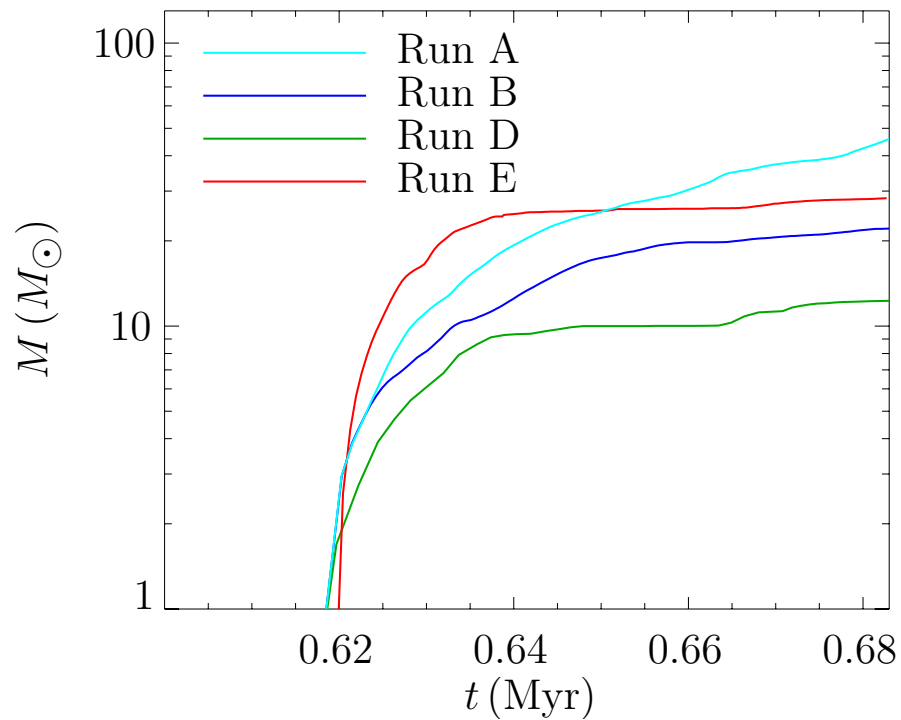
**mass load onto the disk
exceeds inward transport**
--> becomes gravitationally
unstable (see also Kratter & Matzner 2006,
Kratter et al. 2010)

fragments to form multiple
stars --> explains why high-
mass stars are seen in clusters

Peters et al. (2010a, ApJ, 711, 1017),
Peters et al. (2010b, ApJ, 719, 831),
Peters et al. (2010c, ApJ, 725, 134)

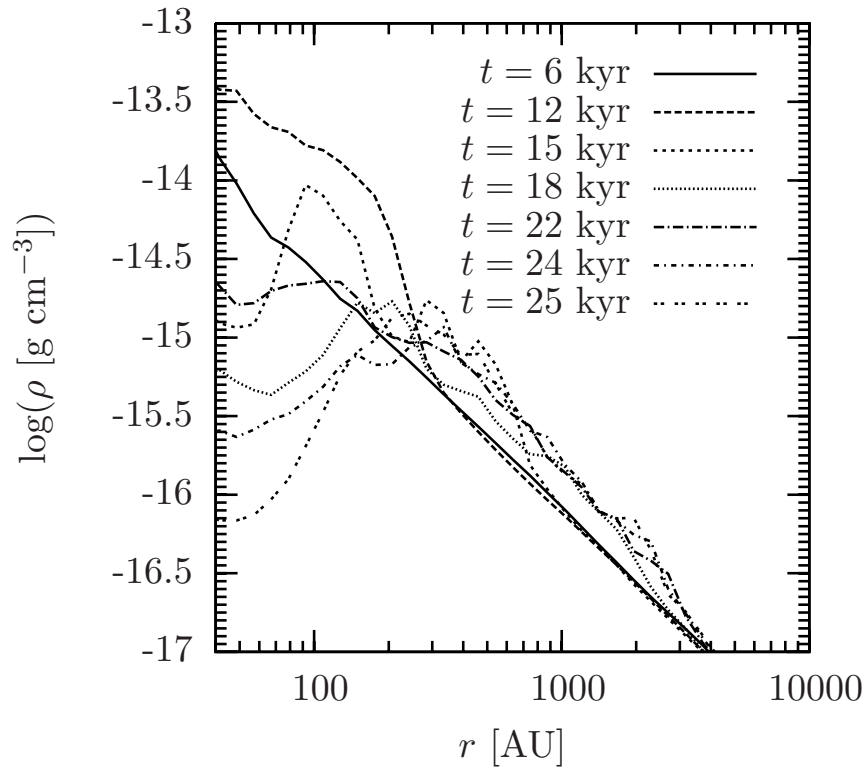


- compare with control run without radiation feedback
- total accretion rate does not change with accretion heating
- expansion of ionized bubble causes turn-off
- no triggered star formation by expanding bubble

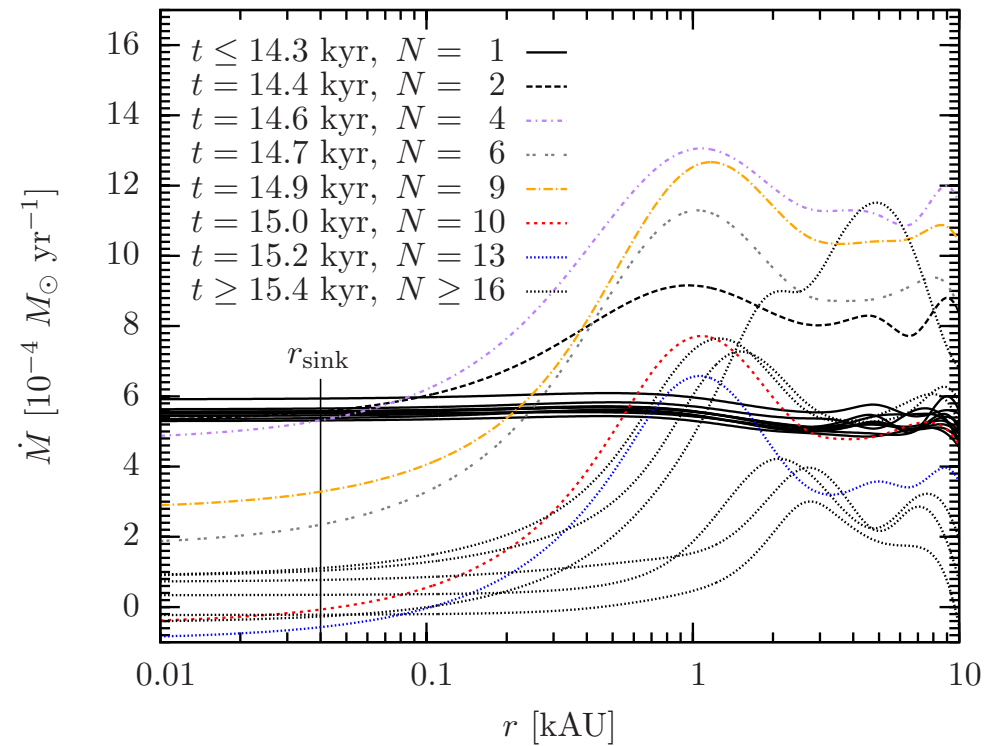


- magnetic fields lead to weaker fragmentation
- central star becomes more massive (magnetic breaking)

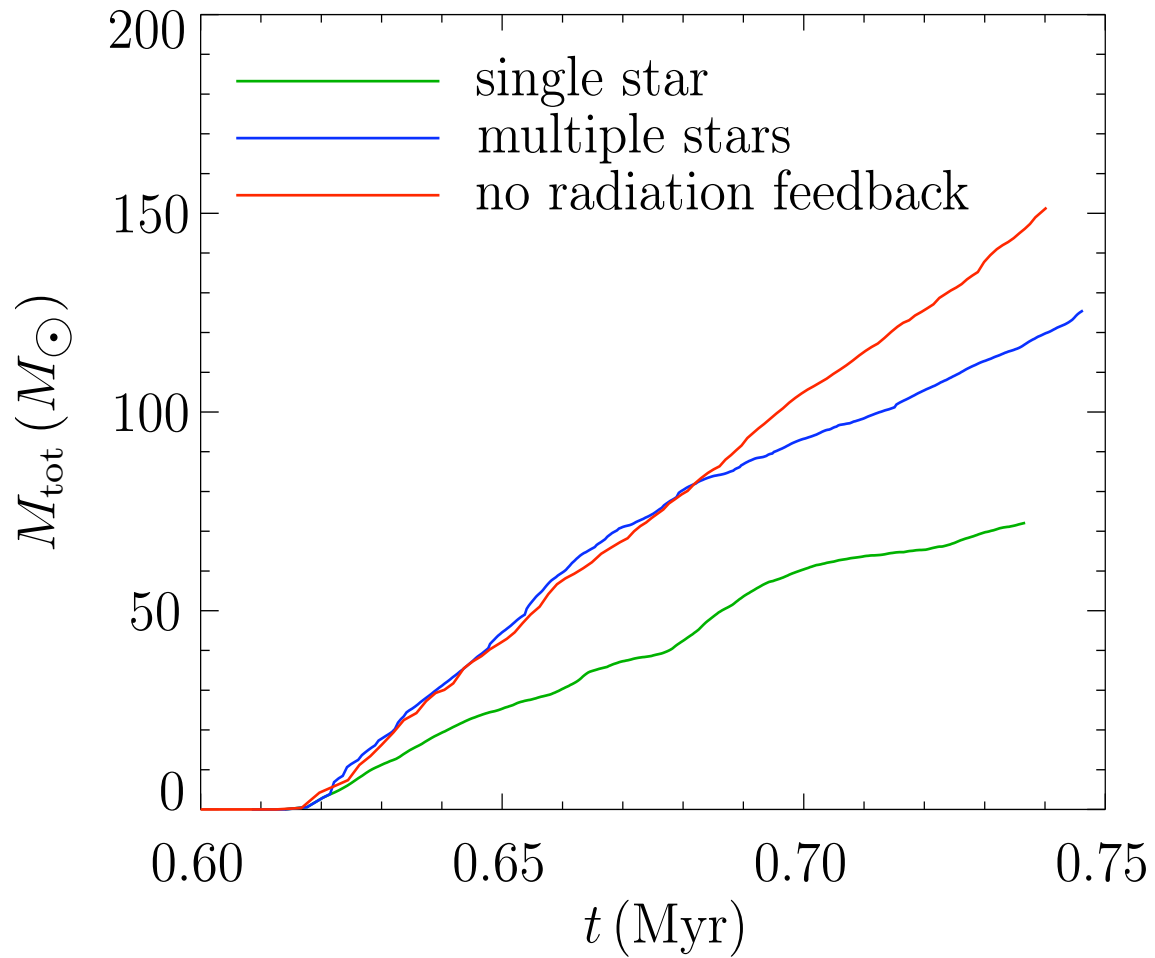
Fragmentation-induced starvation in a complex cluster



gas density as function of radius
at different times

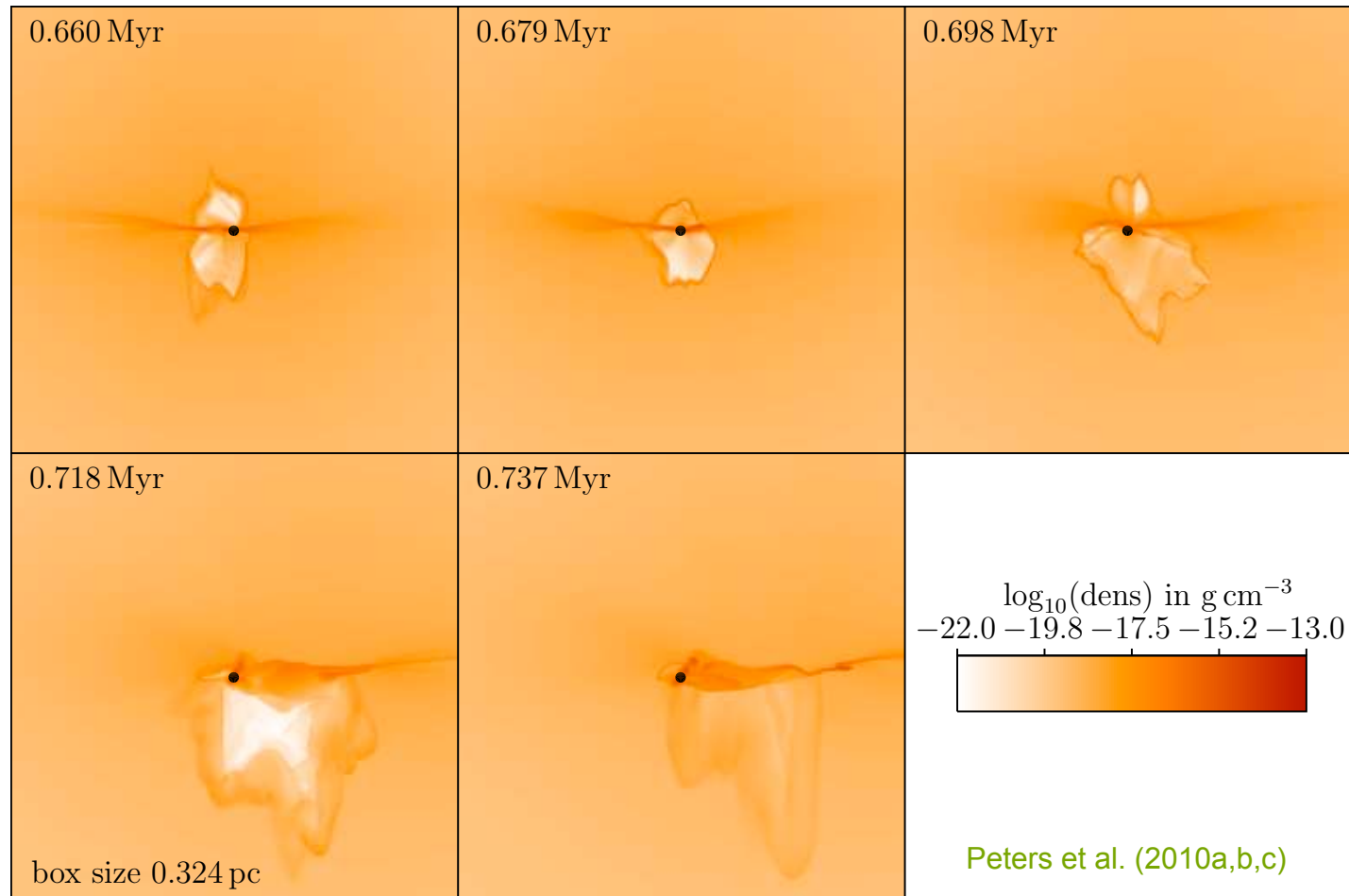


mass flow towards the center as
function of radius at different times

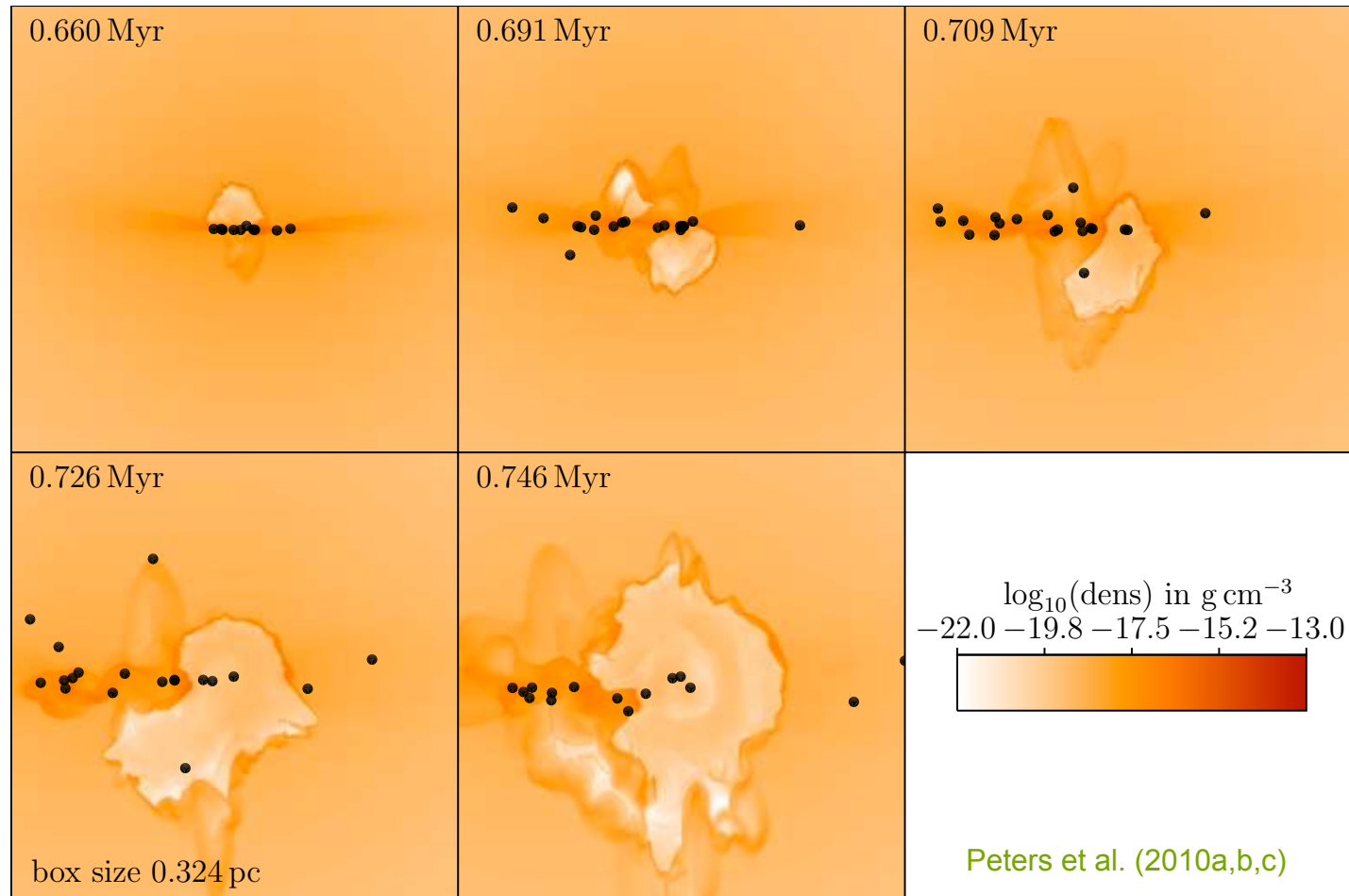


OVERVIEW OF COLLAPSE SIMULATIONS.

Name	Resolution	Radiative Feedback	Multiple Sinks	$M_{\text{sinks}} (M_{\odot})$	N_{sinks}	$M_{\text{max}} (M_{\odot})$
Run A	98 AU	yes	no	72.13	1	72.13
Run B	98 AU	yes	yes	125.56	25	23.39
Run D	98 AU	no	yes	151.43	37	14.64



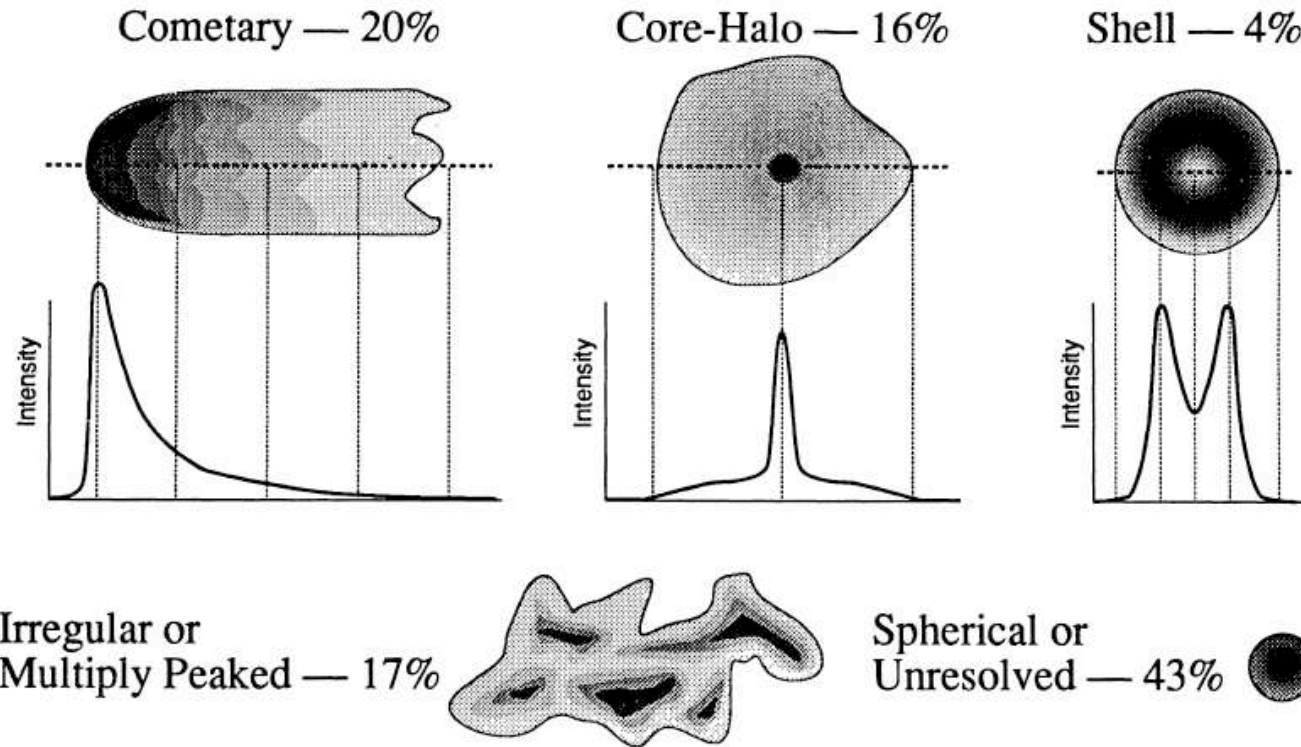
- thermal pressure drives bipolar outflow
- filaments can effectively shield ionizing radiation
- when thermal support gets lost, outflow gets quenched again
- no direct relation between mass of star and size of outflow



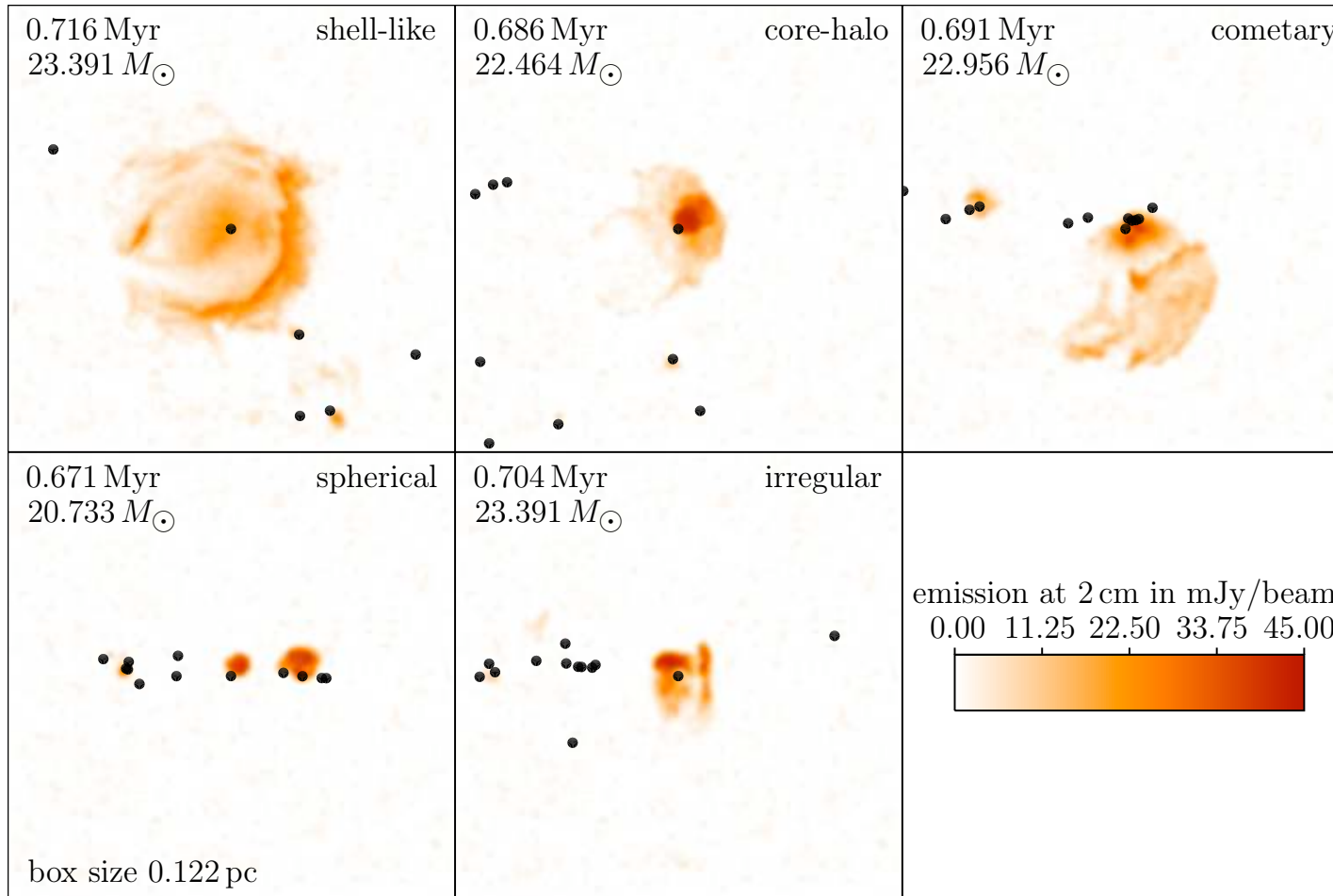
- bipolar outflow during accretion phase
- when accretion flow stops, ionized bubble can expand
- expansion is highly anisotropic
- bubbles around most massive stars merge

- numerical data can be used to generate continuum maps
- calculate free-free absorption coefficient for every cell
- integrate radiative transfer equation (neglecting scattering)
- convolve resulting image with beam width
- VLA parameters:
 - distance 2.65 kpc
 - wavelength 2 cm
 - FWHM 0''14
 - noise 10^{-3} Jy

Ultracompact HII Region Morphologies



- Wood & Churchwell 1989 classification of UC H II regions
- Question: What is the origin of these morphologies?
- UC H II lifetime problem: Too many UC H II regions observed!



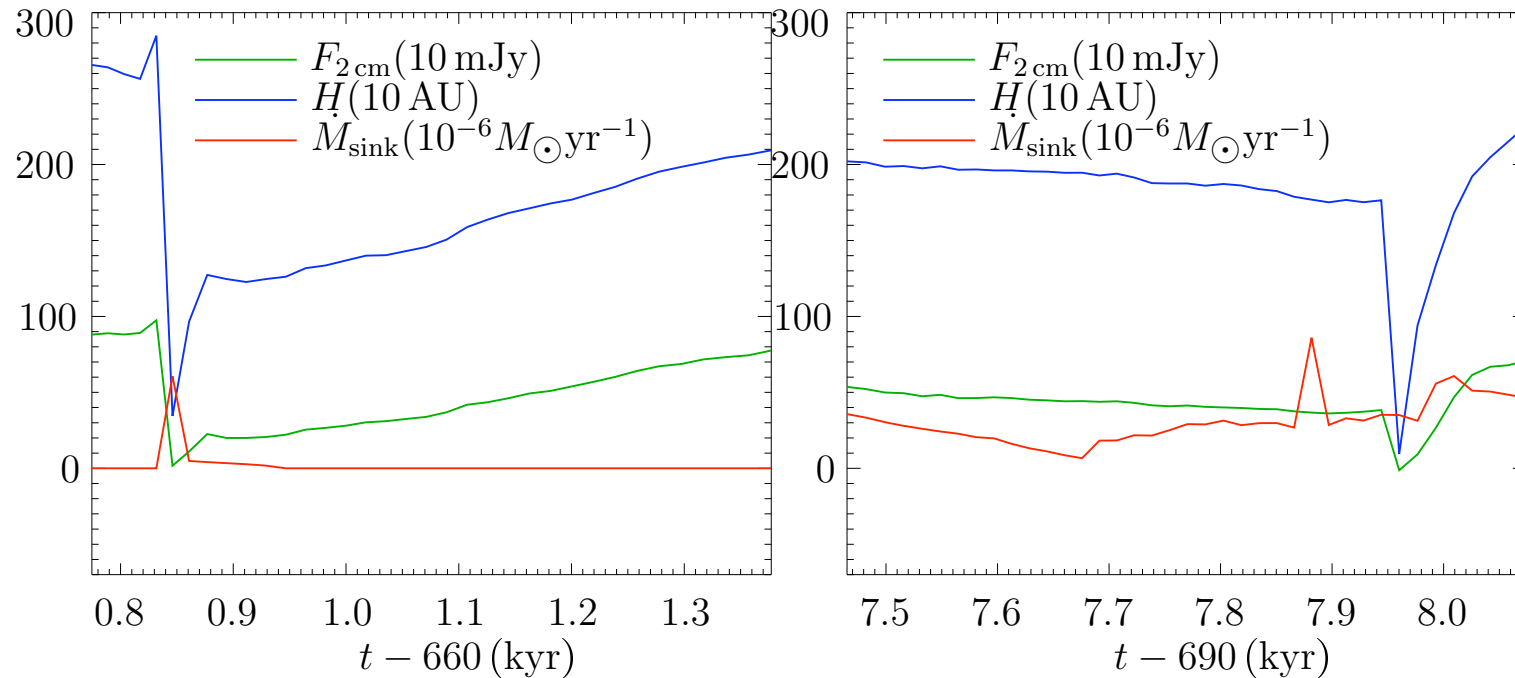
- synthetic VLA observations at 2 cm of simulation data
- interaction of ionizing radiation with accretion flow creates high variability in time and shape
- flickering resolves the lifetime paradox!

Type	WC89	K94	single	multiple
Spherical/Unresolved	43	55	19	60 ± 5
Cometary	20	16	7	10 ± 5
Core-halo	16	9	15	4 ± 2
Shell-like	4	1	3	5 ± 1
Irregular	17	19	57	21 ± 5

WC89: Wood & Churchwell 1989, K94: Kurtz et al. 1994

- statistics over 25 simulation snapshots and 20 viewing angles
- statistics can be used to distinguish between different models
- single sink simulation does not reproduce lifetime problem

time variability



- correlation between accretion events and H II region changes
- time variations in size and flux have been observed
- changes of size and flux of $5\text{--}7\% \text{yr}^{-1}$ match observations

Franco-Hernández et al. 2004, Rodríguez et al. 2007, Galván-Madrid et al. 2008

(Galvan-Madrid et al. 2011)

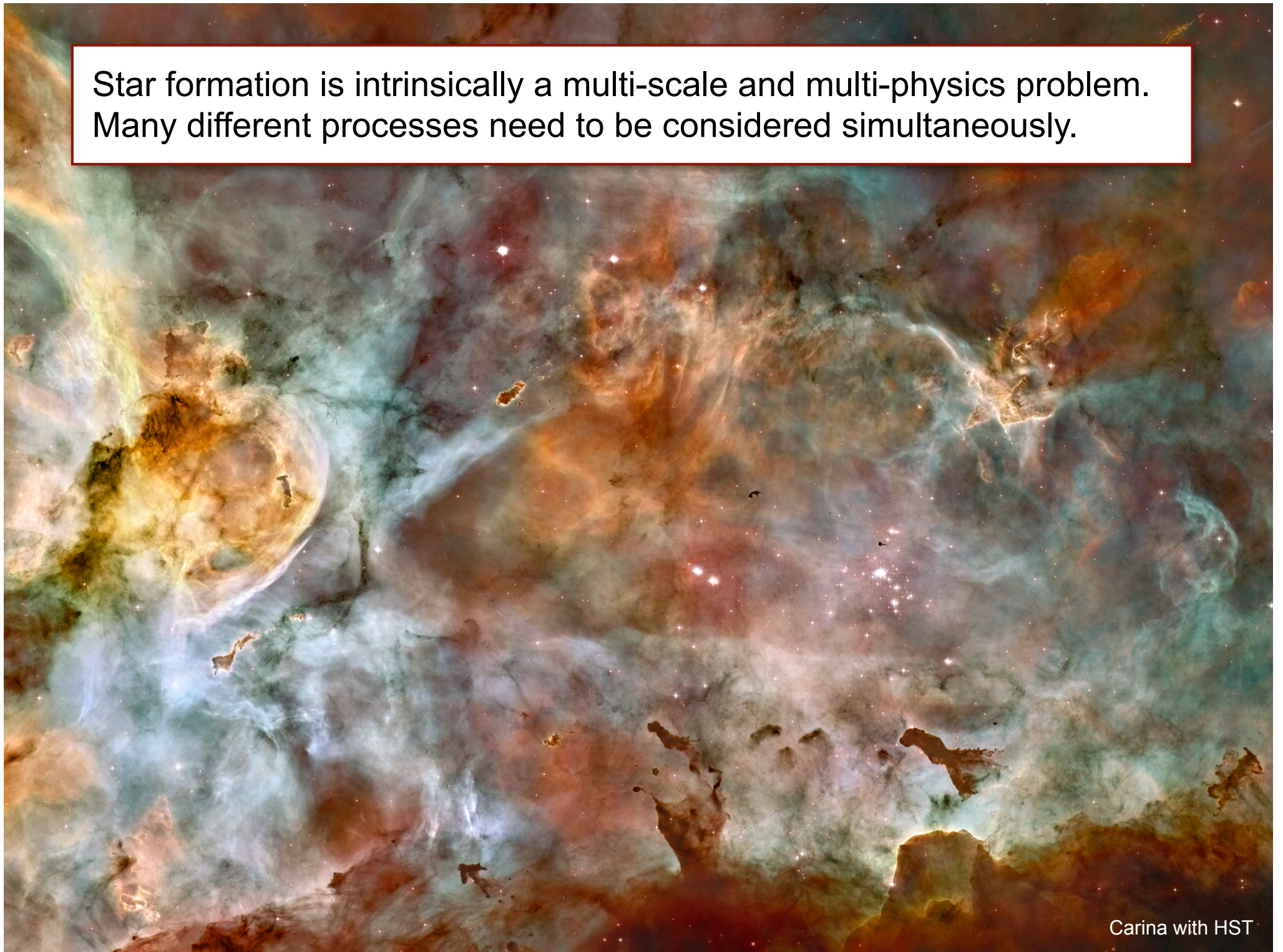
Some results

- ionization feedback cannot stop accretion
- ionization drives bipolar outflows
- HII regions show high variability in time and shape
- all classified morphologies can be observed in one run
- lifetime of HII regions determined by accretion timescale (and not by expansion time)
- rapid accretion through dense and unstable flows
- fragmentation limits further accretion of massive stars

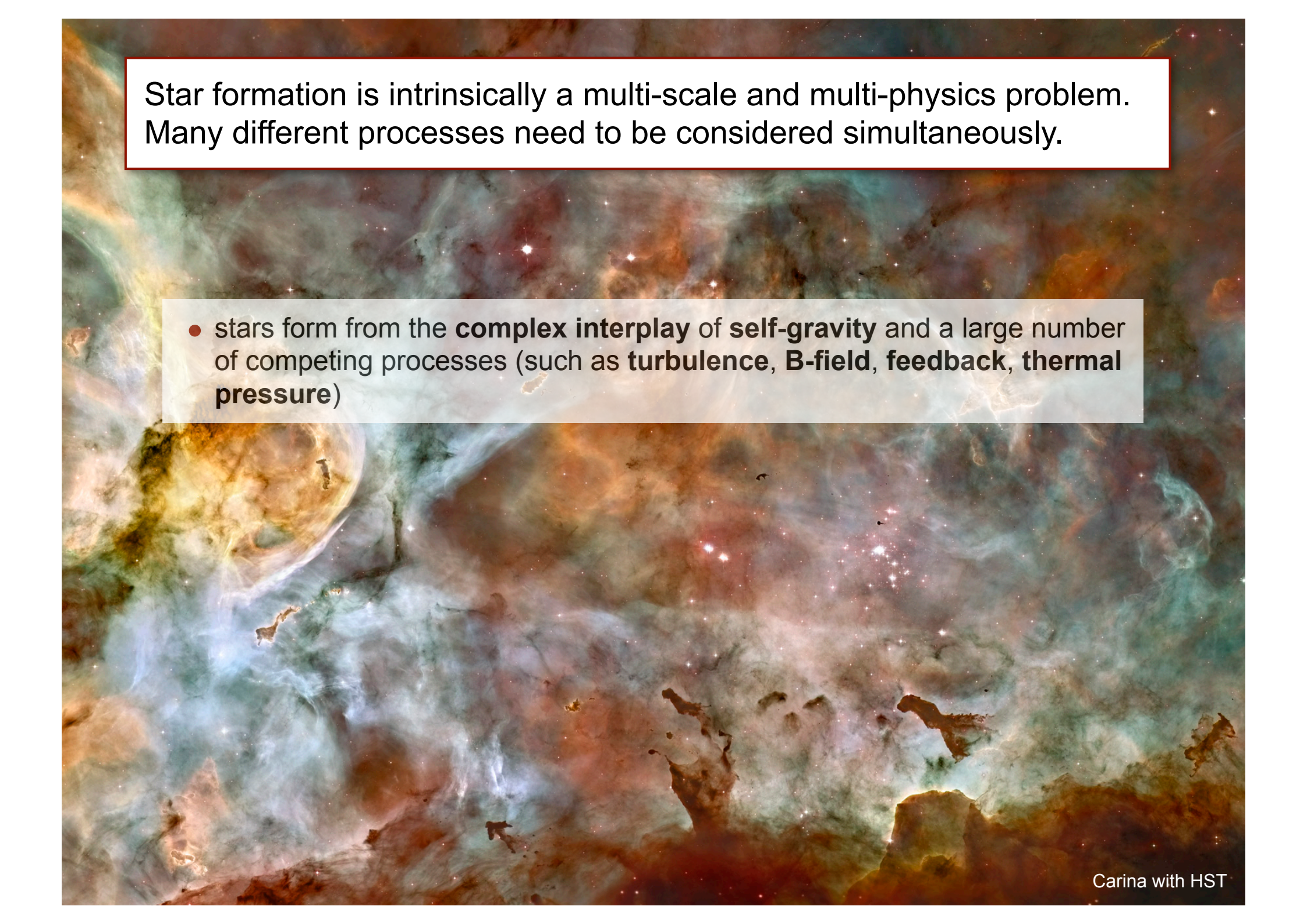


Carina with HST

Star formation is intrinsically a multi-scale and multi-physics problem. Many different processes need to be considered simultaneously.

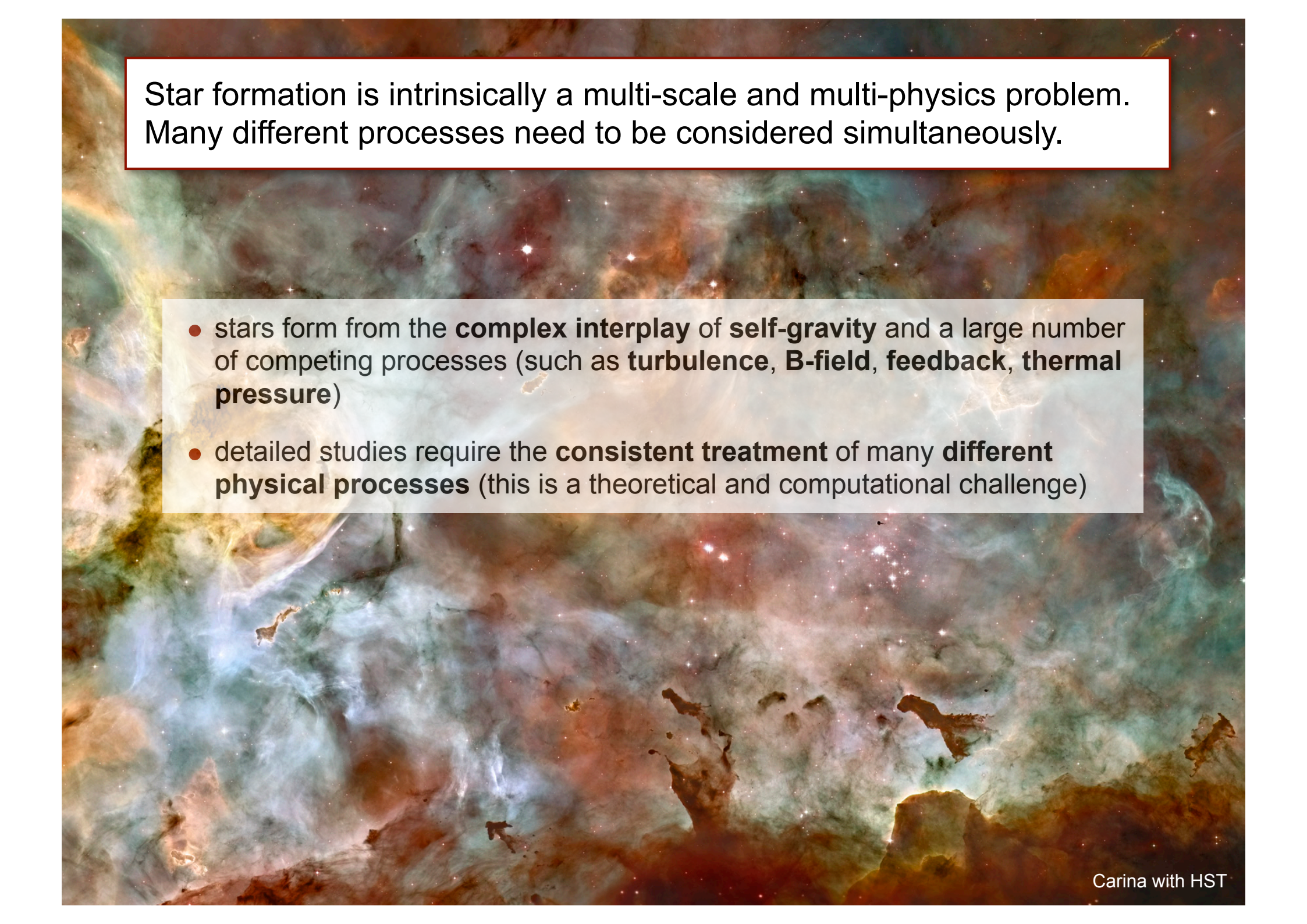


Carina with HST



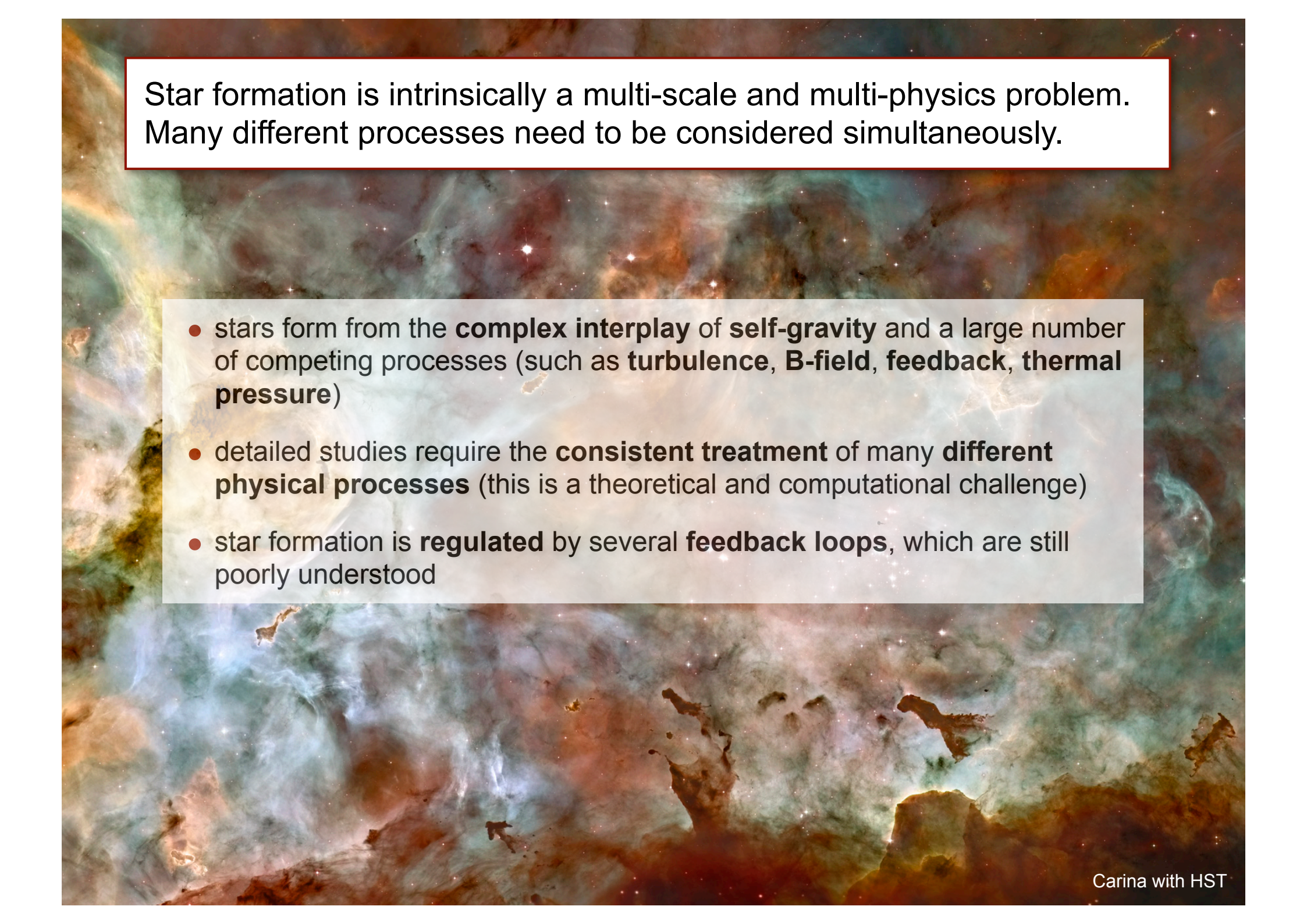
Star formation is intrinsically a multi-scale and multi-physics problem. Many different processes need to be considered simultaneously.

- stars form from the **complex interplay** of **self-gravity** and a large number of competing processes (such as **turbulence**, **B-field**, **feedback**, **thermal pressure**)



Star formation is intrinsically a multi-scale and multi-physics problem. Many different processes need to be considered simultaneously.

- stars form from the **complex interplay** of **self-gravity** and a large number of competing processes (such as **turbulence**, **B-field**, **feedback**, **thermal pressure**)
- detailed studies require the **consistent treatment** of many **different physical processes** (this is a theoretical and computational challenge)




Star formation is intrinsically a multi-scale and multi-physics problem. Many different processes need to be considered simultaneously.

- stars form from the **complex interplay** of **self-gravity** and a large number of competing processes (such as **turbulence**, **B-field**, **feedback**, **thermal pressure**)
- detailed studies require the **consistent treatment** of many **different physical processes** (this is a theoretical and computational challenge)
- star formation is **regulated** by several **feedback loops**, which are still poorly understood



thanks



Protostars and Planets VI in July 15 - 20, 2013

*... hope to see you there!!!
(www.ppvi.org)*